University of California, Merced

Efficient Solar Cooling:

First Ever Non-tracking solar collectors powering a double effect absorption chiller

A thesis submitted in partial satisfaction of the requirements for the degree of

Master of Science

By

Heather Marie Poiry

2011

The thesis of

Heather M. Poiry is approved:

Professor Roland Winston

Professor Gerardo Diaz

Professor Yanbao Ma

University of California, Merced

Fall 2011

Efficient Solar Cooling:

First Ever Non-tracking solar collectors powering a double effect absorption chiller

By:

Heather M. Poiry

Acknowledgments

To arrive at my Masters in Mechanical Engineering there were many mentors, family and friends that helped me achieve this success.

First I would like to thank my family. There were many sacrifices that I had to make but none as great as the sacrifices all of you made for me to have the opportunity for a higher education. To my mother, for all of the hard work and love that she put into me, to my grandparents for all the support they lent to me throughout the years and to my siblings, aunts and uncles for giving me the courage to preserve through the hardest times. And lastly, to my late father, who taught me how to dream.

To my friends, without you I truly couldn't have made it through. Anne, Paul, Amanda, Yang and Alex. You are the ones who inspired me, developed me and became part of making me who I am today. I am so grateful for your patience and so appreciative of our friendship!

To my mentors, it was you who guided me and gave me the encouragement to pursue my dreams. To Dr. Roland Winston, you believed in me in ways that no one ever had before and because of your investment in me I am a confident engineer who is inspired to change the world. To Dr. Viney, you showed me the hidden potential that I had in myself all along and I thank you for helping me to shed light on that, and to Nuno and Bruce, thank you for sanity checks!

To a great team of colleagues who made this project possible and taught me a lot about team work, Kevin Balkoski and Kevin Rico, Chris, Bennett, Lun and Roy were all fundamental characters who each in their own profound way taught me a lot about life and engineering.

Lastly, to my boyfriend Mario. Thank you for your love and support, but most of all your patience. You taught me balance and tranquility and I am deeply appreciative to have you in my life and for your presence with me during this journey.

Thank you, to all of you, for everything!

Sincerely,

Heather M. Poiry

Table of Contents

1. Introduction 11
2. Background 12
2.1 Solar 12
2.1.1 Motivation for a Solar Thermal Medium Temperature Collector 12
2.1.2 Non-Imaging Optics 13
2.1.3 The External Compound Parabolic Concentrator 14
3. Cooling 24
3.1.1 Motivation for Solar Cooling 24
3.1.2 Heat driven cooling technologies 25
3.1.3 Market potential 29
3.1.4 Time to commercialization 29
3.1.5 Other considerations 30
3.2 Conclusions 31
4. Solar Cooling System 31
4.1 Chiller 31
4.1.1 How it works 31
4.1.2 Control Logic 33
4.2 Collector 34
4.2.1 Design 34
4.2.2 Size 41
4.2.3 Configuration 41
4.3 Balance of System 55
4.3.1 The Loops 56
Oil Loop 56
4.3.2 Process Flow Diagram of System: 60
4.3.3 Pumps 61

4.3.4 Tanks 63
4.3.5 Heat Exchangers 66
4.3.6 Insulation 68
5. Manufacturing 74
5.1 Reflectors Mold 74
Reflective Adhesive 76
5.2 Collector 81
5.2.1 Frame 81
5.2.2 Attaching Manifold to Collector Frame 86
5.2.3 Manifold Expansion 88
6. Experimental Results 90
6.1 Solar Collector Performance 90
6.2 Chiller Performance 90
7. Results and Discussion 91
7.1 The Collectors 91
7.2 The Chiller: 94
7.2.1 95
7.3 The System: 96
8. Conclusion 97
9. Appendix 100
9.1 Acronyms 100
1.1 Nomenclature 100
9.2 Solar 102
9.2.1 Testing Method: 103
9.3 The System 107
9.3.1 Chiller 107
9.3.2 Computer Programs 108
9.3.2.1 EW vs NS 108

9.3.3 Cooling Load Program 110
9.3.4 Heat Exchanger: Oil to Glycol 112
9.3.5 Fluids 113

List of Figures

Figure 1: Prototype of solar thermal collector at Castle, in 2008. From left to right, Kevin Balkoski-Graduate Student, myself, Dr. Roland Winston. 11
Figure 2: To the left is a standard flat plate solar collector, and to the right is a standard evacuated solar tube system. 12
Figure 3: Left is a linear Fresnel high temperature system, to the right is a parabolic high temperature system. Both tracking technologies. 13
Figure 4: Roland Winston with the prototype at Nasa Ames. 15
Figure 5: Cross sectional view of XCPC with U-tube. 16
Figure 6: Left is the EW reflector design with an evacuated tube shown. Right is the NS design with an evacuated tube shown. 16
Figure 7: An evacuated U-tube. Purple color is the thermal absorber, copper pipes are where the heat transfer takes place. 17
Figure 8: Manifold showing where the evacuated tube goes. 17
Figure 9: Left is a trough, to the right is the collector. 18
Figure 10: Left is a bank, and to the right is the system. 18
Figure 11: Is a North-South collector showing the incoming sun rays, red lines, changing their incidence angle but the incoming rays are still reflected onto the surface are of the tube. 19
Figure 12: Incidence angle modifier for the NS, Reflectech collector with the U-tube 22
Figure 13: This is a numeric model of the North-South, Reflectech, U-tube efficiency performance for various inlet temperatures and flow rates. 23
Figure 14 BROAD's double effect lithium bromide chiller. 26
Figure 15: Is a diagram of an adsorption chiller. 27
Figure 16: (a) solid and (b) liquid systems. 28
Figure 17: BROADS double effect 6.6 Lithium Bromide absorption chiller, and me. Circa 2009. 31
Figure 18: Is a depiction of what the HTG looks like, with a natural gas burner below the tank and wrapped coils that have the hot solar thermal fluid flowing through, represented by the red arrow. 33
Figure 19: Break even analysis for the NS collector, with Reflectech and the U-tube, with an ambient temperature of 35°C. 38
Figure 20: The diagram to the left is a depiction of 2 banks in parallel, each bank is a collector of 80 tubes in parallel. The diagram to the right is two banks in parallel, each with two collectors that run in parallel as well, with 40 tubes per collector. 44
Figure 21: Mass flow through each tube for various configurations. 45
Figure 22: Pressure drop for various configurations of the collector systems. 46
Figure 23: The selected collector system. 46
Figure 24: Vertical pipe flow to show elevation losses. 47
Figure 25: Horizontal pipe flow. 48
Figure 26: Pipe flow through a 90° bend, showing minor losses 48
Figure 27: A cylindrical shell showing an elemental control volume for application of energy conservation principle. 49
Figure 28: Balance of system. 55
Figure 29: The three closed loops are what the solar cooling system is comprised of. 55

Figure 30: Oil loop process flow diagram. 56
Figure 31: Process flow diagram of glycol loop. 57
Figure 32: Process flow diagram for entire system. 60
Figure 33: Oil pump performance graphs showing pressure head, volumetric flow rate, power and efficiency 62
Figure 34: Storage tank retention temperature for various volume tanks. 64
Figure 35: Manifold, and junction. 68
Figure 36: Galvanized steel pipe 68
Figure 37: Fiberglass pipe insulation. 69
Figure 38: Fiberfrax layer rolled up. 69
Figure 39: Microtherm quilt 69
Figure 40: Heat loss in thermal watts from the collectors to the chiller. 73
Figure 41: Reflector 3-d renderings for the mold. 74
Figure 42: Slight angle added to mold for reflector manufacturing. 75
Figure 43: Is the foundational base of the frame. Top picture is the loads and constraints, bottom is the stress contours. 82
Figure 44: Final frame design. 84
Figure 45: Top figure is the final frame design with load and constraints applied. Bottom picture is the stress contour. 85
Figure 46: Design of tube, frame and attachment. 87
Figure 47: Real picture of manifold attachment. 87
Figure 48: Picture of our manifold to manifold connection with flex hoses 88
Figure 49: Delta T of the solar collectors during an efficiency experiment. 92
Figure 50: Collector efficiency comparison of extra insulation 93
Figure 51: Collector efficiency comparison of the collectors dirty vs. clean. 93
Figure 52: COP comparison on maintenance of chiller. 95
Figure 53: Outlet temperature of the chiller when it is maintained vs. when it is not. 95
Figure 54: Power of solar, chiller, natural gas and sun vs. operational time. 96
Figure 55: Top and cross sectional view of the XCPC with a counter flow tube. 102
Figure 56: Schematic of the test facility for CEC grant. 105
Figure 57: Kinematic Viscosity vs. temperature for the mineral oil. 113
Figure 58: Glycol/Water vapor pressure vs. temperature. 113

List of Tables:

Table 1: Comparison of the pros and cons for various solar thermal technologies. 15
Table 2: Lists the variables for the XCPC design that were experimented..... 20
Table 3: North-South, Reflectech, U-tube collector description..... 21
Table 4: Performance characteristics of the NS, Reflectech, U-tube..... 23
Table 5 Chiller types with their temperature and COP ranges..... 26
Table 6: Temperature algorithm for the BROAD chiller..... 34
Table 7: NS vs EW characterization..... 36
Table 8: Priority and scores for the EW and NS collector designs..... 41
Table 9: Building Characteristics of office trailer..... 58
Table 10: Load of building. 60
Table 11: Glycol expansion tank calculations 66
Table 12: Heat exchanger requirements..... 66
Table 13: Microtherm vs. FiberFrax for Junction..... 70
Table 14: Thickness comparison of fiberglass for piping sections. 71
Table 15: Oil storage tank calculations for FiberFrax insulation..... 72
Table 16: Oil expansion tank calculations for FiberFrax insulation. 72
Table 17: Glycol expansion tank calculations for FiberFrax insulation 72
Table 18: Input data for the expansion analysis of the manifold. 89
Table 19: The expansion results of the manifold for the temperature increase. 89
Table 20: Chiller burner refrence table. 107

1. Introduction

Solar thermal technologies have been successfully applied for water heating and power generation for several decades. While solar collectors for water heating are low cost, individual units that operate at less than 100°C, solar thermal power plants are utility scale investments and installations that operate at temperatures beyond 300°C. What is needed is a cost effective solar thermal collector capable of producing heat at 100-300°C.[i]

When the University was established in 2004 Dr. Roland Winston came with an extensive background in solar energy; and had an idea about how to design a solar thermal collector that could achieve 100-300°C while being economically competitive with traditional fuel sources. To achieve this goal he began a solar thermal research group at UC Merced that attracted many students including myself as a freshman in the fall of 2005. The group consisted of multiple graduate students as well as undergraduates and together we extensively studied physics, optics, solar energy, etc. that allowed us to design and model solar thermal collectors. In 2007 our group was awarded a California Energy Commission, CEC, grant that allowed us to build and test our designs over two years to determine the characteristics of each design.

What came of it was an optimal design for the collectors and an ideal application for them, a double effect absorption chiller. Our group chose to purse designing, building and testing this solar cooling system in 2009, the year I graduated with my B.S. and I chose to continue this research and take on the role of being the lead engineering and project manager.

This thesis reviews the work that was done before my time as a graduate student so that one may understand the solar thermal technology and specific design, and why a double effect absorption chiller was chosen as the ideal application; and how we designed, built and tested the first ever non-tracking solar powered double effect absorption chiller.

Figure 1: Prototype of solar thermal collector at Castle, in 2008. From left to right, Kevin Balkoski-Graduate Student, myself, Dr. Roland Winston.

2. Background

2.1 Solar

2.1.1 Motivation for a Solar Thermal Medium Temperature Collector

Low temperature thermal systems primarily consist of two technologies: flat plate collectors and evacuated tubes, as shown in Figure 2 below. To date, flat-plate collectors for hot water generation serving the residential and commercial sectors have been implemented for several decades and have achieved a high degree of reliability, being one of the most widespread solar thermal technologies.[ii] Flat plate collectors for water heating are inherently limited due to their design to the low temperature region; however, well-engineered devices can achieve operating temperatures beyond 100°C at low pressures for water, and some degrees higher with other fluids.[iii] Flat plate collectors can effectively be used as pre-heaters to assist several processes and increase the overall fuel efficiency, such as the solar assisted air conditioning program (SACE) in Europe.[iv] Other collectors sharing the same principles of the flat type have been proposed for drop drying as well as other applications.[v]

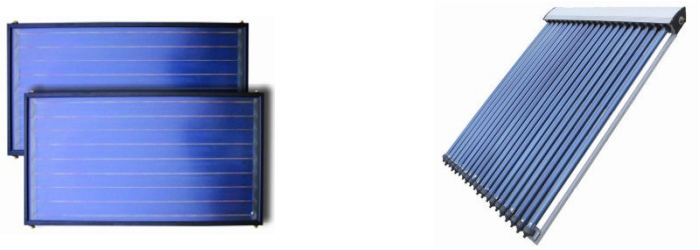

Figure 2: To the left is a standard flat plate solar collector, and to the right is a standard evacuated solar tube system.

High temperature thermal systems with working fluid temperatures in the range of 300°C to 1000 °C are generically known as Concentrating Solar Power, CSP, technologies. Examples of these technologies are parabolic and linear Fresnel mirrors, and are shown in Figure 3 . To date, any technology in the market today that can achieve $^{+}$ 300°C are tracking technologies. These types of systems have focused primarily on power generation and are large scale installations able to generate power in the tens of megawatts. The economics of these systems only make sense at the electrical utility scale.[vi]

Figure 3: Left is a linear Fresnel high temperature system, to the right is a parabolic high temperature system. Both tracking technologies.

Medium temperature solar collectors have an operating range between 120-250°C. In contrast to the extensive literature and development of low and high temperature solar collectors, recent surveys on commercially deployed solar thermal technologies do not report any development of medium temperature collectors. What happens is that industry attempts to bring expensive high temperature tracking solar collectors down to the medium temperature range or the non-tracking inefficient low temperature technologies up to the medium temperature range. The result is that both approaches are inefficient.

What is needed is a solar thermal collector that has a low cost design and is simple to use, and can effectively achieve temperatures in the medium temperature range.

2.1.2 Non-Imaging Optics

For most of its history, the field of optics had been devoted to the collection and concentration of the visible light reflected or generated by objects, onto a plane or directly transmitted to the human eye. The main motivation was to form a visible image of distant or minuscule objects that otherwise would escape the human eye's resolution capacity. Contemporary optics however, has expanded its field of study and applications beyond image formation and beyond the spectrum of visible light.

Image-forming optical systems are devices such as cameras, telescopes, microscopes and similar others. One strict requirement of these systems is that the light at the output of the optical system must preserve the same spatial distribution of the incoming light. In other words, using geometrical optics each ray originated at each single point of the object that is collected by the optical system, must occupy the same relative position of the input (source), at the output (image plane or receiver). The better the optical system can achieve this condition, the better the image at the output will resemble the image at the input.

Non-imaging optics is a relatively new field in optics that studies the collection and concentration of light without the requirement of transmitting the same spatial distribution of light radiated by the source, to the output of the optical system. Therefore, the image at the output of a non-imaging device won't necessarily bear any resemblance to the image at the input. This relaxation in the performance requirements of the optical system also relaxes the design approach for non-imaging devices, as typical aberrations for image-forming optical devices are not necessarily important to address.

For solar energy applications what matters is the collection, transmission or concentration of the incoming energy, with no interest in reproducing the precise image of the sun at the output of the optical system, which would be the input of the energy conversion system. Therefore, non-imaging optical components are of great interest in the design of solar energy systems.

The discovery and development of non-imaging optics has enabled non-tracking (fixed) concentrating solar collectors generating heat up to 300°C. In March 2002, Bergquam Energy Systems completed a project to design and optimize solar absorption chillers. This project, funded by PIER Renewables (contract number 500-02-035), was the first demonstration worldwide showing that a double effect absorption chiller can be powered by a solar thermal system, based on non-imaging optics for the concentration of sunlight. That specific collector is called an integrated compound parabolic concentrator, ICPC. Several companies overseas took up this technology concept and developed similar products to be commercialized. However, these products were, in most cases, not cost-competitive and not geared to California's climate.

2.1.3 The External Compound Parabolic Concentrator

Building on the foundation of the ICPC an idea for an external parabolic concentrator, XCPC, was pursued at the University of California, Merced, UCM, through a CEC grant #500-05-021. The goal was for the XCPC to be a low-cost, medium-temperature solar thermal collector system ready for mass production. Table 1 outlines the pros and cons of various solar thermal technologies against the XCPC. Working with corporate participants Sol Focus and United Technologies Research Center, the research team at the UCM developed an innovative non-tracking system consisting of a series of stationary evacuated solar thermal absorbers paired with external non-imaging reflectors. This system is able to operate with a solar thermal efficiency of

50% at a temperature of 200°C. The XCPC can be readily manufactured at a cost of $15 - $18 per square foot meeting the economic goals for the project.

Table 1: Comparison of the pros and cons for various solar thermal technologies.

Technological concept	Pros	Cons
Flat plate collector	Stationary	Limited to temperatures well below 100°C
Parabolic Trough	Can operate up to 315°C	Tracking required
Integrated Compound Parabolic Concentrator (ICPC)	- No tracking required - Can operate up to 260°C	Expensive
External Compound Parabolic Concentrator (XCPC) [our approach]	- No tracking required - Amenable to low cost mass production ($15 - $18 psf)	Limited to temperatures up to 200°C

During the course of this project, a total of seven different XCPC configurations were created and tested at UC Merced. After improving the reflector technology and incorporating a new evacuated thermal absorber design, a prototype was then constructed and tested. After further improvements and adjustments, a 10kW prototype was manufactured and tested at the NASA/Ames facility by SolFocus. This prototype has been in operation since the spring of 2008. Figure 4 below is a picture of this prototype.

Figure 4: Roland Winston with the prototype at Nasa Ames.

Before getting into the specifics of the design it is important to understand the various components that the collector is comprised of and how the system is referred to.

Components:

To have a general understanding of the external compound parabolic concentrator, cross sectional view of the collector in Figure 5, a brief description of each component of the system and how they fit together and operate is provided.

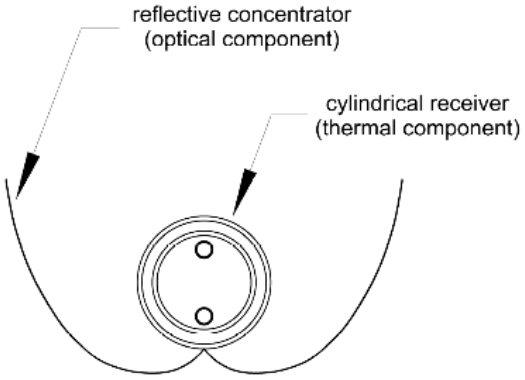

Figure 5: Cross sectional view of XCPC with U-tube.

Reflector:

The reflector is designed via non-imaging optics and is orientated for the NS or EW direction. It has a reflective coating so that it can reflect the solar insolation. Figure 6 shows the NS and EW designs to scale.

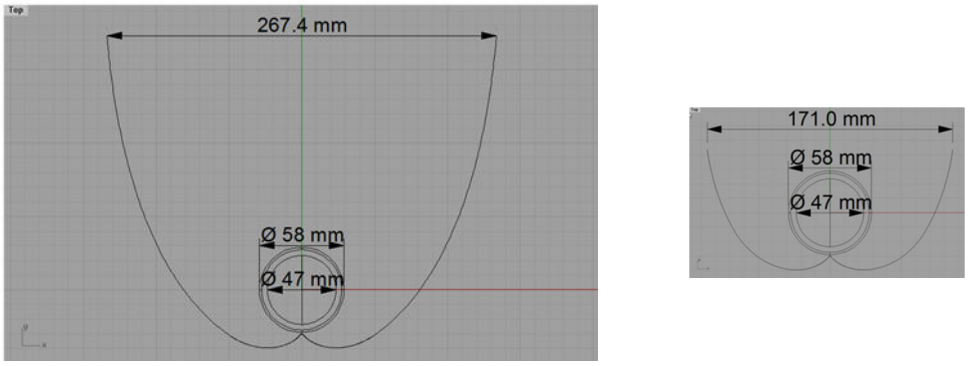

Figure 6: Left is the EW reflector design with an evacuated tube shown. Right is the NS design with an evacuated tube shown.

Evacuated Tube:

The thermal component includes an envelope (glass tube), absorber and the absorber-to-fluid element. Figure 7 is a model of an evacuated U-tube.

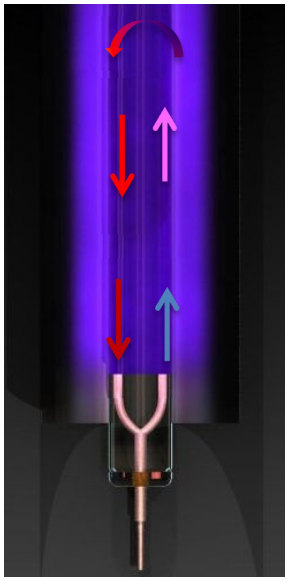

Figure 7: An evacuated U-tube. Purple color is the thermal absorber, copper pipes are where the heat transfer takes place.

- *Envelope:*

The envelope is a hermetically sealed, evacuated glass cylinder that encloses the thermal absorber and the absorber-to-fluid element. This glass cylinder, tube, provides a transparent medium for the incoming solar radiation and is made of commercial grade borosilicate. The vacuum gap between the thermal absorber and the glass limits the thermal losses by convection.

- *Thermal Absorber*

The thermal absorber is a cylindrical surface coated with an optically selective thin film. The selective coating provides a high absorptivity of radiant energy in the visible and near UV band of the solar spectrum while reducing the emissivity in the thermal spectrum.

- *Heat Transfer from Absorber to Fluid*

This absorber then transfers the heat collected to the working fluid circulating through the thermal circuit pipe. The main heat transfer mechanism is by contact of the working fluid with the thermal absorber.

Manifold

There is a copper pipe that connects all of the evacuated tubes to one another. It has a supply pipe and a return pipe which is connected to the tube itself. Figure 8 is a depiction of what a section of manifold looks like for a single evacuated tube.

Figure 8: Manifold showing where the evacuated tube goes.

Vocabulary of XCPC System

To lay the foundation for the terminology of this paper in regards to speaking of the XCPC in components vs. various 'systems' the standard terms used in industry are the following:

Trough:

A single reflector with an evacuated tube

Collector:

A system of multiple troughs, coupled with evacuated tubes and as single manifold.

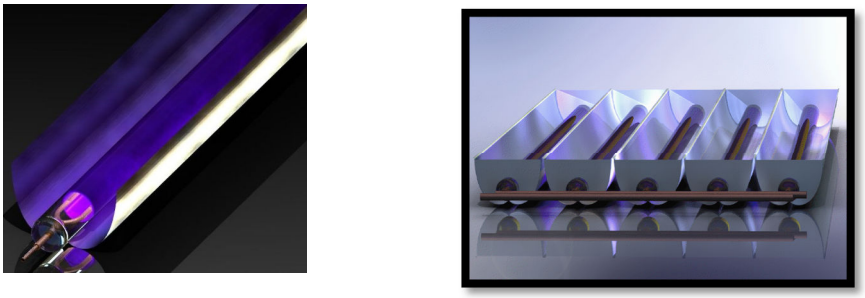

Figure 9: Left is a trough, to the right is the collector.

Bank:

A bank consists of multiple collectors, whether they are in series or parallel, in one row which gives a single input and a single output.

System:

Multiple banks.

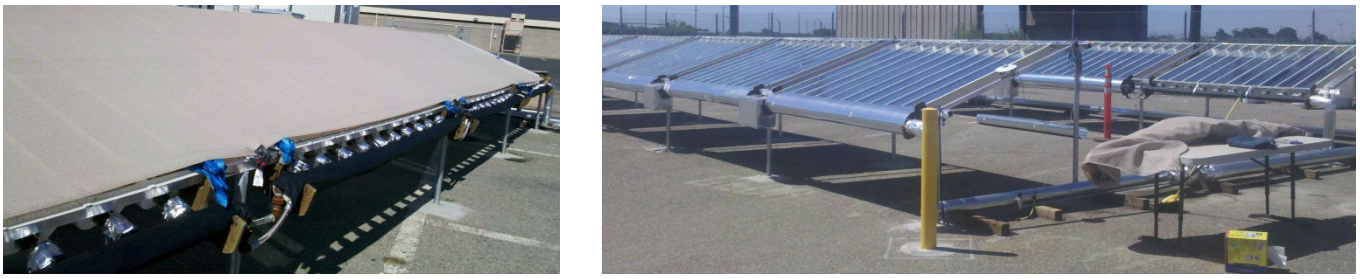

Figure 10: Left is a bank, and to the right is the system.

The Design

The operation of the XCPC unit is relatively simple in concept. The solar irradiance incident at the collector aperture is directed to the glass enclosure (tube) by means of the reflecting surfaces, increasing the density of radiant energy over the tube. Figure 11 shows incoming sun angles can vary throughout the day but are always reflected to surface area of the tube.

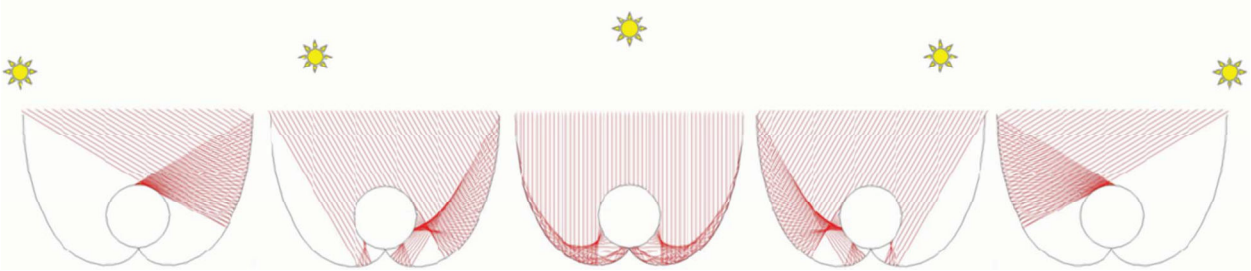

Figure 11: Is a North-South collector showing the incoming sun rays, red lines, changing their incidence angle but the incoming rays are still reflected onto the surface are of the tube.

The concentration ratio of the XCPC varies on whether the design is for the North-South, NS, orientation or East-West, EW. For NS it is1.2 and EW is 1.8. The solar irradiance reflected by the optical component to the evacuated tube is transmitted through the glass envelope and to the absorber element. The absorber element in turn, transfers the energy absorbed to the fluid circulating through the thermal circuit. The absorber element and the thermal circuit are enclosed by the evacuated glass envelope to avoid energy losses by convection, and the number of contact points between the glass envelope and all elements within are reduced in quantity and surface area to minimize heat losses by contact. The flow of energy from the input of the system to the output will be defined by the energy-matter interactions occurring at each material interface. The properties of all the different materials and manufacturing finishes at each one of the interfaces then limits the total amount of energy that be effectively transferred to the working fluid. For instance, the reflector will introduce some energy losses due to material defects, absorption and heterogeneities in the reflective coating, as well as shape distortions of reflectors from ideal geometry. Similarly the glass will absorb and reflect back to the atmosphere some of the incoming radiation. The absorber will reflect some of the incoming radiation and will become an energy emitter due to the temperature at which it operates. The capacity of this element to absorb and transfer most of the incoming energy is a very important defining factor for the XCPC thermal efficiency. Finally, the thermal circuit and working fluid will lose by absorption some of

that transferred by the absorber. In the appendix there is a top and cross sectional view of this design that shows where these materials are relative to the system.

To understand how the collector designs would perform multiple designs were manufactured and tested. Table 2 outlines these variables.

Table 2: Lists the variables for the XCPC design that were experimented.

Collector Designs	Reflector Material	Tube Design
East-West, EW	Alanod	X-tube
North-South, NS	Reflectech	U-tube
		Dewar
		Cross Flow

In analyzing all systems the following variables were chosen as an optimal collector design for the medium temperature application that could be readily manufactured. For the design of the collector both the EW and NS were competitive with each other pending on the geographic region's solar insolation. This is due to the EW design having a higher concentration it can achieve both higher temperatures and higher efficiencies; however, it cannot collect as much diffuse light as the NS design. Reflectech was chosen as an optimal design for the reflector material and the design for a tube came down to the U-tube.

To understand the characterization of this collector the following experimental results have been summarized.

Collector Description

Table 3: North-South, Reflectech, U-tube collector description.

Orientation	North-South
Concentration C_x	1.15
Effective Collector Area A_A	2.076 m^2
Tube Type	U-Tube
Number of Tubes	6
Reflector	Reflectech (95%)

Optical Efficiency

The optical efficiency of the North-South U-Tube with Reflectech collector was measured on 10/23/08 with an average inlet temperature of 30°C and an average ambient temperature of 21°C. The optical efficiency based on an effective irradiance ($G = G_{DNI} + G_{diffuse}/C_x$) was found to be 71.3%. The optical efficiency based on direct normal irradiance ($G = G_{DNI}$) was found to be 88.5%.

Collector Incident Angle Modifier (IAM) and All-Day Performance

The IAM was measured by positioning the collector due south and tilted to be normal to the sun at solar noon (not tracking) and recording the instantaneous thermal collector efficiency at a collector inlet temperature of 140 °C over the course of the day. In this measurement the instantaneous efficiency was based on the direct normal insolation only that was measured with a Normal Incidence Pyrheliometer on a separate tracker. Figure 12 shows the relative drop in efficiency during the day as the sun angle varies between -51° and +59° at 90% relative to normal incidence. The acceptance angle was measured as +/- 55°. The test used to determine the IAM chart and the acceptance angle can also be used to understand the collector's all-day performance. During the test, the collector performed within 90% of the nominal efficiency for roughly 7.3 hours.[vii]

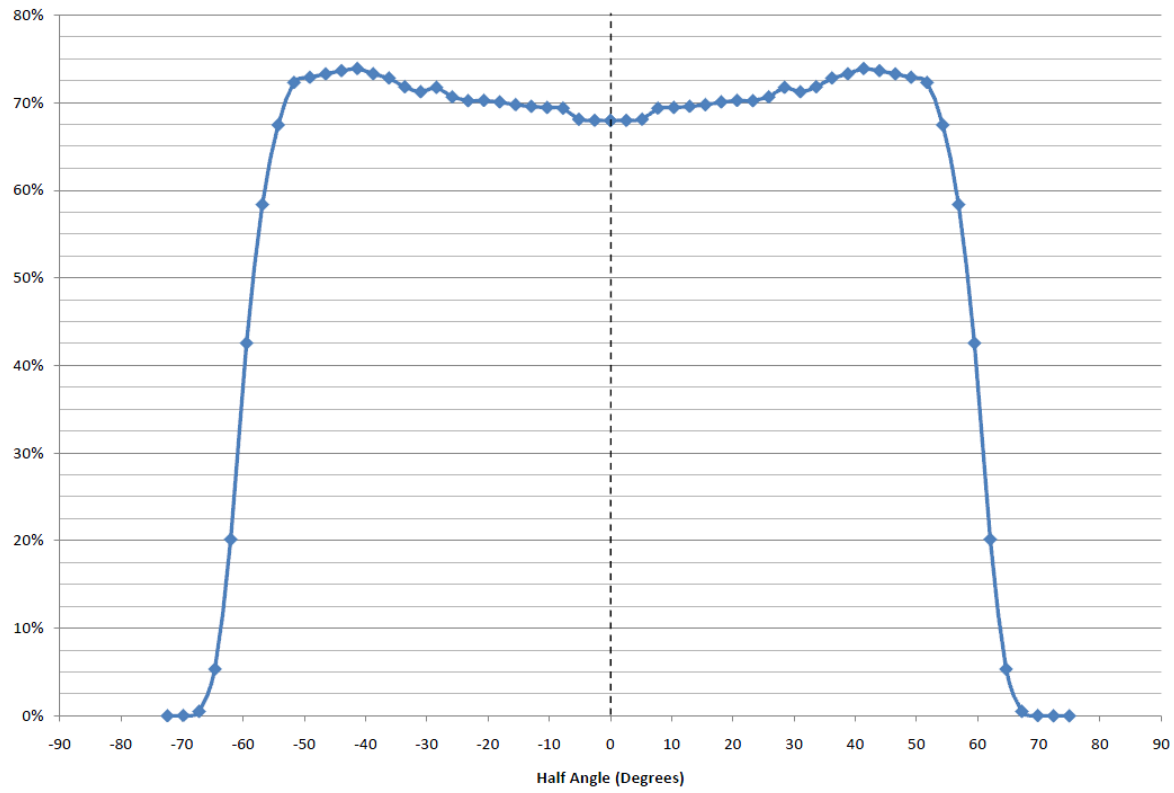

Figure 12: Incidence angle modifier for the NS, Reflectech collector with the U-tube.

Collector thermal efficiency

The efficiency of the XCPC was measured from 10/23/08 – 3/19/09 using the following collector inlet temperatures: 80°C, 100°C, 120°C, 140°C, 160°C, 180°C, and 200°C; and at the following flow rates: 80 g/s, 100 g/s, 120 g/s, 140 g/s, and 160 g/s. The method for how this experiment was tested is in the appendix, as "Testing Method".

The performance characteristics are tabulated in Table 4 and the collector efficiencies are depicted in Figure 13. This assumed an ambient temperature of 25°C and an effective insolation of 1,000 W/m^2 that is captured by the XCPC. The displayed efficiency is based on the effective irradianceG_E.

Table 4: Performance characteristics of the NS, Reflectech, U-tube.

NS RT UT	$G=G_E$
Optical Efficiency η_o	71.3%
Efficiency at 100 °C	61.9%
Efficiency at 200 °C	35.8%
Loss coefficient (1) a_1	0.664 W/m^2-K
Loss coefficient (2) a_2	0.00780 W/m^2-K^2
Overall heat loss coefficient U	2.068 W/m^2-K

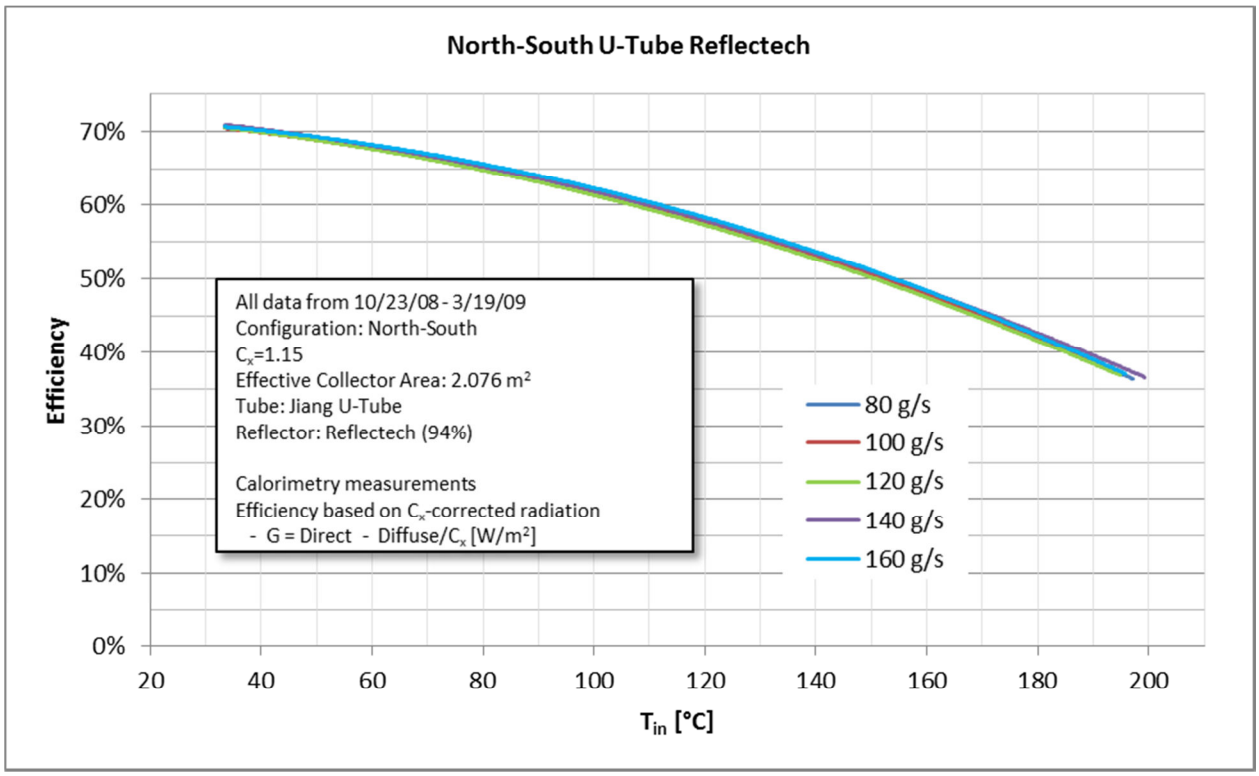

Figure 13: This is a numeric model of the North-South, Reflectech, U-tube efficiency performance for various inlet temperatures and flow rates.

3. Cooling

3.1.1 Motivation for Solar Cooling

Buildings today are responsible for 41% of the primary energy used in the U.S. 30% of that demand is for cooling, and that demand as a whole has grown 300% in the past 50 years.[viii] [ix] Hundreds of power plants were constructed, distribution lines were set and pricing structures were created to control the supply and demand of that electricity. However, it is now becoming difficult to supply. Spiked peak loads occur during brief periods of time, primarily in the summer due to air conditioning systems.[x] [xi] Areas which are densely populated are feeling this effect even greater due to increased air temperatures. These spikes surpass the average peak load by an uneconomical amount. Conventional energy fuel based generation technologies have reached their maturity and are leaving little to no room for significant cost reductions.[xii] Although it is difficult to predict what the price of fuels will be in the future, forecasts have shown that crude oil will be significantly depleted within the next 40 years. Researchers and industries may debate about the rate at which these prices will increase, but it is no argument that they will.[xiii]

It is therefore not valuable for the consumer or the owner to develop larger power plants to meet these rare needs. Thereby blackouts have occurred within the last two decades because power plants cannot provide enough electricity to its consumers during these peaked hours.[xiv] The need to develop an economical solution for cooling, not powered by electricity and to be most effective during the hottest months of the year is now more than ever evident by all. Scientists have produced results that have shown spiked demands for cooling aligns with the solar irradiation peak.[xv] [xvi] Showing, that in some ways solar energy is better suited to space cooling and refrigeration than to space heating. The seasonal variation of solar energy is extremely well suited to the space cooling requirements of buildings. The principal factors affecting the temperature in a building are the average quantity of radiation received and the environmental air temperature. Since the warmest seasons of the year correspond to periods of high insolation, solar energy is the most available when comfort cooling is most needed.[xvii]

Within the past 50 years there has been a lot of research focused on solar powered cooling which has amounted to systems that work but are not cost competitive with traditional fuel

sources. What society needs is an effective cooling machine powered by solar energy that is simple, cheap and efficient for their needs.[xviii] [xix]

3.1.2 Heat driven cooling technologies

The following is an analysis that was done within the CEC grant to understand which application would be best to couple with the XCPC collectors. Various applications such as power generation, water desalination and cooling were taken into consideration, but for this report it will be narrowed to only the evaluation of the heat driven cooling technologies.

There are three major types of thermally active cooling technologies that could work with solar thermal collectors. These include: absorption chillers, adsorption chillers and desiccant systems.

Technology Basics

Absorption Chillers

Briefly, the absorption chiller uses a thermal method for compressing the refrigerant vapor compared to the mechanical method (compressors) used in most electric vapor compression (VC) chillers. The equipment typically uses a working fluid pair such as ammonia-water or lithium bromide-water and the amount of cooling provided can range from a few refrigerant tons for residential applications to more than one thousand tons for commercial applications. The ammonia-water pair has been in limited usage for several years due to the toxicity issues associated with ammonia. In current lithium bromide – water based chillers, water is the refrigerant and aqueous lithium bromide is the absorbent. Water in vapor phase exiting the evaporator is absorbed by the lithium bromide solution in the absorber and this solution is pumped to the generator where heat is used to remove the water from the lithium bromide solution which is subsequently pumped back to the absorber. Several designs use natural gas or other fuel driven methods to provide heat to the generator. Thermal energy obtained from industrial waste heat sources, solar etc. could be used as an alternative method for heating the generator stage and this can provide added benefits of reduced emissions and minimizing energy costs (less fuel consumed). The performance metric for cooling cycles is the coefficient of performance (COP) and enhancing the amount of water produced using the refrigerant vapor from a high stage generator can enhance performance of the absorption chiller. Absorption chillers are thereby offered as single effect, double effect and triple effect chillers with the key

distinction among the three technologies being the number of generators used in the chiller and the temperatures at which they operate. Figure 14, shows a schematic of BROAD's double effect absorption chiller where the heat is generated by burning natural gas.

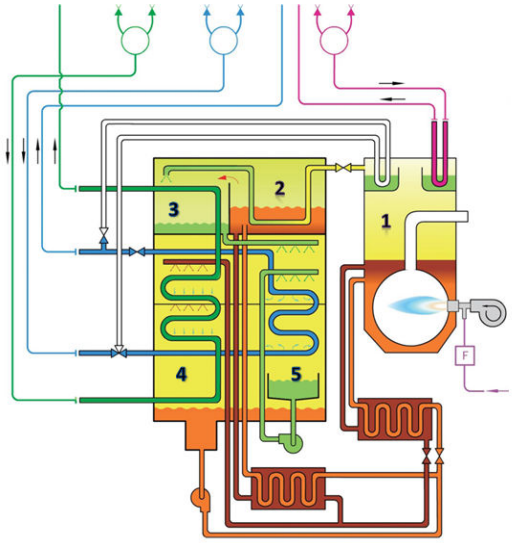

*Orange Liquid is $LiBr + H_2O$
*Green Liquid is H_20

1. High Temperature Generator
2. Low Temperature Generator
3. Condenser
4. Absorber
5. Evaporator

Green Loop is cooling water loop (goes to cooling tower)
Blue Loop is chilled water loop (goes to house AC system)
Purple Loop is hot water loop (goes to house hot water)

Figure 14 BROAD's double effect lithium bromide chiller.

Table 5 below summarizes the generator temperatures and associated COPs typical for the three types of absorption chiller technologies

Table 5 Chiller types with their temperature and COP ranges.

Chiller type	Temperature range	COP range
Single effect	> 85°C	0.5-0.75
Double effect	> 140°C	1.1-1.4
Triple effect	> 175°C	1.5-1.8

Adsorption Chillers

Adsorption chillers have been considered as alternatives for absorption chillers because of their lower operating temperatures and potential advantages such as no corrosion issues, no hazardous leaks etc. (primarily associated with lithium bromide solutions in absorption chillers). A typical working pair in the adsorption chiller is water (refrigerant) and silica gel (adsorbent). In this system there are two adsorbent beds that alternate between a generation stage and an adsorption stage. The generation stage requires heat and this heat can be provided by various renewable and non-renewable sources. The heat source temperatures for these systems can be in the 50 ^{o}C to 90 ^{o}C range and their COPs are usually lower than single effect absorption chillers (close to 0.6). Figure 15, shows a schematic of an adsorption chiller cycle.

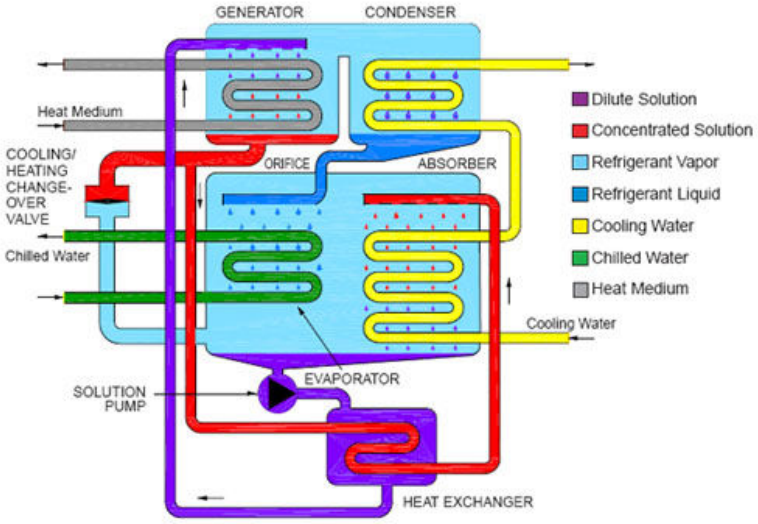

Figure 15: Is a diagram of an adsorption chiller.

Desiccant Cooling

Desiccant cooling is a popular method for humidity control and the basic principle for this technology is the use of a sorbent material to remove moisture from an air stream. The sorbent material can be solid (silica gel, alumina etc.) or liquids (lithium chloride, glycol etc.). Thermal energy is used to regenerate the sorbent material and waste heat or solar could be one of the sources of this thermal energy. Several companies including Carrier, Munters, AIL Research etc. to name a few offer desiccant based humidity control products. Figure 16 shows the liquid and air desiccant systems.

(a) **(b)**

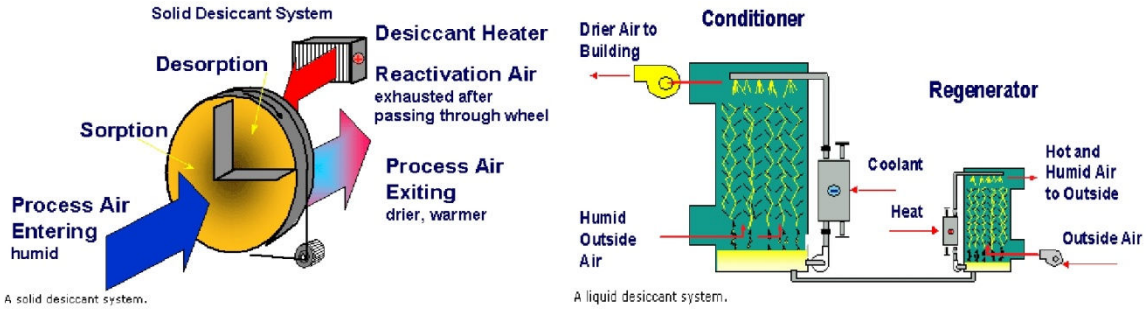

Figure 16: (a) solid and (b) liquid systems.

Technical feasibility and viability

Absorption chillers have been successfully demonstrated for several integrated applications with waste heat. Solar driven absorption chillers were demonstrated by Carrier in the 1970s and additional demonstration work has been performed by Broad and other major HVAC companies as well. All the work done so far suggests a high degree of technical feasibility for a XCPC driven absorption chiller.

Adsorption chillers are present in the Japanese market today and HIJC in the US is marketing a Japanese product. Integration of this device with the XCPC while feasible may not necessarily be the best use of the high quality heat that is obtained from the XCPC.

Most of the desiccant systems can operate with low quality waste heat (as low as 65°C) and while it is technically feasible to interface this with the XCPC, this particular application may not be the best use of the high quality thermal energy obtained from the collectors.

Economic Competitiveness

Economic competitiveness for the integrated XCPC with the absorption chiller system largely depends upon the ability of the XCPC to hit cost targets of <$100/$m^2$.[xx] In doing so the operational expenditures for the system is comparable to absorption chillers operating on natural gas (~4 cents/kWh). Rising fuel costs further enhance the attractiveness of the absorption chiller option.

Adsorption chillers at a COP of 0.6 could compete favorably with single effect chillers from a cost and reliability perspective. Double effect machines with higher COPs (more cooling capacity per unit of thermal energy input) are economically more competitive than current adsorption chillers.

The desiccant systems can be expensive products and the economic competitiveness of an integrated system will primarily depend on making the collector prices competitive with the current method used for regenerating the sorbent material. Since the quality of heat required to regenerate sorbent materials in desiccant systems is quite low, there are cheaper off the shelf low temperature thermal collectors that may be a better choice for an integrated solution.

3.1.3 Market potential

Absorption chillers in the US market compete with electrically driven vapor compression chillers and cheap electricity prices have prevented their mass adoption in this market. The VC systems have COP's in the range of: 3-4. This implies that the higher the COP of the TAT chiller, the greater the chance it has of capturing the market share, particularly when consumer electricity prices are on the rise (California especially).

Adsorption chillers could compete well as cooling technology offered in markets where low grade waste heat (<95°C) is readily available. The low COP of these devices makes their ability to displace vapor compression chillers even more difficult than double effect absorption chillers.

Market potential for desiccant based dehumidifiers was projected to be $300 M in North America in 2006[xxi]. The market share for solar driven desiccant dehumidifiers is not significant and it is unclear if the XCPC would offer any benefit in terms of penetrating into this market.

3.1.4 Time to commercialization

Single and double effect chillers have been available in the commercial space for several years,

and Kawasaki has recently introduced triple effect chillers in the Asian market. This implies that successful commercial development of the XCPC in two years could lead to integrated chiller product offerings within five years.

Adsorption chillers are available in the market today and while an XCPC integrated adsorption chiller could be commercialized, the current technology with its lower temperature of operation is not the ideal fit for the XCPC collector. Future generation adsorption chillers with higher COPs and higher temperature operations could be better fits; however, no such device is available commercially.

Several desiccant cooling system products exist today and it is conceivable that any potential solar integrated desiccant product can be developed in a span of 1-2 years.

3.1.5 Other considerations

Potential legal and institutional barriers for an integrated XCPC-chiller product will depend primarily on the type of working fluid used in the XCPC and the ability to safely install the collectors and transport this fluid to the chiller. Corrosion issues and refrigerant leaks are the main concerns for absorption chiller systems from a legal and institutional perspective and technology maturity coupled with market adoption dictates how these barriers are overcome. The chiller systems themselves are commercial products and there should be no major institutional barriers for single and double effect chillers. Triple effect chillers on the other hand might require additional qualification before they can penetrate the US market primarily because of the lower technology maturity of these systems

Solid desiccant systems are the most prevalent in the market today; and, there are almost no legal or institutional barriers preventing the adoption of this technology. However, working fluid in the solar collector, and the need to pump corrosive fluids in liquid desiccant systems could be of concern from an institutional stand point.

There seem to be no major legal or institutional barriers that might prevent the current water-silica gel based adsorption chillers from entering the market. Attempts to improve the COP might require moving to refrigerants such as ammonia and this may introduce barriers primarily due to concerns about toxicity of the refrigerant.

3.2 Conclusions

Based on the assessment in this report it was recommended that an ideal near term focus for a future project would be XCPC integration with absorption cooling. Specifically, the double effect absorption chiller, with it being readily manufactured, was the cooling technology chosen.

4. Solar Cooling System

The first item purchased and the foundation of the system was the chiller. It is a double effect lithium bromide, LiBr, 6.6 United States refrigeration ton, USRT system. Figure is a picture of me with the chiller. The chiller had the following input requirements: 21 thermal kilowatts, at an inlet temperature of 175°C with an outlet temperature of 160°C. The company would only warranty the product if a glycol water mixture was used, meaning that the fluid loop inlet to the chiller would have to be pressurized. The following is a description of how the system works.

Figure 17: BROADS double effect 6.6 Lithium Bromide absorption chiller, and me. Circa 2009.

4.1 Chiller

4.1.1 How it works

Refer to Figure 14 for a schematic of the chiller, and the numbers go along with this process.

1. Solution Pump – A dilute lithium bromide solution is collected in the bottom of the absorber shell. From here, a hermetic solution pump moves the solution through a shell and tube heat exchanger for preheating.

2. Generator – After exiting the heat exchanger, the dilute solution moves into the upper shell. The solution surrounds a bundle of tubes which carries either steam or hot water. The steam or hot water transfers heat into the pool of dilute lithium bromide solution. The solution boils, sending refrigerant vapor upward into the condenser and leaving behind concentrated lithium bromide. The concentrated lithium bromide solution moves down to the heat exchanger, where it is cooled by the weak solution being pumped up to the generator.

3. Condenser – The refrigerant vapor migrates through mist eliminators to the condenser tube bundle. The refrigerant vapor condenses on the tubes. The heat is removed by the cooling water which moves through the inside of the tubes. As the refrigerant condenses, it collects in a trough at the bottom of the condenser.

4. Evaporator – The refrigerant liquid moves from the condenser in the upper shell down to the evaporator in the lower shell and is sprayed over the evaporator tube bundle. Due to the extreme vacuum of the lower shell [6 mm Hg (0.8 kPa) absolute pressure], the refrigerant liquid boils at approximately 3.9°C, creating the refrigerant effect. (This vacuum is created by hygroscopic action - the strong affinity lithium bromide has for water - in the Absorber directly below.)

5. Absorber – As the refrigerant vapor migrates to the absorber from the evaporator, the strong lithium bromide solution from the generator is sprayed over the top of the absorber tube bundle. The strong lithium bromide solution actually pulls the refrigerant vapor into solution, creating the extreme vacuum in the evaporator. The absorption of the refrigerant vapor into the lithium bromide solution also generates heat which is removed by the cooling water. The now dilute lithium bromide solution collects in the bottom of the lower shell, where it flows down to the solution pump. The chilling cycle is now completed and the process begins once again.

4.1.2 Control Logic

The high temperature generator, HTG, is in the structure described as the following: The upper part of the HTG is a coiled pipe in which the solar thermal medium is circulated. The LiBr solution is sprayed onto the coiled pipes. Right beneath are the smoke pipes of the natural gas burner, in which the 1100°C hot air from natural gas burner is run through. Figure 18 is a depiction of what the HTG looks like, and how it is set up. At the bottom of the HTG is a thermo sensor for the HTG. The highest temperature of HTG is 155°C, and can be manually set to be lower. Temperatures above this however, will make the LiBr in the HTG start to crystalize. The normal operational temperature for the HTG to start working is 140°C.

Figure 18: Is a depiction of what the HTG looks like, with a natural gas burner below the tank and wrapped coils that have the hot solar thermal fluid flowing through, represented by the red arrow.

If the temperature of the solar thermal medium is below 145°C, then there is really no reason for turning on the natural gas, because the 1100° C of natural gas burner is way above the solar heat source, and the natural gas will be used to heat up the solar loop.

If, the temperature of the solar loop is above 145°C, it means that we can entrust the solar heat source to heat up the HTG. If the HTG is too big of a load for the solar loop, the inlet temperature of the solar loop will drop, and the system will start to switch back to natural gas.

If the solar loop is so powerful that the HTG begins to go above 155°C, then the machine will turn down the solar valve to lower percentages, such as 75%(stage 3), 50%(stage 2) etc.

To conclude, the chiller does not go back and forth between using natural gas and using solar thermal energy. There is a solar valve that limits the solar heat source from overheating the HTG. The temperature range for HTG is too narrow, and the distance between solar pipes and burner is too close to each other. It is difficult to design it in a way to use the solar heat source to first elevate the HTG for a small temperature and then to use natural gas to lift the temperature to

meet the HTG requirement. Therefore, the system is either programmed to run on natural gas or on solar thermal energy before it will switch pending on the temperature range. Table 6 demonstrates this algorithm. T1 will be the HTG temperature, T2 will be the solar inlet temperature to the chiller. In the appendix is a more detailed table.

Table 6: Temperature algorithm for the BROAD chiller.

HTG Temperature (T1)	Condition to Open Solar Valve and turn off Natural Gas	Condition to close the solar valve and switch to Natural Gas
$145 \leq °C$	$T2 > T1 + 2°C$	$T2 \leq T1 + 1°C$
$130°C \leq T1 < 145°C$	$T2 > T1 + 4°C$	$T2 \leq T1 + 2°C$

4.2 Collector

4.2.1 Design

EW vs. NS from an Energy Perspective

When designing non-tracking compound parabolic concentrators, CPC, solar thermal systems the first decision to be made is whether you want your collectors to be aligned in the North-south or East-West direction. The physical difference being in which direction the evacuated tubes are aligned, and the optical difference being that the EW design allows for a higher concentration while the NS accepts more diffuse light.

There are multiple factors that directly impact the two designs at a strictly technical level, such as: The concentration of the collectors, operational temperature, ambient temperature, and the percentage of diffuse irradiation specific to the geographic region.

For lower temperatures the NS design has a higher efficiency than that of the EW. The primary reason for the NS being more efficient at lower temperatures is due to its optical efficiency being greater than that of the EW. Analyzing the efficiency equation, Equation 1, one can observe that at lower temperatures the loss term in the efficiency equation are low, and since the optical efficiency is higher for the NS the NS's overall efficiency is greater. Thereby, at lower temperatures, regardless of the diffuse, the NS design is more efficient.

Table 7 shows the experimental results compared for both the NS and EW design, with Reflectech and the U-tube.

For higher temperatures, the EW is the more efficient design, depending on your level of diffuse irradiation. The primary reason for this is the surface area of the absorber area. At higher temperatures the absorber will want to radiate heat back into the environment; however, since the EW has less surface area than the NS, and the EW has a higher concentration than the NS, the ratio of heat gained vs. heat loss is higher for EW than that of NS. The question then becomes, what is considered to be a low and high temperature?

Methodology

On a strictly fundamental level, we want to know which design will provide us with the most energy. To do this, one can calculate a breakeven analysis of the power for the EW vs. NS. This is done by taking into account the power and efficiencies of both designs, as seen below:[xxii]

$$\eta_{EW} * P_{EW} = \eta_{NS} * P_{NS} \quad \text{Equation 1}$$

Power is calculated by:

- Assuming that the area is $1m^2$
- Z is a variable for the total solar irradiation

$$\Phi = \left(\frac{1-C}{C*(I_d)} + z\right) \quad \text{Equation 2}$$

$$Power = \Phi * Area * \eta \quad \text{Equation 3}$$

Efficiency is calculated by:

$$(\eta = \eta_o - a_1 * T^* - a_2 * \Phi * T^{*2}) \quad \text{Equation 4}$$

Reduced Temperature[1]:

$$T^* = \frac{T_{in}-T_{amb}}{\Phi} \quad \text{Equation 5}$$

The inputs are:

- Ambient temperatures
- Concentrations

[1] This is not actually a temperature, it has units of $\left(\frac{Km^2}{W}\right)$

- Efficiencies

Table 7: NS vs EW characterization.

	NS RT UT	EW RT UT
η_o	71.30%	64.40%
$\eta(100℃)$	61.90%	58.10%
$\eta(200℃)$	35.80%	41.70%
a_1	0.664	0.488
a_2	0.0078	0.00463
U	2.068	1.321

The out-put will be the breakeven point at every diffuse level, and at any inlet temperature.

Solving for its zeros determines the breakeven point.

Equation to analyze $\boldsymbol{\eta_{EW} * P_{EW} = \eta_{NS} * P_{NS}}$ Equation 6:

$$\eta_{EW} * P_{EW} = \eta_{NS} * P_{NS} \quad \text{Equation 6}$$

$$\eta_{EW} * \left(\frac{1-C_{EW}}{C_{EW}} * I_d + 1000\right) = \eta_{NS} * \left(\frac{1-C_{NS}}{C_{NS}} * I_d + 1000\right) \text{Equation 7}$$

$$\left(\eta_{o\,EW} - a_{1EW} * \frac{T_i - T_{amb}}{1000} - a_{2EW} * \left(\frac{1 - C_{EW}}{C_{EW}} * I_d + 1000\right) * \left(\frac{T_i - T_{amb}}{1000}\right)^2\right) * \left(\frac{1 - C_{EW}}{C_{EW}} * I_d + 1000\right) = \left(\eta_{o\,NS} - a_{1NS} * \left(\frac{T_i - T_{amb}}{1000}\right) - a_{2NS} * \left(\frac{1 - C_{NS}}{C_{NS}} * I_d + 1000\right) * \left(\frac{T_i - T_{amb}}{1000}\right)^2\right) * \left(\frac{1 - C_{NS}}{C_{NS}} * I_d + 1000\right)$$

Results

The results show that for any temperature one can evaluate what their given ambient and inlet temperatures are, coupled with the percent diffuse, i.e.: 10% diffuse is 100 watts on these graphs (Based off of $1000\,\frac{W}{m^2}$), and determine whether they are below, above or at the breakeven point. The following three graphs were produced using the breakeven analysis Matlab codes outlined in the appendix. The analysis was done for three different ambient temperatures: 25, 35 and 45° C.

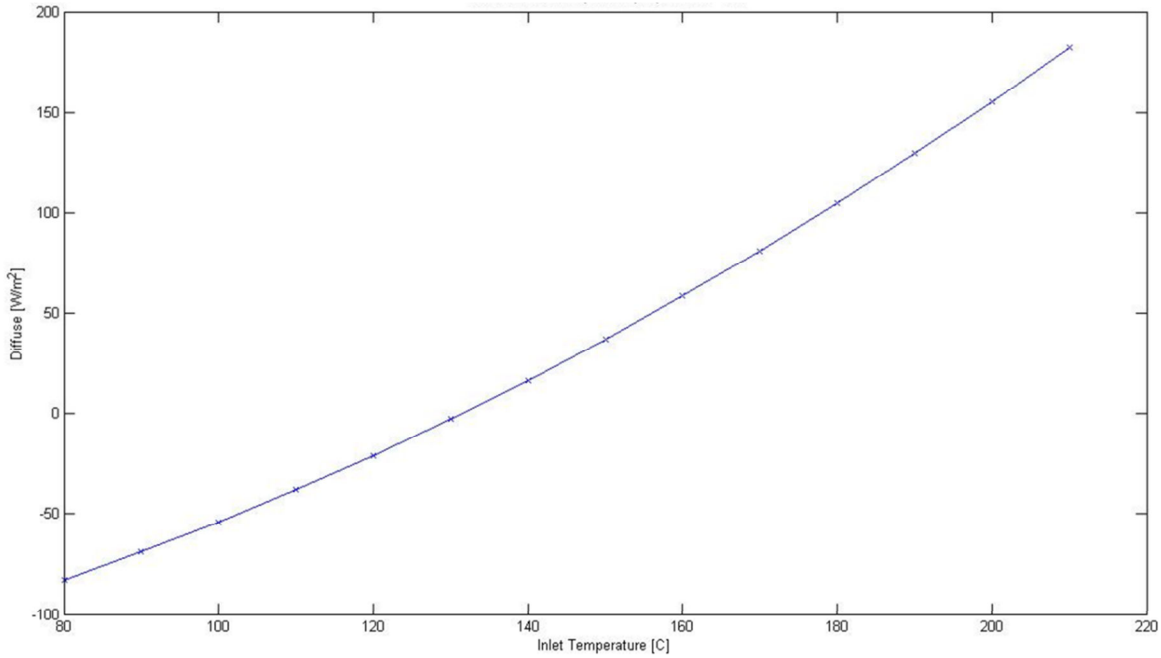

Figure 19 represents the 35°C value. The 25 and 45°C were extremely similar to the 35°C.

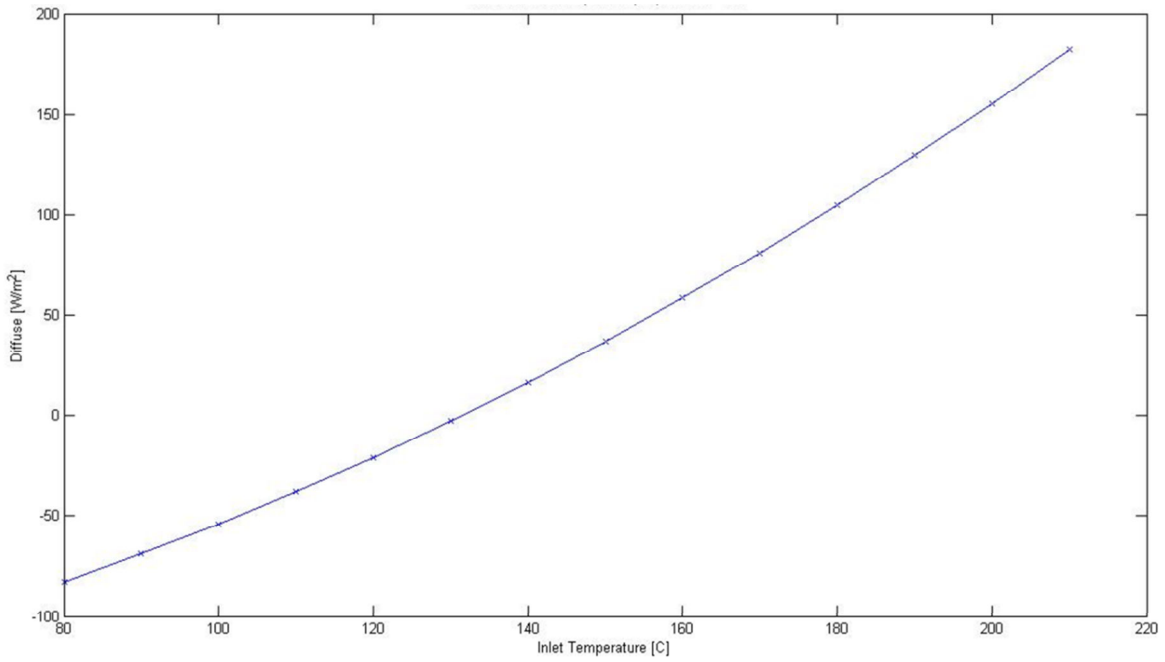

Figure 19: Break even analysis for the NS collector, with Reflectech and the U-tube, with an ambient temperature of 35°C.

Discussion

At any inlet temperature, relatively low inlet temperatures, where the diffuse level shown is negative, unreal, the design is automatically NS. If below the breakeven point, that means that either design will suffice for the given conditions; thereby, EW would be the chosen design since has a higher concentration. If above the breakeven point this means that the system will need to capture more diffuse and NS is the optimal design. If right at, or near the breakeven point then from an energy perspective, the designs are even.

For the UCM Solar Cooling Project, the diffuse level for Merced, CA is approximately 10%, with an inlet temperature of 180℃, and ambient temperature, during the summer, of approximately 35℃. According to the breakeven analysis we were right at the breakeven point. This can be seen from Figure 19. From an energy perspective, both designs are even. In order to choose which design would be optimal, further analysis taking in other variables is necessary in order to truly conclude the holistic optimal design.

EW vs. NS Beyond Energy

Manufacturability:

In terms of physical structure and manufacturing the biggest difference between the EW and the NS is the orientation of the manifolds. For the EW the manifolds are aligned in a vertical position, while the NS manifolds are aligned horizontally. Having a solar thermal system connecting multiple manifolds proves to be very difficult when trying to connect the EW manifolds due to their angles. There would be a lot of elbows and it would be difficult not only to design, but also to construct. On the other hand, the NS manifold connections are easy since they are all on the same plane.

Maintenance

Weather and the environment are the largest issues at hand in dealing with the differences between the NS and EW. Rain is a large issue in terms of CPC. The EW design being aligned horizontally captures water and it is then difficult to remove from the collectors. This also goes for dirt, leaves and other particulates in the air. Since the NS is aligned vertically, one can drill holes at the bottom of the collector to allow rain and debris to drain at the bottom .

Finances

In comparing the EW vs. NS, the same amount of power per system, the EW has fewer tubes than that of the NS; thereby, in terms of tubes, the EW is cheaper than that of NS. When doing a financial comparison of both systems overall, then one must consider the different options for producing the collectors themselves, and the cost of their respective materials.

Choice Table

In choosing what the optimal design choice is, it is critical to understand the priorities associated with the different factors that influence which design is best for you. Below is a table, filled out with the UCM Solar Cooling Project data, and this table interprets the priorities vs. what the design is capable of.

The first step is to associate your priorities levels. For the UCM Solar cooling project, being a University finances are our highest priority is research, therefore, energy was allotted the top priority. Following is our ability to manufacture and construct the system, then the energy of the system and lastly is the maintenance of the system. (Since we are a University, our priorities will be different than that of a business. Whereas we will always have students to clean the system and help maintain the system, a business may not; therefore, different priority levels would be assigned.) Lastly are finances, which, for both systems, a raw cost may be equivalent, but further analysis would need to be conducted. (For now, an equivalent score has been given.)

Next, is scoring each category: Energy, Manufacturing, Maintenance and Finances of the EW vs. NS. For the UCM Solar Thermal, the EW vs. NS in terms of energy was a break-even. Therefore, each design received a score of 1. In terms of manufacturing, the manifold issue did present a problem to us whereas the NS structure and manifolds are feasible, therefore, NS receives 1 and EW receives 0. In terms of maintenance, the NS is preferred every time; and, financially both the EW and NS received an equivalent score. This is due partly to the fact that although there would be fewer tubes, the cost for the collectors may have been more for the EW vs. the NS; therefore, financially the designs were scored as equivalent.

The score is calculated by the following equation:

$$\sum Piority(Energy) * Score(Energy) + Priority(Manufacturing) * Score(Manufacturing) + \cdots \text{Equation 8}$$

Table 8: Priority and scores for the EW and NS collector designs.

Factor	Priority
Energy	40%
Manufacturing	30%
Maintenance	10%
Finances	20%

	Energy	Manufacturing	Maintenance	Finances	Score
EW	1	0	0	1	0.6
NS	1	1	1	1	1

For the UCM Solar Cooling Project the final score shown is that the NS design, after considering all factors associated with the realistic system, outperforms the EW design.

4.2.2 Size

The chiller requires 21 thermal kilowatts at an inlet temperature of 175°C. According to Figure 13 the collectors should be operating at an approximate efficiency of 40%. Considering that each individual collector produces approximately 150 watts, and expecting a 10% loss from the collectors to the chiller, the collectors would need to produce 23 kilowatts of thermal energy. This would be approximately 160 individual units.

4.2.3 Configuration

Tilt Angle of Collectors

Since the solar thermal system will be in high demand during the summer, we want to favor the summer insolation. This can be done by orientating the collectors 14° West of South, to be in the direction of true North-South, not magnetic; and by calculating the declination angle for a hot summer day and using that data to derive the proper tilt angle for the collectors.

Day Chosen: July 23rd, 2009

Location: Merced, Ca

$\delta = Declination\ Angle$

$n = Day\ of\ year\ number$

$\beta_n = Zenith\ angle\ between\ the\ sun\ and\ collector\ plane$

$\beta = Zenith\ angle\ between\ ground\ and\ collector\ plane$

$$\delta_{July} = 23.45 \sin\left[\left(\frac{360}{365}\right)(n - 81)\right] => (n = 204) = 20° \text{Equation 9}$$

$$\beta_n = 90 - L - \delta = 90° - 37° - 20° = 73° \text{Equation 10}$$

$$Tilt\ Angle = 90° - \beta_n = 90° - 73° = 17° \text{Equation 11}$$

For practical purposes the collectors will be placed at a 20° tilt from the ground.

Layout of Collector System

There are two questions to be answered at this time, how many troughs per collector and in which configuration should they be placed in?

To answer these questions a thorough pressure drop analysis is needed. There are many factors that are to be considered for the system, such as fluid type, size of the piping, material selections for the plumbing, the flow rate of the fluid and all of these amounts to a pressure drop in the system which defines not only a pump size but also a configuration. To account for these factors a matlab program was developed which has the following structure, where the black lettering is the title of the m-file in the appendix.

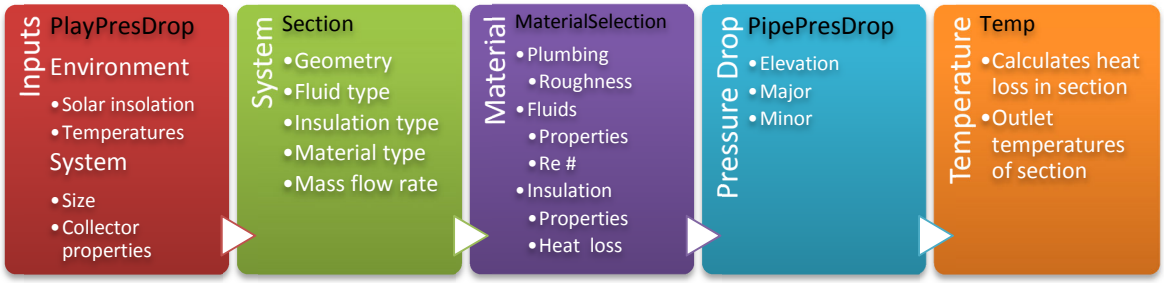

The pressure drop analysis begins with the input file where the user inputs the environmental conditions of their geographic region, operational temperature, etc. and also the system size, ie: how many individual troughs, how many in parallel vs. series, and all of the properties of each trough. Then it begins to process the next file, Section. Because the plumbing was going to be complicated and there was going to be various elements to the structure of the system it was

decided best to split the system into different sections so as to simplify the calculations for the pressure. Another benefit of splitting the system into different sections is that it would allow the reconfiguration of the system easily so to analyze multiple configurations and see how the pressure drops would change. The basic sections were: pipe, manifold, tube. These variables were inputs to the material selection which held all of the properties for any fluid that would be used in the solar cooling system, all pipe material and all insulation material. These were then inputs to the pipe pressure drop which calculated the pipe pressure drop due to elevation, major and minor losses. The Material properties were also input to the temperature file which calculated the output temperature of the section and this was then used as the input temperature to the next file, and the pressure drops were added from each section to amount to the total pressure drop and final temperature of the system.

This code was used to analyze various configurations and to which design would be optimal for our system. The following section is the results of that analysis followed by a detailed analysis of the function files for the pressure drop code so as to understand how the calculations were formulated.

The Configuration

The following configurations were plausible designs for our system that we tested.

1. Tubes per collector (# of Collectors)
    a. 5 (32)
    b. 10 (16)
    c. 16 (10)
    d. 40 (4)
2. Collector Configuration
    a. All in series (1X)
    b. 2 banks in parallel (2X)

c. 4 banks in parallel (4X)

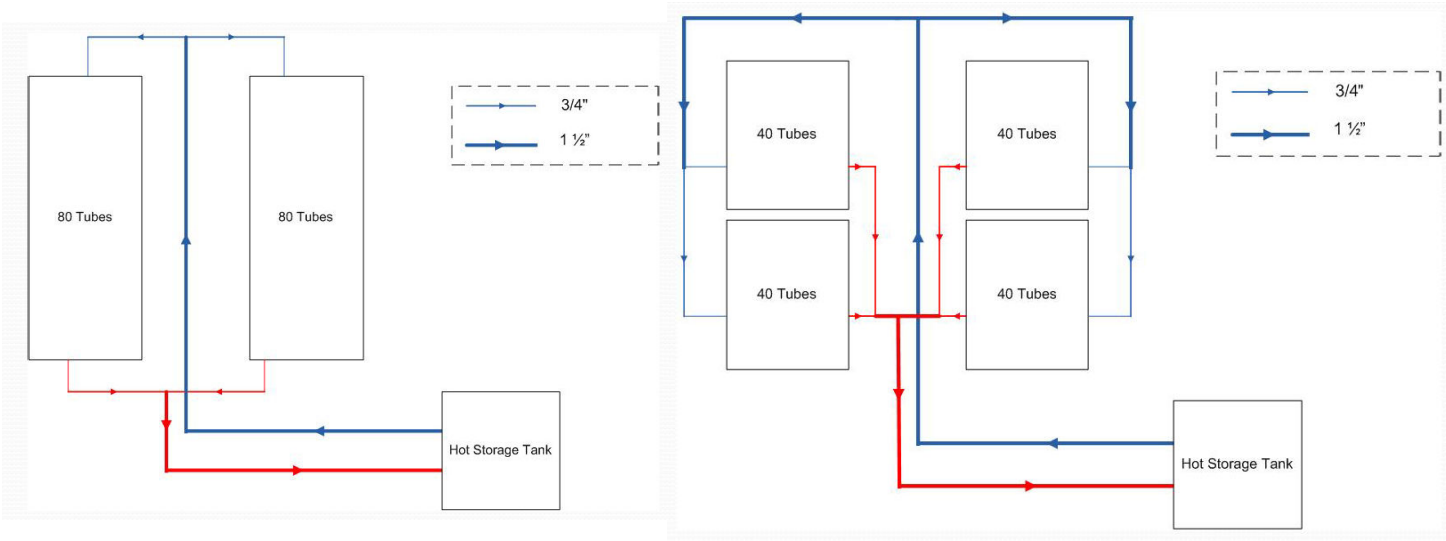

Figure 20: The diagram to the left is a depiction of 2 banks in parallel, each bank is a collector of 80 tubes in parallel. The diagram to the right is two banks in parallel, each with two collectors that run in parallel as well, with 40 tubes per collector.

The critical factors are the mass flow rate through each tube, pressure drop for the whole system and the volumetric flow rate for the system. Figure 21and Figure 22 shows the mass flow through each tube and the pressure drop of the collector systems for each of the top four configurations.

The initial goal for the mass flow rate through each tube was 11-14 g/s. This value came from previous research that has shown that for the U-tube, NS, system this is an optimal mass flow rate through the tube. There are three configurations that met that goal, the 40(4x1) at a delta T=15, the 10(4x4) at delta T=10, and the 40(2x2) at delta T=10.Looking at the pressure drops of the systems for the plausible mass flow rate conditions for all pressure drops were plausible for a pump that could be found on the market.

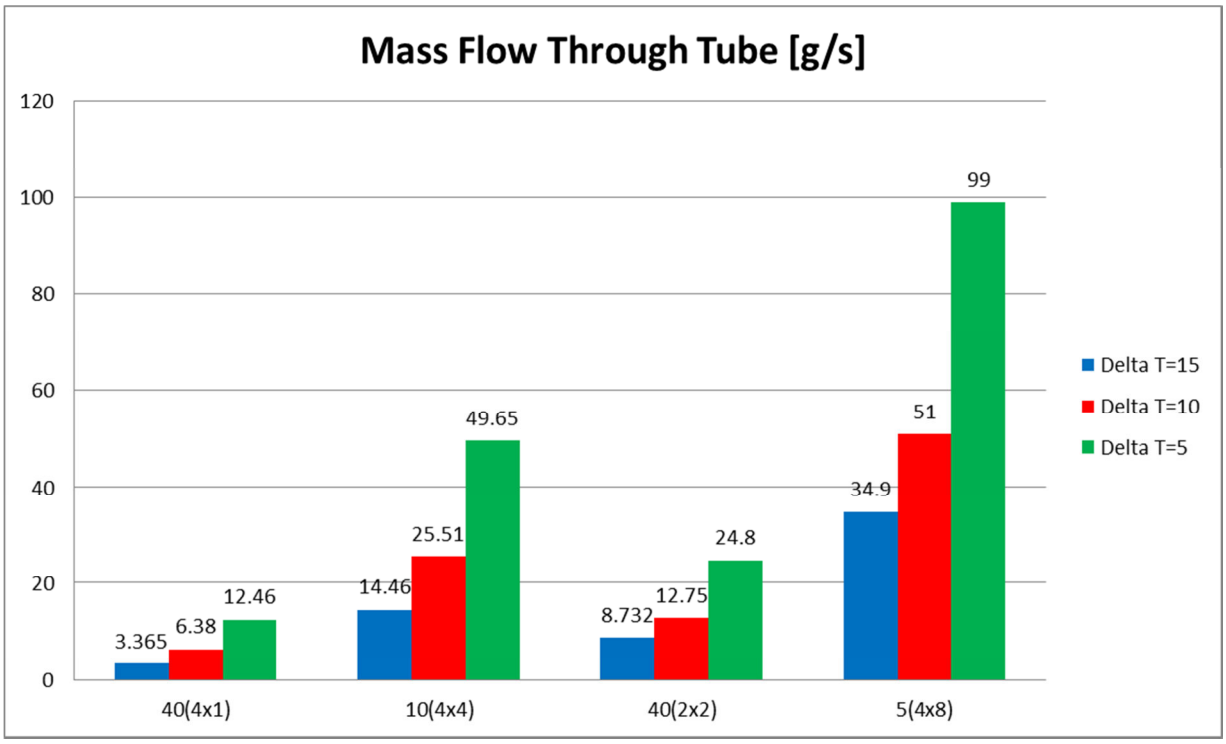

Figure 21: Mass flow through each tube for various configurations.

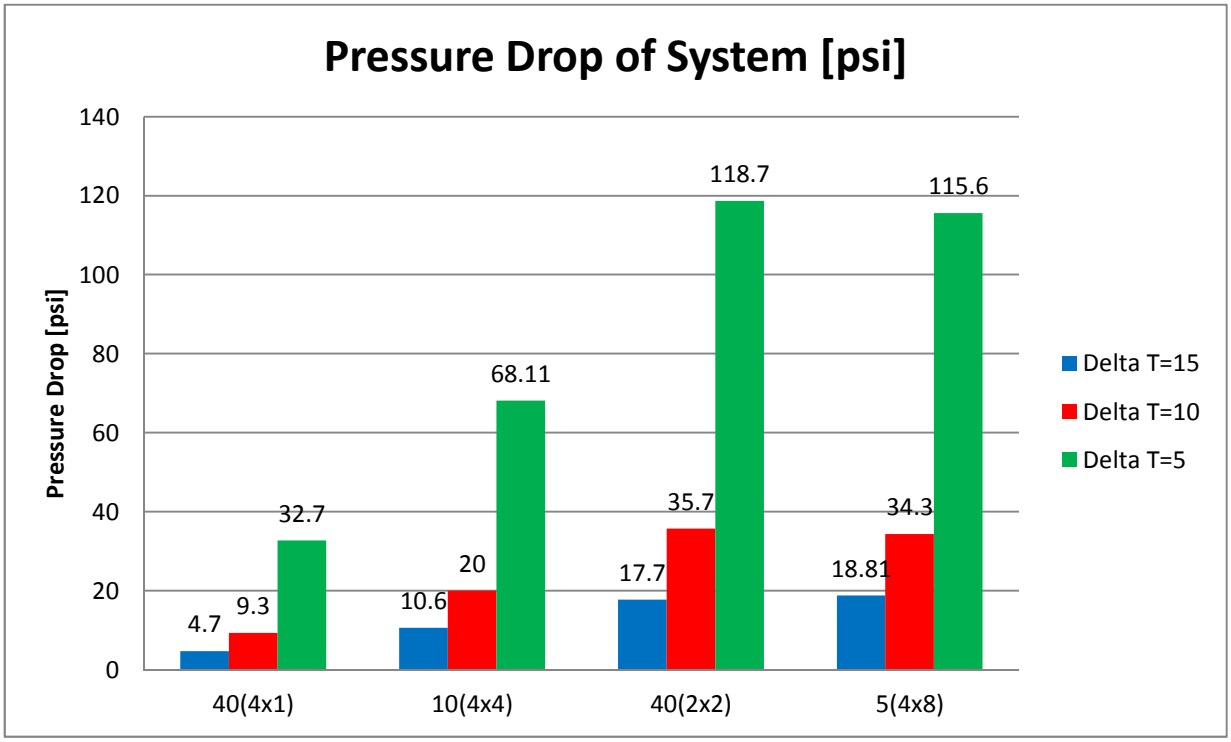

Figure 22: Pressure drop for various configurations of the collector systems.

Two very important variables that then came into play were the amount of material as well as the delta T. From previous experiments it was best to look for a ΔT of approximately 6°C per tube which results in the 40(2x2) configuration and the 10(4x4) configuration. The amount of material needed and installation costs, land area, etc. for the 40(2x2) was less than the 10(4x4) and thus, the 40(2x2 configuration was chosen.

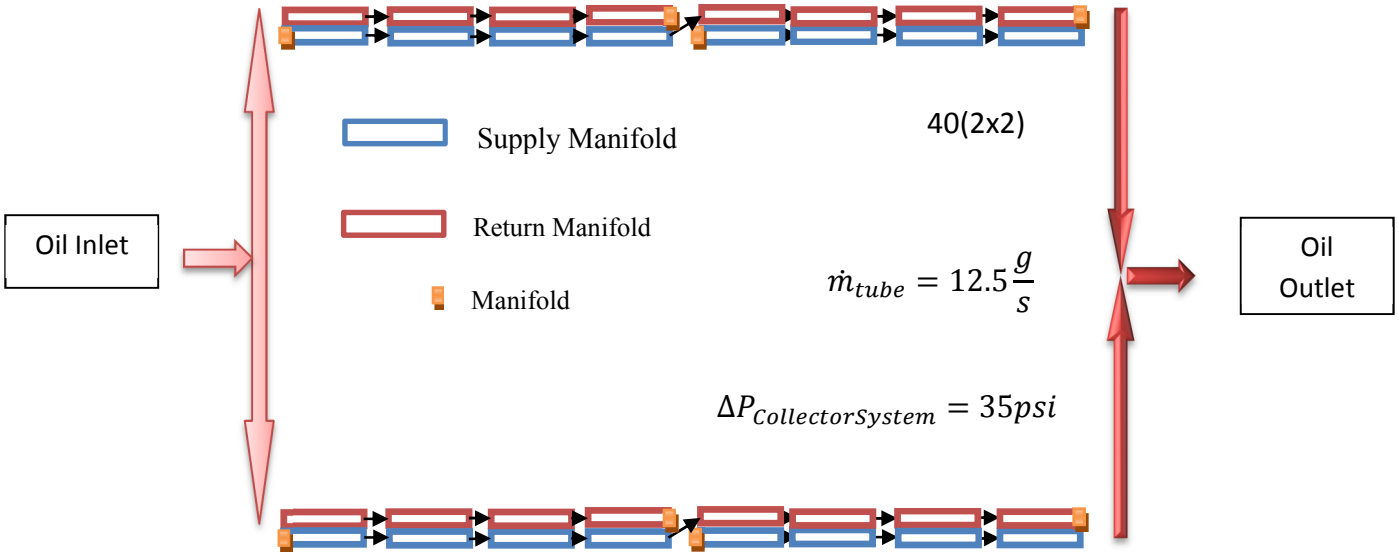

Figure 23: The selected collector system.

Pressure Drop[xxiii]

A typical pipe system usually consists of various lengths of straight pipe interspersed with various types of components (valves, elbows, etc.). The pressure drop, ΔP for the pipe system consists of the elevation change, termed ΔP_e, head loss due to viscous effects in the straight pipes, termed *major loss,* and denoted ΔP_{major}, and the head loss in the various pipe components termed the *minor loss* denoted ΔP_{minor},

$$\Delta P = \Delta P_e + \Delta P_{major} + \Delta P_{minor} \quad \text{Equation 12}$$

Elevation Losses

To begin, I took the energy equation for incompressible, steady flow between two locations:

$$\frac{p_1}{\rho g} + \alpha_1\left(\frac{V_1^2}{2g}\right) + z_1 = \frac{p_2}{\rho g} + \alpha_2\left(\frac{V_2^2}{2g}\right) + z_2 + h_f \quad \text{Equation 13}$$

$$\Delta P_e = (p_2 - p_1) = \rho g\left(\frac{(\alpha_1 V_1^2 - \alpha_2 V_2^2)}{2g} + (z_1 - z_2) - h_f\right) \quad \text{Equation 14}$$

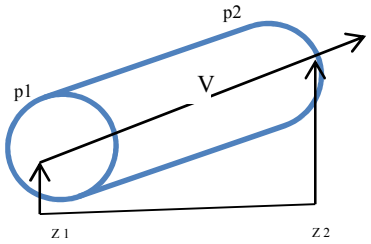

Figure 24: Vertical pipe flow to show elevation losses.

Where ρ is the density of the fluid, α is the kinetic energy coefficients, and was taken as 1 for a fully develop flow and 2 for turbulent; V is velocity, g is gravity, z represents the height from ground, and h_f is the head loss of the pipe. The following calculation is for the head loss.

$$h_f = f\left(\frac{L}{D}\right)\left(\frac{V^2}{2g}\right) \quad \text{Equation 15}$$

L represents the length of the pipe, D is the diameter, V is the velocity, g gravity and f is the friction factor. To calculate the friction factor one must first determine if the flow is laminar, having only one component of velocity, or turbulent, random components of velocity normal to flow. To determine whether the flow is laminar or turbulent one calculates the Reynolds Number below and if the number is below 2100 it is laminar, above 4000 turbulent, and if it's in-between that is transitional and I chose those properties to be turbulent. Re_D Represents the Reynolds number for a pipe of diameter D, and is calculated by the following equation, where μ is the dynamic viscosity. This is a dimensionless number.

$$Re_D = \frac{\rho V D}{\mu} \quad \text{Equation 16}$$

The functions for the friction factor are listed below for both laminar and turbulent flows.

$$f_{laminar} = \frac{64}{Re_D} \quad \text{Equation 17}$$

$$f_{turbulent} = \left(-1.8 \log \left(\left(\frac{6.9}{Re_D} \right) + \left(\frac{\frac{\epsilon}{d}}{3.7} \right)^{1.11} \right) \right)^{-2} \quad \text{Equation 18}$$

Major Losses

To begin, I took the energy equation for incompressible, steady flow between two locations:

$$\frac{p_1}{\rho g} + \alpha_1 \left(\frac{V_1^2}{2g} \right) + z_1 = \frac{p_2}{\rho g} + \alpha_2 \left(\frac{V_2^2}{2g} \right) + z_2 + h_f \quad \text{Equation 19}$$

With the assumption of a constant diameter thereby a constant velocity, $V_1 = V_2 = V$, and horizontal $z_1 = z_2$, fully developed flow, $\alpha_1 = \alpha_2$, the equation for the pressure difference due to major losses is:

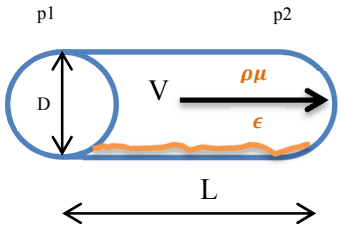

Figure 25: Horizontal pipe flow.

$$\Delta P_{major} = h_f = f \left(\frac{L}{D} \right) \left(\frac{V^2}{2g} \right) \quad \text{Equation 20}$$

Minor Losses

Losses due to pipe system components are given in terms of loss coefficients. The loss coefficients, are represented by K_L and each component has it's own value, ie: a 90° flanged bend, as shown in figure 13, has a $K_L = 0.3$. The pressure drop due to minor losses can then be calculated as:

$$\Delta P_{minor} = K_L \left(\frac{V^2}{2g} \right) \quad \text{Equation 21}$$

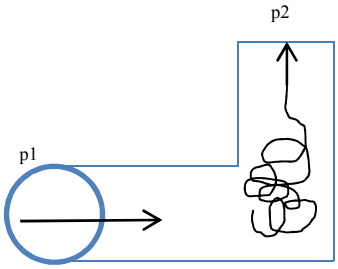

Figure 26: Pipe flow through a 90° bend, showing minor losses.

Temperature

It is important to understand the temperature of the system, that is divided into two parts: an insulated pipe and the evacuated tube. The following details are how formulations were developed.

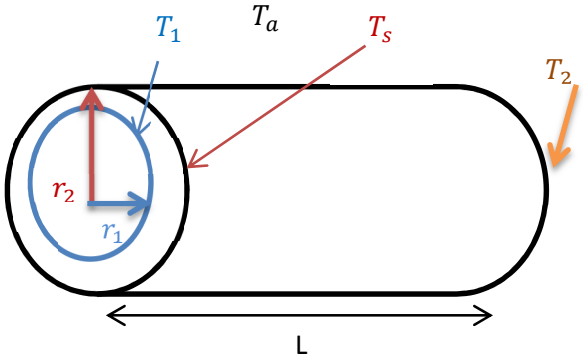

Figure 27: A cylindrical shell showing an elemental control volume for application of energy conservation principle.

Insulated Pipe:

Figure 27 shows an insulated pipe with a fluid flowing through. It has an inner radius of r_1 and an outer radius of r_2, with a length of L. T_1 represents the inlet fluid temperature, T_s is the surface temperature of the insulated pipe, and Ta is the ambient temperature. T_2 Is the outlet temperature of the fluid which is the unknown to be solved. For this analysis conduction and convection are the primary source of heat loss and so the energy analysis will be limited to these.

Conduction

Fourier's law of heat conduction, which states that in a homogenous substance, the local heat flux is proportional to the negative of the local temperature gradient:

$$\frac{\dot{Q}}{A} = q_{conduction} \qquad q_{conduction}\ \alpha\ \frac{dT}{dx} \qquad \text{Equation 22}$$

Where is the heat flux, or heat flow per unit area perpendicular to the flow direction$\left[\frac{W}{m^2}\right]$, T is the local temperature$[°C]$, and x is the coordinate in the flow direction $[m]$. When $\frac{dT}{dx}$ is negative, the minus sign gives a q in the positive x direction. Introducing a constant of proportionality k,

$$q_{conduction} = -k\left(\frac{dT}{dx}\right) \qquad \dot{Q}_{conduction} = -kA\left(\frac{dT}{dx}\right) \qquad \text{Equation 23}$$

Where k is the thermal conductivity of the substance and, by inspection of the equation, must have units$\left[\frac{W}{m^{2}°C}\right]$. The thermal conductivity varies for each material and can vary with temperature.

By taking Fourier's law and integrating across a wall:

$$\left(\frac{\dot{Q}}{A}\right)\int_0^L dx = -\int_{T_1}^{T_2} dT \quad \text{Equation 24}$$

$$\dot{Q}_{conduction} = \frac{T_1 - T_2}{\frac{L}{kA}} \quad \text{Equation 25}$$

Steady one-dimensional conduction in cylinders requires that temperature be a function of only the radial coordinate r. For a cylindrical shell of length L, the area for heat flow is $A = 2\pi rL$; A increases with increasing r. Figure 14 shows a cylindrical shell of length, L, with inner radius $r_1$and outer radius of r_2. The inner surface is maintained at temperature $T_1$and the outer temperature surface is maintained at temperatureT_2. An elemental control volume is located between radii r and $r + \Delta r$. If temperatures are unchanging in time and $\dot{Q}_v = 0$, the energy conservation principle requires that the heat flow across the face at r equal that at face $r + \Delta r$. Since $\dot{Q}$ is independent of r, we can use Fourier's law in the following form:

$$\dot{\mathbf{Q}}_{\mathbf{conduction}} = \mathbf{Aq} = \mathbf{2\pi rL}\left(-\mathbf{k}\left(\frac{\mathbf{dT}}{\mathbf{dr}}\right)\right) \quad \text{Equation 26}$$

Assuming that the conductivity k is independent of temperature, and dividing by $2\pi kL$,

$$\left(\frac{\mathbf{Q}}{\mathbf{2\pi kL}}\right) = -\mathbf{r}\left(\frac{\mathbf{dT}}{\mathbf{dr}}\right) = \mathbf{Constant} = \mathbf{C_1} \quad \text{Equation 27}$$

This is a first-order ordinary differential equation for T(r) and can be integrated easily:

$$\left(\frac{\mathbf{dT}}{\mathbf{dr}}\right) = -\frac{\mathbf{C_1}}{\mathbf{r}} \Rightarrow \mathbf{T} = -\mathbf{C_1}\,\mathbf{ln(r)} + \mathbf{C_2} \quad \text{Equation 28}$$

Two boundary conditions are required to evaluate the two constants; these are:

$r = r_1;\quad T = T_1 \qquad\qquad r = r_2;\quad T = T_2$

Taking the temperature equation with the boundary equations, two equations were yield:

$T_1 = -C_1 \ln(r_1) + C_2; \qquad\qquad T_2 = -C_1 \ln(r_2) + C_2$

Which are two algebraic equations for the unknowns C_1 and C_2. Subtracting the second equation from the first:

$$T_1 - T_2 = -C_1 \ln(r_1) + C_1 \ln(r_2) = C_1 \ln\left(\frac{r_2}{r_1}\right) \quad \text{or,}\ C_1 = \frac{T_1 - T_2}{\ln\left(\frac{r_2}{r_1}\right)}$$

Using either of the two equations then gives

$$C_2 = T_1 + \frac{T_1 - T_2}{\ln\left(\frac{r_2}{r_1}\right)} \ln(r_1)$$

Substituting back into the temperature equation then gives

$$\frac{T_1 - T}{T_1 - T_2} = \left(\frac{\ln\left(\frac{r}{r_1}\right)}{\ln\left(\frac{r_2}{r_1}\right)}\right)$$

The heat flow, for conduction through a cylinder is found by:

$$\dot{Q}_{conduction} = 2\pi kLC_1 = \left(\frac{2\pi kL(T_1 - T_2)}{\ln\left(\frac{r_2}{r_1}\right)}\right)$$

Convection

Convection is used to describe heat transfer from a surface to a moving fluid, i.e.: to air. In an external forced flow, the rate of heat transfer is approximately proportional to the difference between the surface temperature T_s and the temperature of the free stream fluid T_a. The constant of proportionality is called the convective heat transfer coefficient h_c.

$$q_s = h_c \Delta T \qquad \text{Equation 29}$$

Where $q_s$is the heat flux from the surface into the fluid, $\left[\frac{W}{m^2}\right]$ and h_c has units $\left[\frac{W}{m^2 °C}\right]$ and $\Delta T = T_s - T_e$. For the convective heat transfer of insulation, the properties of each material were given and are included as a value in the material selection file of the pressure code program.

The convection equation can be re-written for heat flux as:

$$\dot{Q}_{convection} = \frac{\Delta T}{\frac{1}{h_c A}} = \frac{T_s - T_1}{\frac{1}{h_c * 2\pi r_2 L * k}} \qquad \text{Equation 30}$$

Thermal Resistance

Thermal resistance can be analogous to electrical resistance, and then the resistance R for thermal is:

$R_{conductive} \cong \frac{L}{kA}$ $R_{convection} = \frac{1}{h_c A}$

If there are composite walls for two slabs of material, the heat flow through each layer is:

$$Q = \frac{T_1 - T_2}{\frac{L_a}{k_a A}} = \frac{T_2 - T_3}{\frac{L_b}{k_b A}}$$

Rearranging,

$\dot{Q}\left(\frac{L_a}{k_a A}\right) = T_1 - T_2$ $\dot{Q}\left(\frac{L_b}{k_b A}\right) = T_2 - T_3$

Adding eliminates the interface temperature and the heat flux becomes:

$$\dot{Q} = (T_1 - \frac{T_3}{R_a + R_b}) \quad \text{Equation 31}$$

Useful Heat of Solar Collector

Useful heat Q delivered by solar collector is related to the flow rate, m, specific heat C_p, and the inlet and outlet temperatures, T1 and T2 by:

$$\dot{Q} = \dot{m}C_p\Delta T = \dot{m}C_p(T_2 - T_1) \quad \text{Equation 32}$$

Insulated Pipe Outlet Temperature

The first step is to understand the temperature of the pipe outside of the insulation, T_s.

1. Energy Equation:

$$\dot{Q} = UA(T_1 - T_s) = \frac{T_1 - T_A}{\frac{1}{UA}}$$

2. Summing the resistances in the thermal network:

$$T_1 \sim Convection \sim Insulation \sim External\ Convection \sim T_s$$

$$R_1(Convection) = \frac{1}{2\pi r_1 L h_{c,i}}$$

$$R_2(\text{Insulation}) = \left(\frac{\ln\left(\frac{r_2}{r_1}\right)}{2\pi L k_A}\right)$$

$$R_3(External\ Convection) = \frac{1}{2\pi r_2 L h_{c,o}}$$

3. Overall heat transfer coefficient and area:

$$\frac{1}{UA} = R_1 + R_2 + R_3 = \frac{1}{2\pi r_1 L h_{c,i}} + \left(\frac{\ln\left(\frac{r_2}{r_1}\right)}{2\pi L k_A}\right) + \frac{1}{2\pi r_2 L h_{c,o}}$$

4. Outlet temperature of the pipe:

$$\dot{Q} = \dot{m} C_p (T_1 - T_2)$$

$$T_2 = T_1 - \frac{\dot{Q}}{\dot{m} C_p}$$

$$T_2 = T_1 - \frac{\left(\left(\frac{1}{2\pi r_1 L h_{c,i}} + \left(\frac{\ln\left(\frac{r_2}{r_1}\right)}{2\pi L k_A}\right) + \frac{1}{2\pi r_2 L h_{c,o}}\right) * (T_1 - T_A)\right)}{\dot{m} C_p}$$

Evacuated Tube

To evaluate the outlet temperature of the evacuated tube we start with the energy equation from equation 33:

$$\dot{Q}_{loss} = \Phi A_{ap}\eta - \dot{m}C_p\Delta T$$

$$\Phi A_{ap}\eta = \dot{m}C_p(T_2 - T_1)$$

$$\frac{\Phi A_{ap}\eta}{\dot{m}C_p} + T_1 = T_2$$

4.3 Balance of System

Now that the solar thermal collector system has been designed to power the chiller we have to design the balance of the system, as shown in Figure 28.

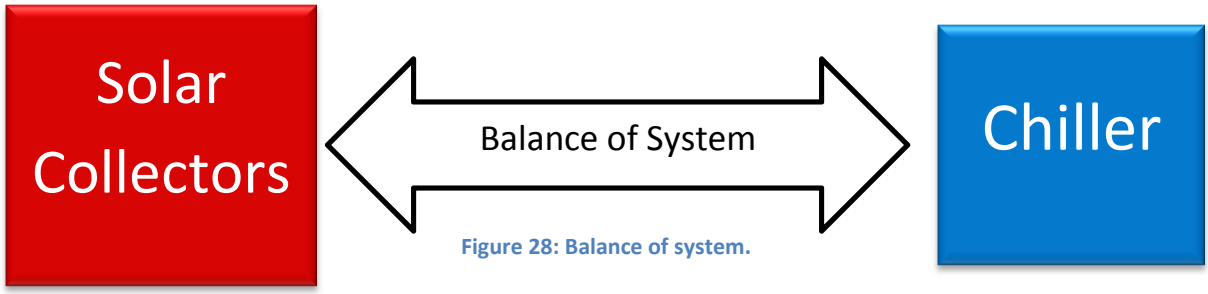

Figure 28: Balance of system.

To begin with there are three separate closed loops in the system, which are shown in Figure 29. The oil loop consists of the solar thermal collector with a mineral oil, Duratherm 600, as the working medium. The heat is exchanged to the glycol loop which is a small loop used as a heat exchanger from the collectors to the chiller. It contains ethylene glycol and water with a 40% ethylene glycol ratio. The glycol loop was incorporated within this system for the chiller. The chiller company did not want mineral oil going through the collector, and we did not want glycol/water mix going through the solar collectors; therefore, it was decided to integrate a small glycol loop in-between the collectors and the chiller. It should be noted however, that a glycol water mix could have gone through the collectors, however, it would have to be pressurized which can be dangerous. Considering that multiple students would be working on this project it was decided to use the mineral oil instead. For the chiller, it could accept mineral oil as the input for the thermal input; however, there is a risk that if the oil leaked in the chiller then it could potentially ruin the machine. It was therefore decided that it would be best to integrate the glycol loop for both systems.

The following sections will give detailed descriptions about each closed loop.

Figure 29: The three closed loops are what the solar cooling system is comprised of.

4.3.1 The Loops

Oil Loop

The oil loop consists of the solar collectors and a heat exchanger. It will require a pump for fluid flow, an expansion tank due to the density of the fluid changing with respect to the increase in temperature, and insulation for minimal heat loss .Our group also made the decision to integrate a storage tank so as to buffer the incoming solar power to the glycol loop so as not to shock the chiller. Figure 30 shows the process flow diagram of the oil loop.

For the configuration of the oil loop it was decided to put the pump just before the collectors and the storage tank immediately after the collectors. This would allow the storage tank to buffer the outlet power of the collectors directly. Immediately after the collector system is the heat exchanger that is thermal transfer unit between the oil and glycol loop. The oil then goes back to the pump to complete a full cycle.

Integrated directly before the pump is the expansion tank. This tank serves a dual purpose in the oil loop. One is for the density decrease of the oil and the second is to put consistent pressure on the line so as not to cavitate the pump. A filter is also placed before the pump to prevent clogs in the line. The last component that is part of the oil loop is a heat dump. In case there was a time where we would want to work on the system or would need to cool down the system we chose to have a heat dump in the system that would allow us that option.

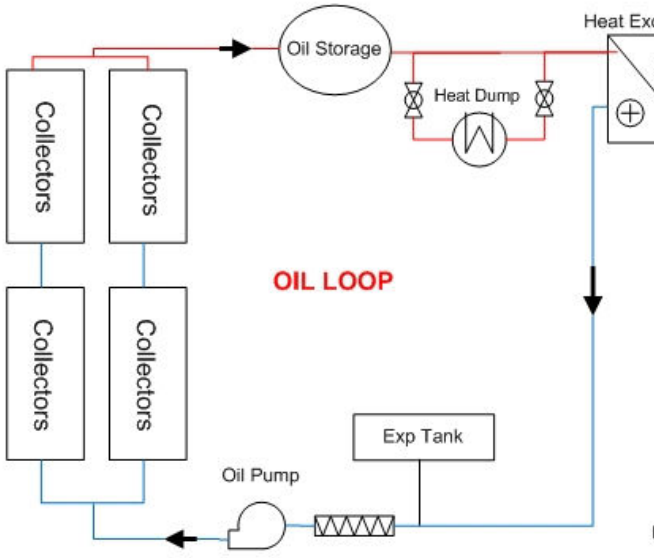

Figure 30: Oil loop process flow diagram.

Glycol Loop

The glycol loop consists of the heat exchanger and the chiller. It will require a pump for fluid flow and an expansion tank due to the density of the fluid changing with respect to the increase in temperature, and insulation for minimal heat loss. Since the glycol loop will undergo a phase change at our operational temperature of 180 $°C$ we are required to pressurize the loop with nitrogen to ensure that does not happen. The glycol/water vapor pressure vs. temperature graph can be seen in Figure 58. At this temperature the loop needed to be pressurized by 7.8 atm. to be to ensure no phase change. The heat goes directly from the exchanger to the chiller, and all other components proceed after the chiller to the exchanger.

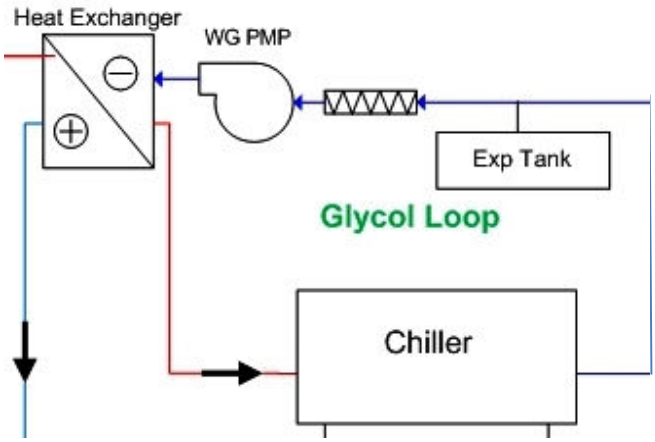

Figure 31: Process flow diagram of glycol loop.

Water Loop

The chilled water loop consists of the chiller and its load, an office trailer, cold dump and a storage tank. These loads will be explained later in detail. The chiller has its own pump within it and a natural gas feed in line.

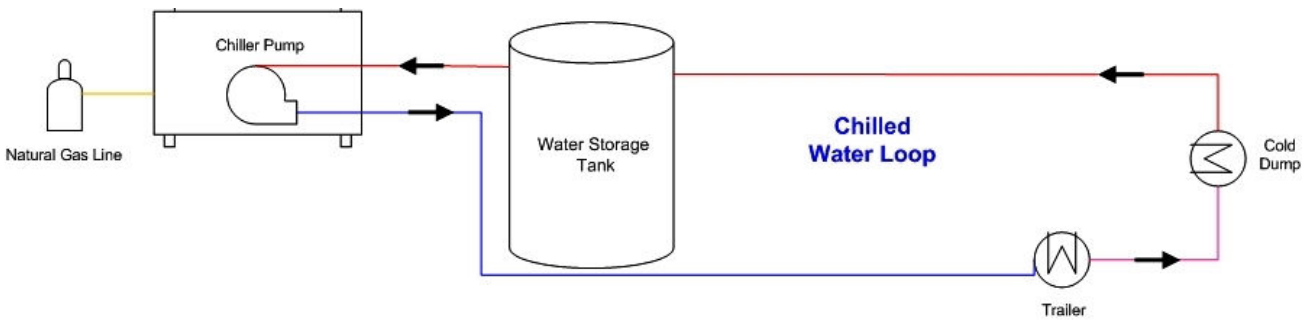

Designing Water Loop

The chiller produces 23 kW[6.6 U.S.R.T] of cooling. Our plan was to buy an office trailer and use the chilled water as a means of cooling the building; however, we could not afford an office large enough for a 6.6 U.S.R.T. So, a more affordable building was purchased a 12 x 56 building and decided to create loads in addition to that building to satisfy the chillers capacity.

The following is the calculations for the buildings load.

Table 9: Building Characteristics of office trailer.

Building Characteristics	Values	Units
Roof		
Type of Roof	Flat, slight tilt	
Area	158	m^2
Walls		
Size, NS	3.35'x17' (two)	
Size, EW	3.35'x3.6'(two)	
Area, NS	1.16	m^2
Area, EW	1.16	m^2
Absorptance, white paint	0.12	
Windows		
Size, NS	3.6 (four)	m^2
Size, EW	3.6 (four)	m^2
Shading Factor	0.1	
Insolation Transmittance	0.6	
Location and Latitude	Merced, CA 33°	
Date	July 23rd, 2009	
Time and Local solar hour angle Hs	Noon, Hs=0	
Solar Declination Angle	20°	
Wall sruface tilt from horizontal	90°	
Temperature outside	72°	
Insolation Transmittance	70°	
U factor for walls	0.061	
Infiltration	NA	
Ventilation	NA	
Internal loads	NA	
Latent heat load, percent	0.3	

Table 9 shows all of the properties of our geographic area plus the buildings characteristics which will be used in the following equations.

Cooling loads are determined using the following equations:[2]

For un-shaded or partially shaded windows, the load is:

$$\dot{Q}_{wi} = A_{wi}[F_{sh} * \tau_{b,wi} I_{h,b} * \left(\frac{cos\, i}{sin\alpha}\right) + \bar{\tau}_{d,wi} I_{h,d} + \bar{\tau}_{r,wi} I_r + U_{wi} * (T_o - T_i)$$

For shaded windows, the load (neglecting sky diffuse and reflected radiation) is:

$$\dot{Q}_{wi,sh} = A_{wi,sh} * U_{wi}(T_o - T_i)$$

For un-shaded walls, the load is:

$$\dot{Q}_{wa} = A_{wa} * \left(\bar{\alpha}_{s,wa}\left(I_r + I_{h.d} + I_{h,b} * \left(\frac{cosi}{sin\alpha}\right)\right) + U_{wa}(T_o - T_i)\right)$$

For shaded walls, the load (neglecting sky diffuse and reflected radiation) is:

$$\dot{Q}_{wa,sh} = A_{wa,sh}\left(U_{wa}(T_o - T_i)\right)$$

For the roof, the load is:

$$\dot{Q}_{rf} = A_{rf} * \left(\bar{\alpha}_{s,rf}\left(I_{h,d} + I_{h,b} * \left(\frac{cosi}{sin\alpha}\right)\right) + U_{rf}(T_o - T_i)\right)$$

Latent load due to infiltration and ventilation is:

$$\dot{Q}_w = \dot{m}_a(W_o - W_i)\tau_w$$

Total cooling load is calculated as follows:

$$Q_{tot} = \dot{Q}_{wi} + \dot{Q}_{wi,sh} + \dot{Q}_{wa} + \dot{Q}_{wa,sh} + \dot{Q}_{rf} + \dot{Q}_w$$

---

[2] Goswami, D. Yogi., Frank Kreith, Jan F. Kreider, and Frank Kreith. "Solar Cooling."*Principles of Solar Engineering*. Philadelphia, PA: Taylor & Francis, 2000. Print.

Table 10 below doesn't add up properly due to rounding errors, but matlab accounts for this.

Table 10: Load of building.

Load	**Magnitude of Load** (Btu/hr except last row)
South facing window	1759
Shaded windows	0
South Facing Wall	19834
Shaded Wall	0
Roof Load	11126
Latent Heat	2327
Total Load	35046
Total Load, USRT	2.9

The office building was going to take 3.8 kW of cooling, so we decided to purchase a Carrier radiator and put it outside that would be another 3 tons of cooling. We also added a 500 gallon storage tank that would be another load but could also be used as storage.

4.3.2 Process Flow Diagram of System:

The final process flow diagram for the whole system is Figure 32.

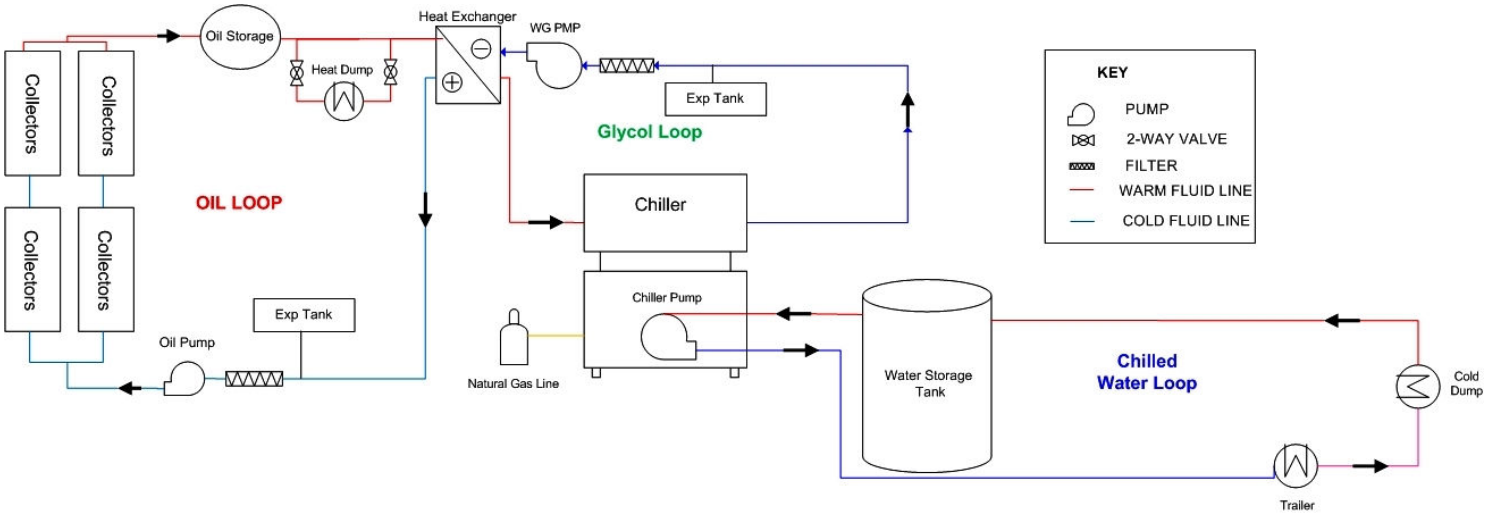

Figure 32: Process flow diagram for entire system.

4.3.3 Pumps

Finding a pump that was high temperature, small horsepower was very difficult. Small pumps are readily available but not for high temperatures; and high temperature pumps are readily available, but not in small sizes. The difficulty with a higher temperature is that the fluid comes into contact with the bearings and the materials used for those components to be made for high temperatures are not cheap. A way around this is to use magnetic pumps, which do not have bearing and can handle high temperatures, but the smallest size we found available in the market was 3 hp, at a cost of $8,000.

The power requirement is:

$$Hydraulic\ Horsepower = V_{flowRate}\Delta P * \left(\frac{7}{12000}\right)$$

The pressure head for the calculation is taken as 4 times the amount due to us wanting to be able to turn on the pump initially at times when the oil may be cold, viscosity is higher thereby the pressure head increases.

Oil & Glycol Pump

The sizing requirements for our pump for the oil loop are:

- High Temperature, ie: 200 $°C$ operational with occasional spikes
- Pressure head of 40 psi to overcome collectors and additional components
- Minimal amount of horsepower to reduce energy demand to pump the working fluid
- Volumetric flow rate of 16 gpm

The calculated horsepower of the pump is 1.5hp. Grundfos had a pump called the vertical centrifugal pump that has an air vent that separates the working medium from the bearings. This allows the fluid to temperatures up to 200$°C$, with a low flow rate at 1.5 hp. Figure 33 shows the performance curves of this specific pump. Considering the size of this system, it is estimated that this pump would circulate oil through the loop at 3 minutes.

For the glycol loop similar calculations were performed and the pump size needed was half the size of the oil loop, ¾ hp. We bought the same Grundfos pump at half the size. Performance ratings were very similar.

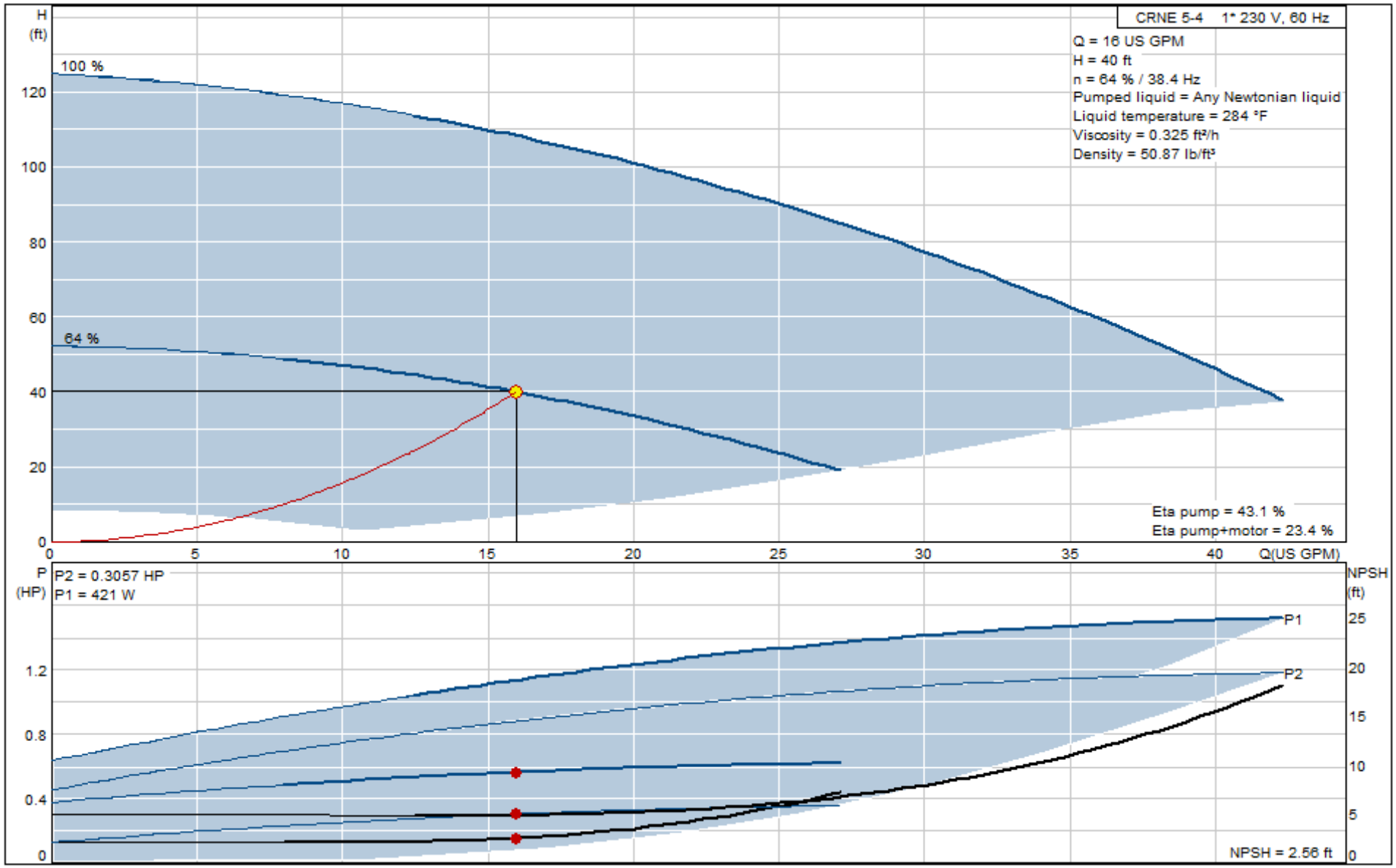

Figure 33: Oil pump performance graphs showing pressure head, volumetric flow rate, power and efficiency.

4.3.4 Tanks

Oil Storage Tank

The Hot Oil Storage Tank was sized based on the amount of time we wanted the oil to mix in the tank. The original purpose of this was to buffer any temperature fluctuations coming out of the collectors, thereby providing controlled power to the heat exchanger. However, another variable that came into play was the pump. We wanted the pump to have a minimal amount of pressure head to overcome and the mineral oil increases it's viscosity with the decrease in temperature. Therefore, our new goal became to design a tank that would retain a temperature above $100°C$ with a retention time of approximately 3 minutes.

The mineral oil's kinematic viscosity, in Appendix 8.4.3, and at approximately $100°C$ there is a turning point for the viscosity of the oil which became our starting point for choosing that size storage tank. The three minutes was calculated as the approximate time that it would take the oil to flow through the loop at one full cycle.

Based of these initial goals the following calculations were used as the foundation to determine the size of the storage tank.

Heat flux for an insulated body:

$$\dot{Q} = \frac{\Delta T}{R} \quad \text{Equation 33}$$

The $\dot{Q}$ is the heat flux of the insulated tank to the ambient environment. The ΔT is the difference in temperature between the oil at night when the system is being turned off and the system in the morning just before we turn it on. The R value is thermal resistance of the insulation. It is related to the thermal conductivity as expressed in the conduction section, by

$$R = \frac{k}{L} \quad \text{Equation 34}$$

Insulation companies typically give R-values for their insulation to characterize its performance. So for this section I will be using equation 33 to study the heat loss in the system, and equation 29 from the convection section. The V is the volume of the tank, the T is the temperature of either the initial temperature of the oil entering the tank and the retention temperature is that of the oil as its about to exit the tank.

$$m = \rho(T) * V \quad \text{Equation 35}$$

$$T_{retention} = T_{initial} - \frac{Q_{loss}}{mh_c(T_{initial})}$$

To calculate the size a matlab program Oil Tank Sizing, which can be found in the appendix, was designed in the following fashion:

Since there were so many variables that were unknown to us we developed a program that would start with initial values, such as:

- R-value, which means specifying an insulation and thickness
  - Thickness were varied but the insulation was the same because it was standard fiberglass
- Temperature
  - Ambient temperatures varied at night from 10-20°C, and in the morning from 30-40°C.
- Volume of Tank
  - Chose a volume of 85 gallons to begin with

The program calculates the initial heat loss and then the retention temperature and if it is not within a given tolerance the program chooses another volume to evaluate given the same parameters. This program was run numerous times for various cases which can be seen in Figure 34 before the final size was chosen.

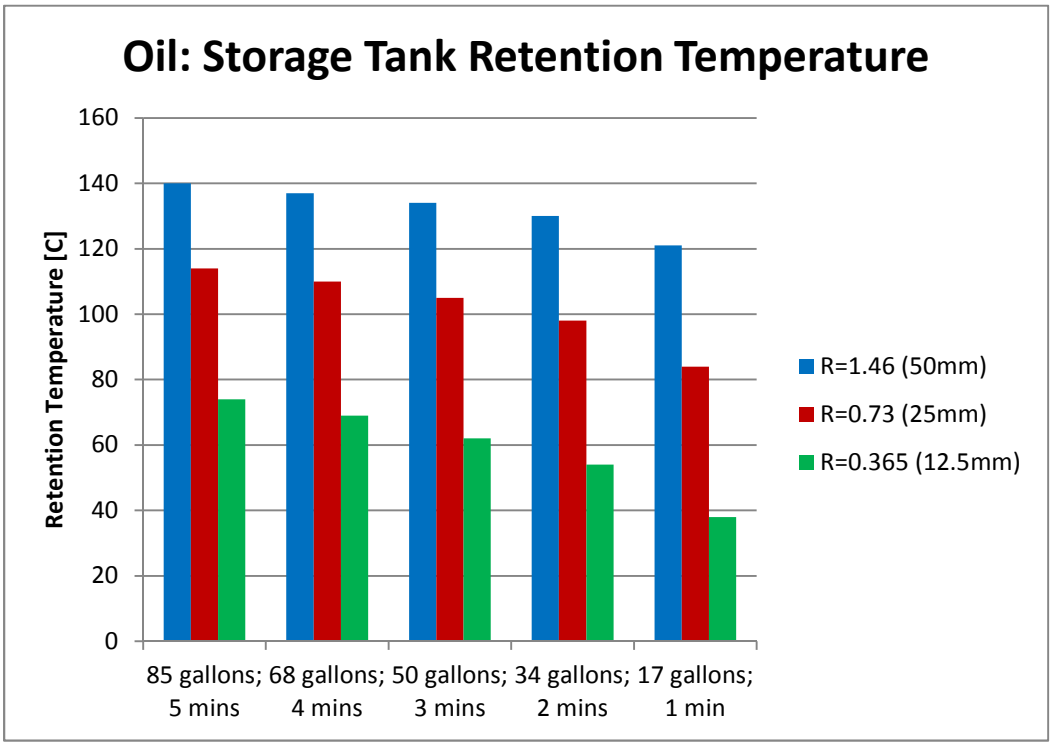

Figure 34: Storage tank retention temperature for various volume tanks.

Looking at Figure 34 we were able to determine that the size of the tank did not have a large effect on the retention temperature, as did the insulation. When considering the expense of the insulation, oil and available tank sizes it was decided to be either the 34 or 50 gallon tank. In analyzing the retention times it was calculated that it would take approximately 3 minutes for the oil to go through the loop once, therefore the 50 gallon tank size was chosen.

Oil Expansion Tank

The storage tank has a direct impact on the size of the expansion tank due to the volume of oil in the system that will be undergoing expansion.

When the oil is at its coldest, 20° C, the expansion tank will be $\frac{1}{3}$ full. This provides an extra amount of oil that can be used in case of leaks, and also allows one to check the amount of oil in the system. When the oil is at its operating temperature, 220° C as a maximum, the expansion tank will be ¾ full. This provides extra headroom in the case of higher temperatures to prevent overflow. Equation 36 and 37 show the volume of the cold oil is related to the volume of the hot oil and can be used to calculate what the volume expansion would be taking into consideration the initial volume in the system, V_{system}.

$$V_{cold} * \rho_{cold} = V_{hot} * \rho_{cold} \quad \textbf{Equation 36}$$

$$V_{expansion} = \frac{V_{hot} - V_{system}}{\rho_{hot}} \quad \textbf{Equation 37}$$

The tank size that was calculated was 40 gallons.

Glycol Expansion Tank

Table X shows the calculations for sizing our expansion tank for our glycol loop which holds approximately 15 gallons of the glycol/water mix and shows the design as super charged, super-c, or not charged. Charged is when you take a tank and pressurize it from the start, ie: with Nitrogen. If we did not super charge the tank it, the expansion tank would be almost 5 times the size and it would phase change. Super charging not only prevents boiling but it has reduced our necessary tank size down to ~4 gallons. Due to costs of tanks and available sizes, a 10 gallon expansion tank was used.

Table 11: Glycol expansion tank calculations

40% Ethylene Glycol			
	no super-c	**super-c**	
System Vol.	.04	.04	m^3
Low Temp	16	16	$°C$
High Temp	185	185	$°C$
Exp. Fctr.	0.13200	0.13200	
Expanded	.005	.005	m^3
Low Press.	344	344	kPa
High Press.	1034	1034	kPa
Accept. Fctr.	0.138	0.60716	
Tank Vol.	.05	.013	m^3

4.3.5 Heat Exchangers

Oil to Glycol

The heat exchanger between the oil and glycol loop was going to have very specific requirements. Our solar collector had very specific requirements, as did the chiller, which can be found in Table 12. Given that we would be dealing with two fluids that would not undergo a phase change, it was decided it would be best to use a flat plate heat exchanger. Properties of which can be found in the appendix, under Heat Exchanger.

Table 12: Heat exchanger requirements.

Design Duty : 21.9 kW				
			Side 1	Side 2
Fluid Name		:	Dowtherm 4000 40%	Duratherm 600
Inlet Temperature	°C	:	161	180
Outlet Temperature	°C	:	170.34	168
Mass Flow Rate	GPM	:	9.16	16
Pressure	bar	:	-	-

Heat Dump

A heat dump was needed in case there is a time where our system overheats. Overheating is based not only on the in-put of the chiller, but also on the boundary conditions for the specific components of the system. Since we do not want to turn on and off the collectors, or rather, cover them and un-cover them, we need a means cooling off the fluid, keeping in mind that there will still be energy being put into the system at the same time; therefore, what is needed to be able to dump a full load of 23kw worth of energy. This sizing was taken into consideration and purchased the following radiator. It is comprised of a pin radiator, along with one fan.

Specs Requested:

To dump 1620 Btu/min from hot oil to the air.

Liquid Name: Duratherm 600

Max Temperature: 220° C

Connector Type: NPT

Oil Inlet Temperature: 180° C

Oil Outlet Temperature: 168°C

Oil Flow Rate: 16 GPM

Air Inlet Temperature: 115 °F

4.3.6 Insulation

To determine which type of insulation and the thickness for each section of the system we broke it down by component first. Each component has different requirements for insulation which means different insulation types would needed to be analyzed in choosing which is best for that component.

The components are broken down by the following list.

Manifold to Tube Junction

- Material: Various
- Size: ~.25in diameter, by 3 inches in length
- Priority: Very High

Figure 35: Manifold, and junction.

Manifolds

- Material: Copper
- Diameter: ~.75 inches
- Priority: Very High

Piping

- Material: Galvanized steel
- Diameter: 1.5 inches
- Priority: High

Figure 36: Galvanized steel pipe

Tanks

- Material: Galvanized steel
- Sizes: Various
- Priority: High

Balance of System

- Material: Various
- Size: Various
- Priority: Medium

The priorities for these components were chosen by concluding from the CEC grant that the majority of the heat loss in the collectors was within the manifolds and manifold to tube junction. This is very important that we lose a minimal amount of heat here. The piping will be the next target of heat loss due to the amount of area available, and the balance of system is of concern but does have the lowest heat loss of these components.

For insulation there are many different kinds of insulation on the market today and after a vast research of high temperature insulations, the following types were analyzed:

Fiberglass

- Description:
    - Fiber reinforced polymer made enforced by glass
    - Lightweight and strong
- Installation: Easy for pipes
    - Can come molded to your pipe diameter and becomes easy to install
    - Hydrophobic: No,
        - Will require weatherization

Figure 37: Fiberglass pipe insulation.

Fiberfrax

- Description:
    - Is like fiberglass, but with ceramics. Great insulator.
- Installation: Easy for complex geometrical objects
    - Fiberfrax comes in layers, and appears like cotton. It can be great to stuff boxes, wrap around abstract objects, etc.
    - Hydrophobic: No
        - Will require weatherization

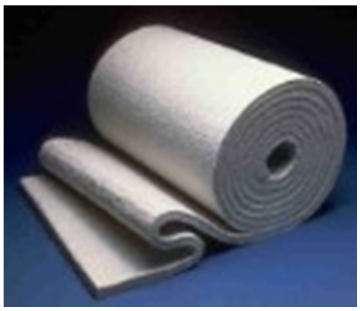

Figure 38: Fiberfrax layer rolled up.

Microtherm

- What is it:
    - Micro porous insulation core is covered in a woven glass cloth outer layer and then stitched into a square matrix.
- Installation: Thought it would be easy for manifolds
    - Comes in a quilt that we were told was malleable and easy to wrap around pipes
    - Hydrophobic: Yes
        - Will not require weatherization against water

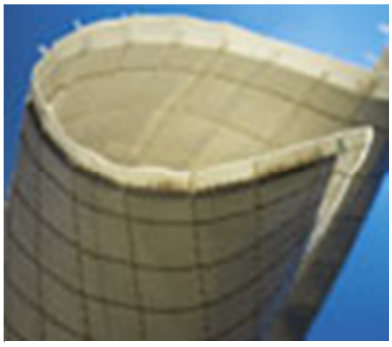

Figure 39: Microtherm quilt.

There are two decisions to be made:

1. Which type of insulation should go with each component?
2. How much insulation will be required for that component, ie: thickness?

Manifold Tube to Junction

There is a 2" gap of exposed pipe between the insulated manifolds and the vacuum tube receivers. Solely based on the geometry on the object it was best to go with FiberFrax or Microtherm. Using the same calculations for heat loss and temperature loss within an insulated pipe, in the temperature section earlier, it was calculated, as seen in Table 13, that Microtherm would have cost $5 a piece ($800 total) for a total loss of ~ 140 watts.
FiberFrax when wrapped to a thickness of 2" would cost approximately $17 and would lose a total of ~ 155 watts, for the summation of all of these components. This would a heat loss of ~0.5% of the system. There is very little difference between the amounts of heat loss between the two products, but Microtherm is 47 times the price of FiberFrax, therefore, we chose FiberFrax.

Table 13: Microtherm vs. FiberFrax for Junction.

Manifold to Tube Junction	Microtherm	FiberFrax
Thickness (in)	0.5	2
Price ($)	$5.00	$1.20
Conductive Resistance (m-K/W)	49.9	47.9
Convective Resistance (m-K/W)	5.2	1.7
Overall Heat Transfer Coefficient (W/K)	0.9	1
Heat Loss (Watts)	**138**	**154**
Total Price ($)	**$800.00**	**$16.80**

The total heat loss for the tube to manifold junction would be ~155 watts.

Manifold:

Since the manifold has an awkward shape and it is so important to have a minimal heat loss, we chose to use Microtherm. In the appendix is a sheet that characterizes its performance. The total heat loss for all manifolds of the system would be 1kW.

Piping

Oil & Glycol

For the geometry of the piping and our experience with FiberFrax we decided it would be best to use pre-molded fiberglass. Table 14 shows the calculations for a thickness of 1 and 2 inches for both the 1.5 and $\frac{3}{4}$ inch diameter piping.

Table 14: Thickness comparison of fiberglass for piping sections.

1½" Diameter Pipe		
Thickness(mm)	25.4	50.8
Heat Loss (Watts)	2809	1959
Total Price ($)	$352.23	$715.08
¾" Diameter Pipe		
Thickness(mm)	25.4	50.8
Heat Loss (Watts)	1867	1391
Total Price ($)	$345.15	$699.15
Combined Heat Loss (Watts)	4677	3351
Combined Price ($)	$697.38	$1,414.23

The heat loss and price difference for 1 or 2 inches of fiberglass is very big. Considering the final difference between heat losses is 1.3 kilowatts is too big of a difference for us. Therefore, we chose for all piping that 2 inch fiberglass pre-molded pieces would be used. This calculated to a total heat loss of 3,351 watts; however, it should be noted here that this does take into consideration the piping used in the glycol loop!

Water

For the water loop a standard pvc pipe insulation foam pre-molded for pipes was used. It wasn't necessary to conserve energy in the water loop; therefore, no energy analysis was needed.

Tanks

The tanks are very critical to insulate because if not they are large heat bodies that can be heat dumps. For the structure it was decided that it would be best for us to FiberFrax, both for ease of installation and financially. To determine the thickness of insulation for each tank, the following tables are shown.

Oil Tanks

Table 15: Oil storage tank calculations for FiberFrax insulation.

Thickness (in)	1	2	3	4
Heat Loss (Watts)	535	300	212	166
Total Price ($)	$29.43	$62.26	$98.59	$138.54

Table 13 shows the FiberFrax insulation of 1 to 4 inches and their respective heat losses for the oil expansion tank. Given the price of the insulation and the heat loss we chose 4 inches for a heat loss of 166 watts.

Table 16: Oil expansion tank calculations for FiberFrax insulation.

Thickness (in)	1	2	3	4
Heat Loss (Watts)	516	294	211	168
Total Price ($)	$31.43	$67.26	$107.59	$152.52

Table 14 shows the FiberFrax insulation of 1 to 4 inches and their respective heat losses for the oil expansion tank. Given the price of the insulation and the heat loss we chose 2 inches for a heat loss of 168 watts but when we went to go insulate, due to the site glass being too close we could only fit 1 inch of insulation, for a heat loss of 516 watts.

Glycol Tank

Table 17: Glycol expansion tank calculations for FiberFrax insulation

Thickness (in)	1	2	3	4
Heat Loss (Watts)	198	115	84	68
Total Price ($)	$12.25	$27.07	$44.56	$64.82

The glycol expansion tank was insulated with the amount of leftover FiberFrax we had. This was based on priority of system insulation at the time of assembly; therefore we only wrapped it with 1 inch of insulation for a heat loss of 198 watts.

Balance of System

Due to the balance of system being the nooks and crannies of each loop, it was decided to use FiberFrax for this insulation.

Heat Loss from Collectors to Chiller

Although a designed heat loss from the collectors to the chiller was10%, ~2.3 kW, the final result was 5.8 kW, which is a 25% loss. Meaning, on a great day of solar insolation, at operational temperatures we would hope to see 17.2 kW. The breakdown of where this heat went to is shown in Figure 40.

The majority of the heat loss is within the tanks. If we were able to use our original design thickness calculations this number would have been significantly reduced. The next largest number is the manifolds. We knew this would be a large heat loss. Next is the piping and balance of system, which includes the heat exchanger. Together they are about 1.5 kW. The junction takes a minimal heat loss. These results are for steady state.

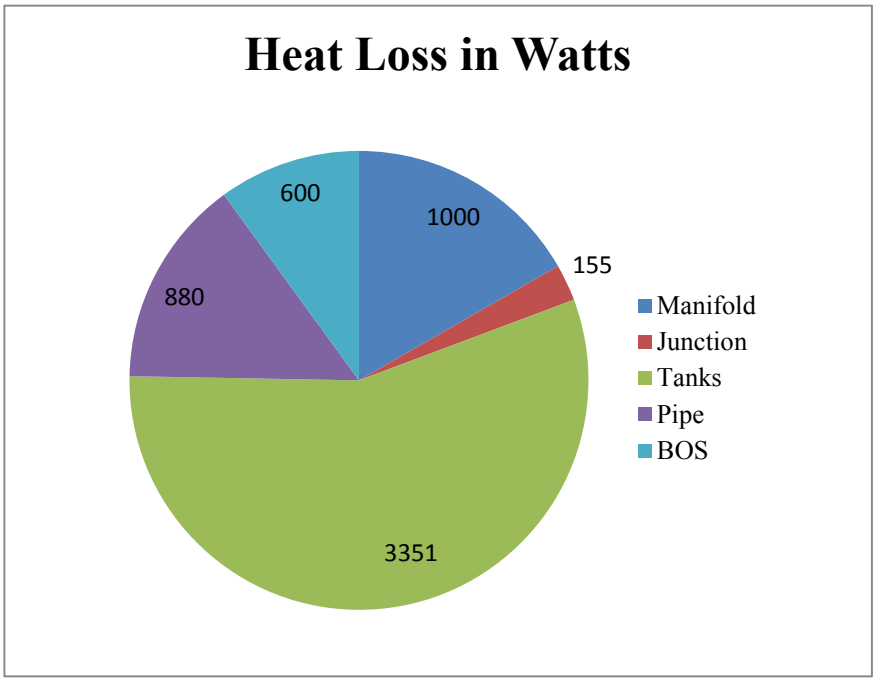

Figure 40: Heat loss in thermal watts from the collectors to the chiller.

5. Manufacturing

Now that the system was designed it was up to our team to manufacture two very important components of the solar thermal system: the reflector, and the collector. The following are descriptions of how we manufactured these components.

5.1 Reflectors

Mold

For the reflectors there were two materials that could have been used: metal or plastic. Although it would have been ideal for the reflectors to be made of metal, the cost just for the tooling, let alone for the materials was out of our budget. Therefore, a plastic mold that would have a reflective adhesive attached to it was used. The optics design was inverted in SolidWorks and a mold was made out of it as shown in Figure 41. This mold, made of wood composite, was taken to a vacuum molding plastic company in town and had them create troughs.

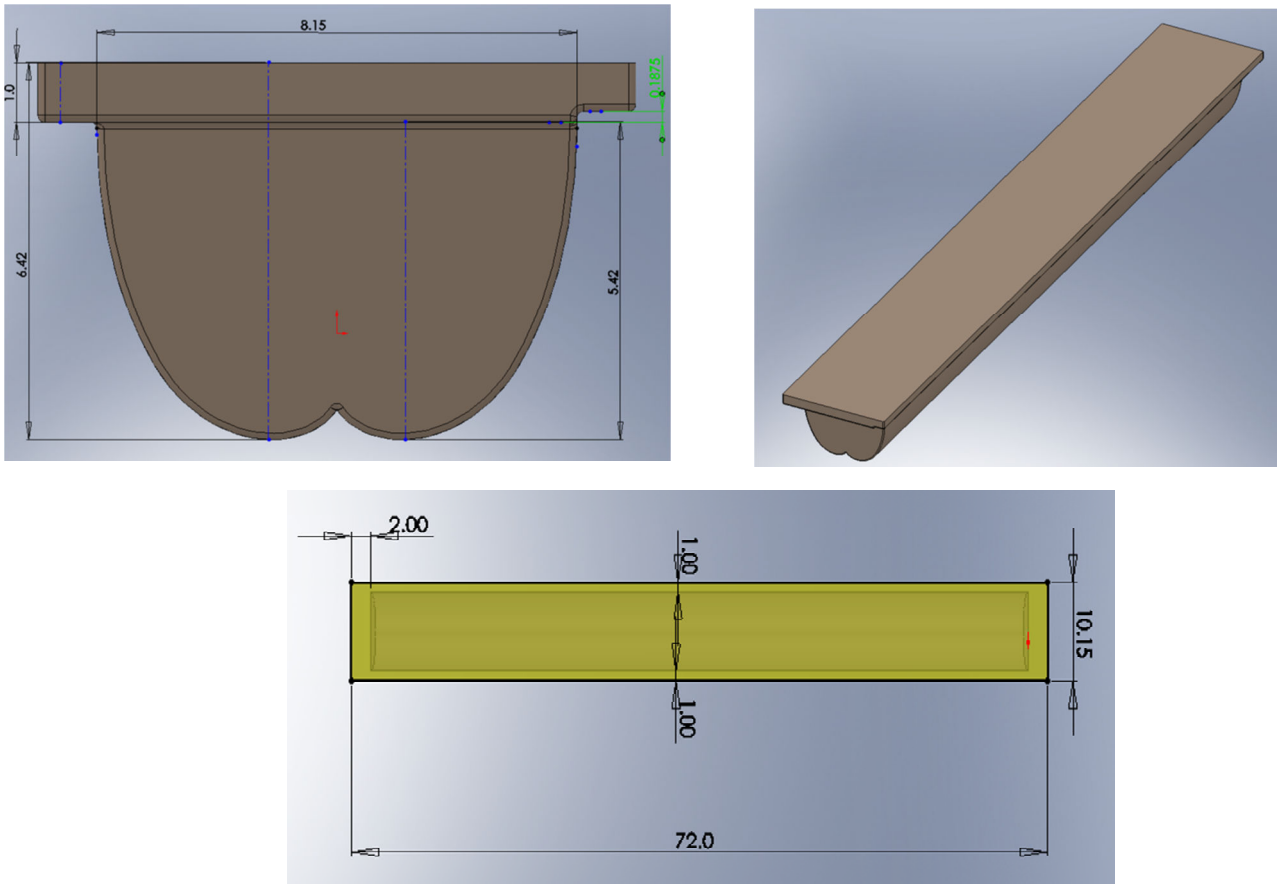

Figure 41: Reflector 3-d renderings for the mold.

The first decision to be made was whether the molds should be for a single trough or for an entire collector. A test was done for a design of a mold for two troughs that were only 20% of the length and test out how the forming would work.

During the test it was observed that the space in-between the collectors were not enough for the plastic to be able to get into the groove and there were holes and extremely thin plastic around those regions. The only option to solve this problem was to have more space in-between the troughs but our manifold was already designed to a specific spacing and we could therefore not change the spacing in-between the troughs. It was by default now that we went with single troughs.

Another problem was also observed during the pilot run. The mold was designed in SolidWorks and did not take into consideration that 90° bends in the mold would be difficult to form the plastic around and to get the plastic off. This posed a large problem; therefore the design was changed for the mold to have an angle to it, as seen in Figure 42.

Now that the spacing issue was solved full length mold was made out of the composite wood for the single trough. Later another problem occurred because a single trough was being used. The mold began to come apart. Originally it was thought that there would be a small amount of molds due to a double trough. Perhaps having groups of 6, but when we did single troughs, then it became pulling at least 160 molds. After ~10 molds were pulled, the mold began to come apart. Luckily the vendor working put in a lot more time and effort and was able to pull off our 160 troughs.

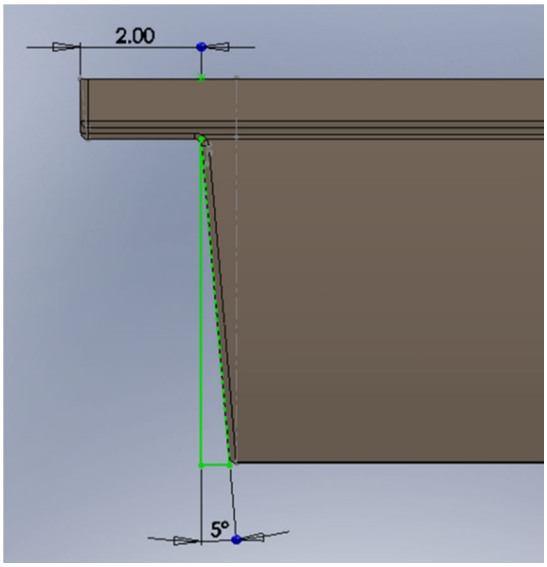

Figure 42: Slight angle added to mold for reflector manufacturing.

Reflective Adhesive

The reflective adhesive chosen is Reflectech. This is the material that was tested in the CEC grant.

Two main reasons for using Reflectech:

1. It has superb reflective properties.
2. Cost

Originally it was proposed to make the collectors out of plastic, and then apply Reflectech onto them. In theory, this process would have been effective and cheap; however, in practice it seems to be everything but both of these. Reflectech is made to be applied to flat surfaces where one can apply a good amount of pressure to the Reflectech and its surface and have a good bond between them. (The adhesive properties of Reflectech work with pressure) However, when trying to apply Reflectech to our curved surfaces there have been bubbles, and were not able to apply the material on smoothly. Because of this, when the collector is left outside, the entire assembly comes apart. The following is a summary of the experimental process in trying to understand how to best apply Reflectech to the troughs:

Brainstorming Reflectech Assembly

1. Why don't we have Reflectech put on during the vacuum mold processing so that the plastic mold already comes with Reflectech on it?

Reflectech would not be able to withstand the temperature, and pressure. Vacuum seal molding is run at a very high temperature, and with the processing procedure used for this type of manufacturing, it would stretch the material and most likely tear holes and come apart.

2. Besides pressure, is Reflectech's adhesive reactive to any other methods?

One idea the team thought of is heat. If Reflectech is reactive to heat, then when we apply the material to the plastic, and we are left with bubbles we could use a heat gun to help with the adhesion and get the air to escape; however, when we used a heat gun on Reflectech we observed that the material would shrink. This means, if we were to use a heat gun on the Reflectech during

the process of applying it, it would create unwanted tension on the material and it would ultimately begin peeling away from the plastic.

3. Are there different methods of applying Reflectech to our curved surface that look promising?

We did contact Reflectech multiple times to ask them how to apply their produce to a curved surface, their response is that they have never worked with applying it to a curved surface before. Their advice is to make sure that we have no bubbles and can apply a lot of pressure evenly on the material to create a strong bond.

4. What is the main problem that we are having in applying Reflectech to the mold, and what have we tried to correct it?

We cannot apply pressure evenly. We have used paint rollers, both hand size and larger. We also have a roller that is almost the length of the collector, but it has a feathery material on the outside. It would be better if it was a solid with some absorption, like rubber.

The adhesive that comes with Reflectech is extremely strong, and once the Reflectech touches the mold it stays. There is no play with being able to move it, and so in applying it on a collector that is over five feet long, with a curved surface, there is plenty of room for error!

So we tried to use water in-between the material and the collector because it would allow a 'slippery surface' to be able to have some flexibility when applying the Reflectech on the mold so that the bond wasn't made instantaneously which allowed us to move the material a bit. Although for the process of applying it worked nicely, the result was that once it dried there were a lot of bubbles and the water process came apart easily. Therefore, we have ruled out making water part of the process.

The strongest points for error is wherever there is an opening for air or weathering to occur that could break the bond. To account for a nicely sealed application, there are a few different methods we are trying:

- Reflectech Tape: This is slightly reflective and is to be used on all edges of Reflectech to prevent degradation, we can use it as a seal

- Superglue: This is to ensure that we have a strong bond that is sealed, and can also be used to prevent degradation
- Calking: To ensure a tight bond at the edges and can be used for degradation

The middle of the trough where there is a peak is usually the first place where the bond breaks. Instead of cutting Reflectech in half and applying it to both sides of the collector, we can fold it down the center and make sure that the Reflectech is centered on the collector and then apply it as once piece; thereby eliminating the most likely area for it to come apart.

Reflectech assembly experiments

The final question became: Is there a solution for using Reflectech on our molds?

In taking all of our analysis and trials and error into consideration we decided to run an experiment where we would apply our best ideas of bonding Reflectech onto our collectors, and then place the collectors outside for a few weeks and see which solution prevailed. The experiments were:

1. Whole piece of Reflectech with a crease down the center. We used 3m adhesive, and left the backing on the Reflectech. We applied it with our long roller, and used the small paint roller after to help apply pressure. Then we cut the edges with a razor and used tape curled at the top to seal the edges. Superglue was used at the ends for a seal.
    a. When we were applying the Reflectech we realized that side 2, we did one side at a time, not only was the pressure not evenly applied on this one, but it began coming up at the sides. This happened for two reasons:
        i. When we applied Reflectech on the first side, everything was relatively smooth, however, we noticed when we applied the second side the tension of it pulling from the first side and the second side was creating bubbles on the second side, right at the valley at the bottom.
        ii. At the very lip at the top of the collector, we didn't cut flesh with the top, there was a little overhang, and so when we applied the tape at the top we stretched the Reflectech over the lip a bit and it created a tension. Within minutes we could already see tiny bubbles occurring.
        iii. 4 people

2. Whole piece of Reflectech with a crease down the center. We used 3m adhesive, and left the backing on the Reflectech. We applied it with our long roller and used the small paint roller after to help apply pressure. Then we cut edges with a razor and used tape at the top and calking on the sides. We were also really careful with applying pressure evenly. This essentially the same experiment as 1 except better.
    a. 4 people
3. Whole piece of Reflectech, sprayed 3m glue on the entire trough and then applied Reflectech as a whole on the trough. Cute the top with a razor and applied calking on the top and sides.
    a. 3 people
4. Same as 3, except this time we only applied 3m spray down the center of the trough so that way we could get the bottoms and the climax of the trough all at once preventing there from being any tension on the center of the trough. Then we applied 3m to one side at a time and used our hands to smooth it out. Then we went for a final run with the small paint rollers. We then cut down the tops with a razor down below the curve of the trough and applied calking around all edges for a good seal.
    a. 3 people

All four collectors were left outside.

Results of Reflectech Assembly Experiments:

We left the experiments out for approximately 3 weeks. The time was from December 22nd to the second week of Jan, 2010. The weather was very cold, extremely wind and very rainy. When we took the collectors off the frame and brought them inside we observed that all of them had diagonal bubbles all along the sides of the collectors. In order to understand where these bubbles came from, we took a razor and carefully cut open the bubbles. The possibilities that we were considering happening were that the Reflectech either separated from its own backing or there were stresses that were separating the Reflectech from the plastic.

One of the troughs with 3M appeared to have in some areas. We were therefore not able to spray the 3M evenly. Then we continued to cut open bubbles on two more troughs, to discover that

they had all not separated from their own backing, but had separated due to stresses and the 3M glue not being able to adhere to both surfaces.
Fortunately, all three methods of securing the edges: caulking, tape and super-glue worked very well. Since Reflectech sold us the tape and aesthetically looks most pleasing, we have decided to use Reflectech tape at the edges on the top. Since tape will be difficult at the front and back of the trough where the *face* is, we have decided to use caulking, with a finger smooth finish.

Interesting result is that we only cut open 3 of the troughs and then depressingly left them inside while we thought of other solutions. We went back 1 week later to find that all of the troughs appeared to be smooth. Especially Number 2, it looked perfect, and luckily that was the one we did not cut, and it had the Reflectech tape with a smooth bond of glue at the edges.

How did it go from having bubbles and not looking good, to being smooth and looking perfect?

Our hypothesis is that the plastic is actually deforming in the weather, due to temperature, and causing stresses on the collector and thus the bond between the plastic and the Reflectech! This made us realize that due to all the stresses in the trough between the plastic and the adhesive it would be best for us to apply the Reflectech in small portions.

The final result for us to assemble the Reflectech to the plastic is: Cut the Reflectech down the center, and partition it into three segments, a total of six pieces per trough. Use their adhesive and their tape to seal edges.

5.2 Collector

There are many factors that go into designing the collector. The following are descriptions of how we designed the collector, which contains the reflectors, manifold and frame.

5.2.1 Frame

Design Problem

The frame is a critical component of the collector. It has to provide support for the troughs and hold up against varying weather conditions. The constraints of this design came down to:

- Budget, being as little as possible
- Feasibility to construct
  - We are dealing with a very limited amount of tools and access to shops, so it had to be easy to manufacture

To design a frame that can meet our needs we used Pro Engineering and Pro Mechanica to model our designs against varying loads and constraints.

Design Parameters

- All force and moment loads were applied with a safety factor of 2
- All welded joints were modeled as a solid connection
- All materials were assumed to be homogenous
- The temperature domain was that of Merced
- All design was done using Pro Engineering
- All analysis was done in Pro Mechanica
- Polynomial Order min1 , max 9
- Percent Convergence was set to 5%

The foundation of the frame was designed and can be seen in Figure 43. This structure was modeled as 6061 Aluminum in Pro Engineering and Pro Mechanica. The constraints would be at the foot of each aluminum vertical post and the load would be evenly distributed along the horizontal frame.

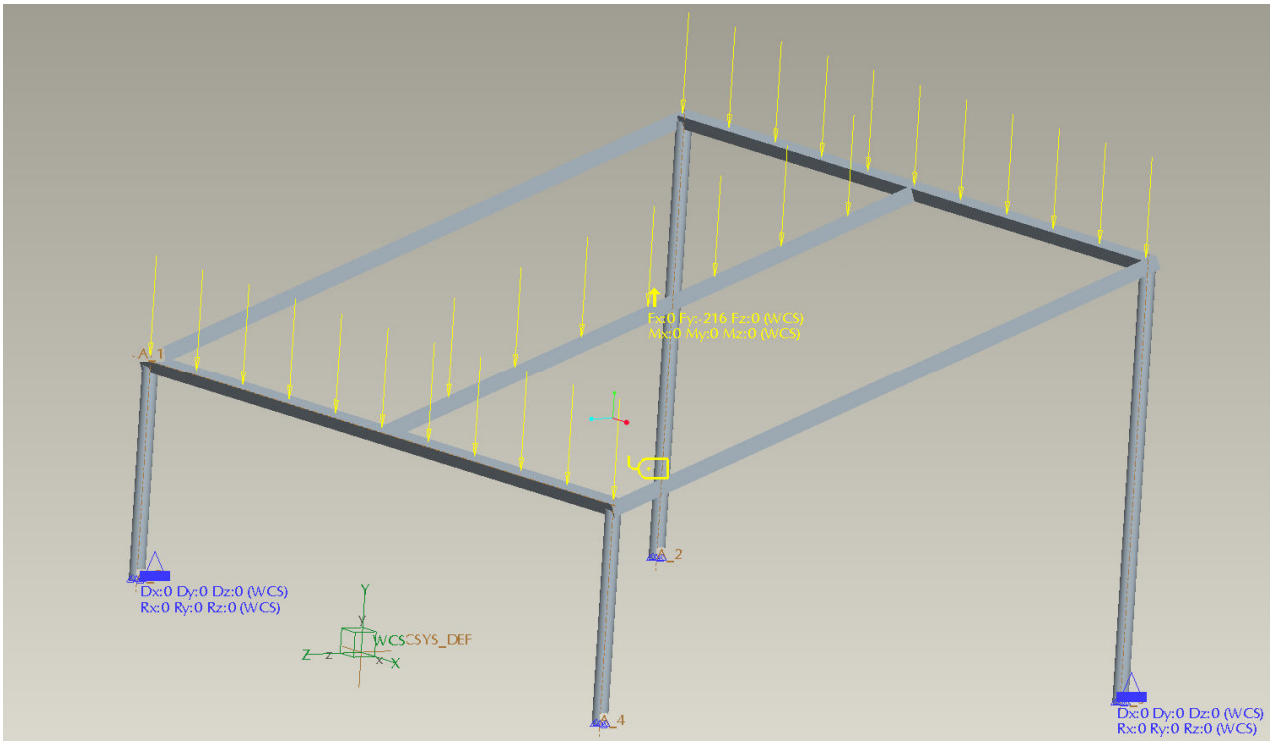

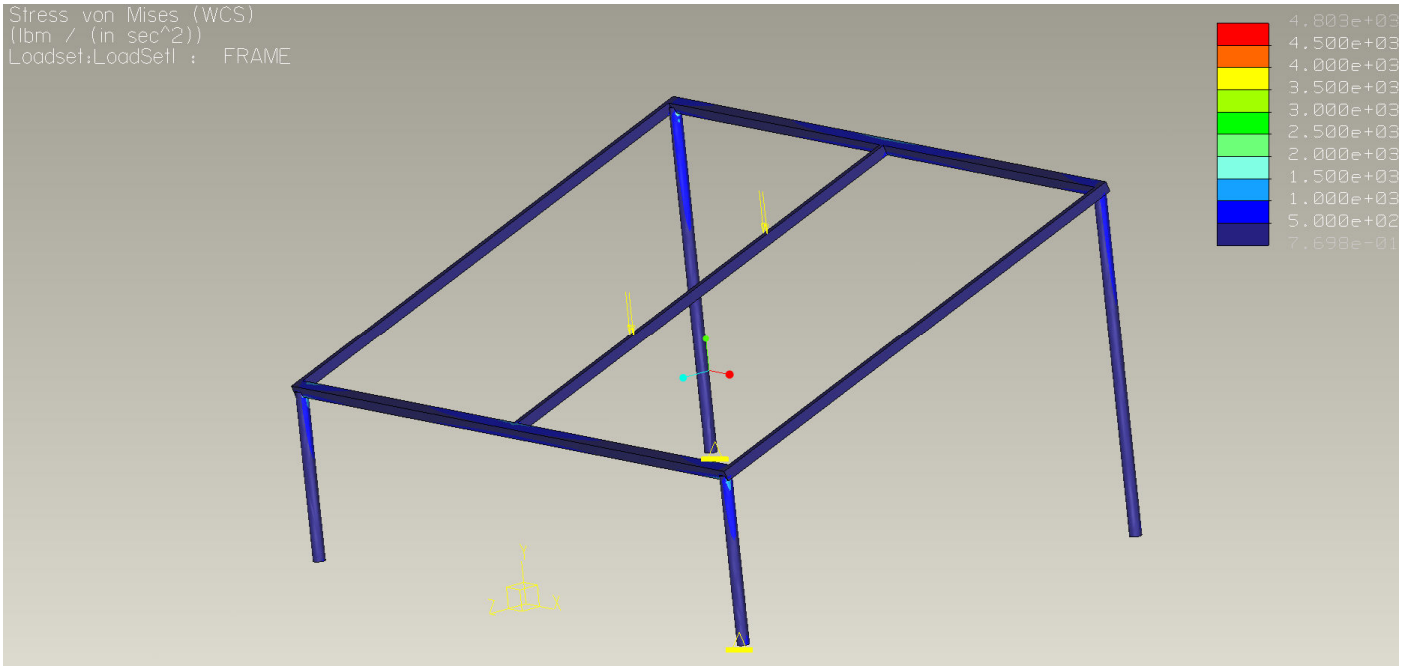

Figure 43: Is the foundational base of the frame. Top picture is the loads and constraints, bottom is the stress contours.

Analysis 1

Loads:

- Collector Tubes: 6 lbs.
- Reflector Troughs: 4 lbs.
- Manifold: 8 lbs.

Total weight load, with a safety factor of 2 is: 216 pounds.

Constraints:

The four supporting poles were held static in all directions.

The results show that the deflection caused by this load is nominal and this design is structurally sound, and will experience minimal deflections.

Analysis 2

Took the frame in Figure 43 and applied a wind loading of 150 mph to test the analyze contours of the frame. They load was placed in the direction of the back of the collectors which would cause the troughs to pull away from the frame.

The analysis showed that there were stresses throughout the frame but they were very minimal proofing that this design will hold up against the weather.

Analysis 3

Considering that the base of the frame was done it was now time to design the portion of the frame that would allow for the 20° tilt for the troughs.

20° wedges will be used to align a 20 in long section of square tubing aluminum at the proper angle. This 20 in long section will act as a receptacle to insert the longer sections of tubing that will support the through, as well as provide suitable spacing between the manifolds. An additional wedge as well as a nut will then be placed on top to hold it all together. This can be seen in Figure 44.

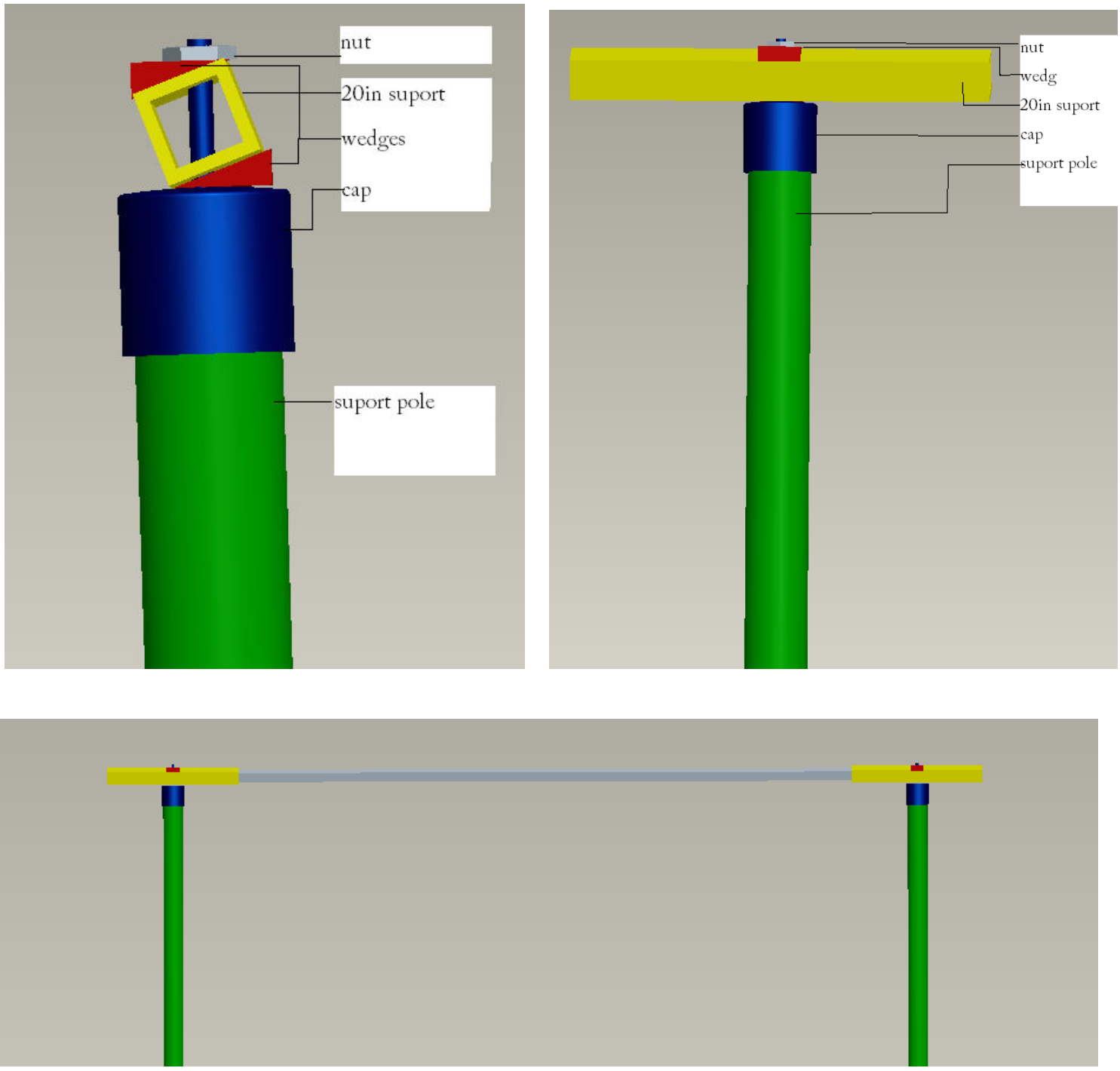

Figure 44: Final frame design.

For the analysis on the final design a load of 216 lbs. was applied as shown in as a distributed load across the section that will be supporting the collectors and troughs. The constraints were held at the ends where the aluminum pole would be attached to the support poles.

Based on these results, most notably the max displacement in the x direction, a confident conclusion can be drawn that we are well within specified criteria, regarding the bending of the support structure. This design was chosen as our final design.

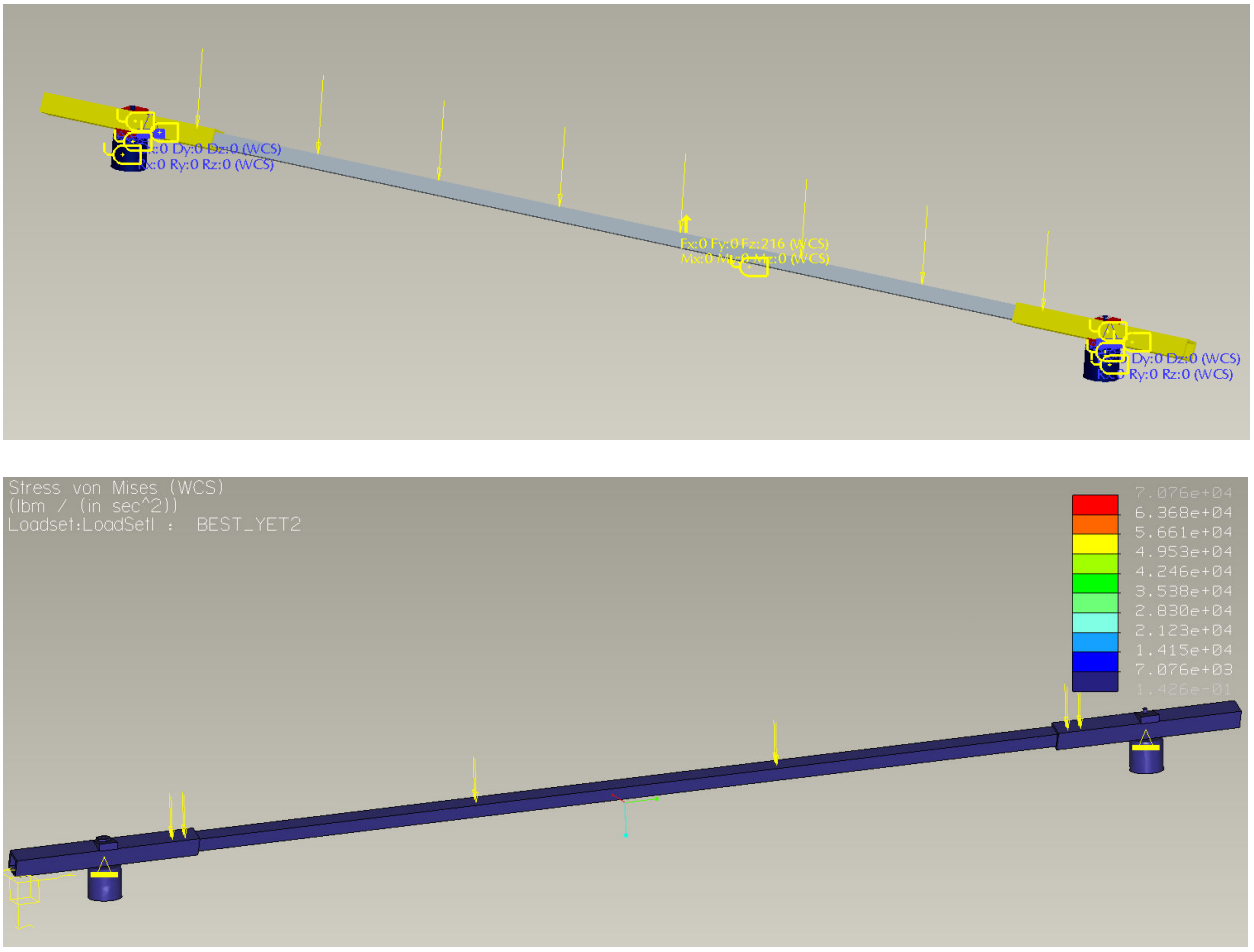

Figure 45: Top figure is the final frame design with load and constraints applied. Bottom picture is the stress contour.

5.2.2 Attaching Manifold to Collector Frame

Design Problem

The collector frame holds 10 troughs at a 20 degree incline. Because of this incline, the vacuum tubes in each trough and the manifold they are attached to will slide out of the bottom of the frame. Therefore, we need some method for holding the tubes and manifold in place to prevent them from falling and breaking. In the experiment for the CEC the manifolds were attached to the collector frame using an aluminum strip. This resulted in a heat loss via conduction from the manifolds to the aluminum strip and a resulting loss in efficiency.

In the current setup, the collector frame will be made of aluminum and thus the problem will be magnified if there is a pathway for conduction to the aluminum frame. Therefore, we must insulate the connection between the tubes and manifolds and the aluminum frame. The pieces that hold the tubes and manifolds will be part of the collector frames. These collector frames are a secondary component of the system and as such should not contribute significantly to the cost. The insulation surrounding the manifolds should be weatherproofed to ensure the maximum lifetime of the insulating material. Lastly, the solution to this problem should be simple to implement and allow for maintenance along the manifolds and tubes.

Design Constraints

1. Must be able to hold weight of 10 tubes (including oil) and manifold from sliding off of the collector stand.
2. Must provide thermal barrier between hot tubes and manifold and the aluminum frame.
3. Must be economical
4. Must provide weatherproofing for manifolds
5. Should provide easy access to tubes and manifolds, for removal, installation and maintenance.

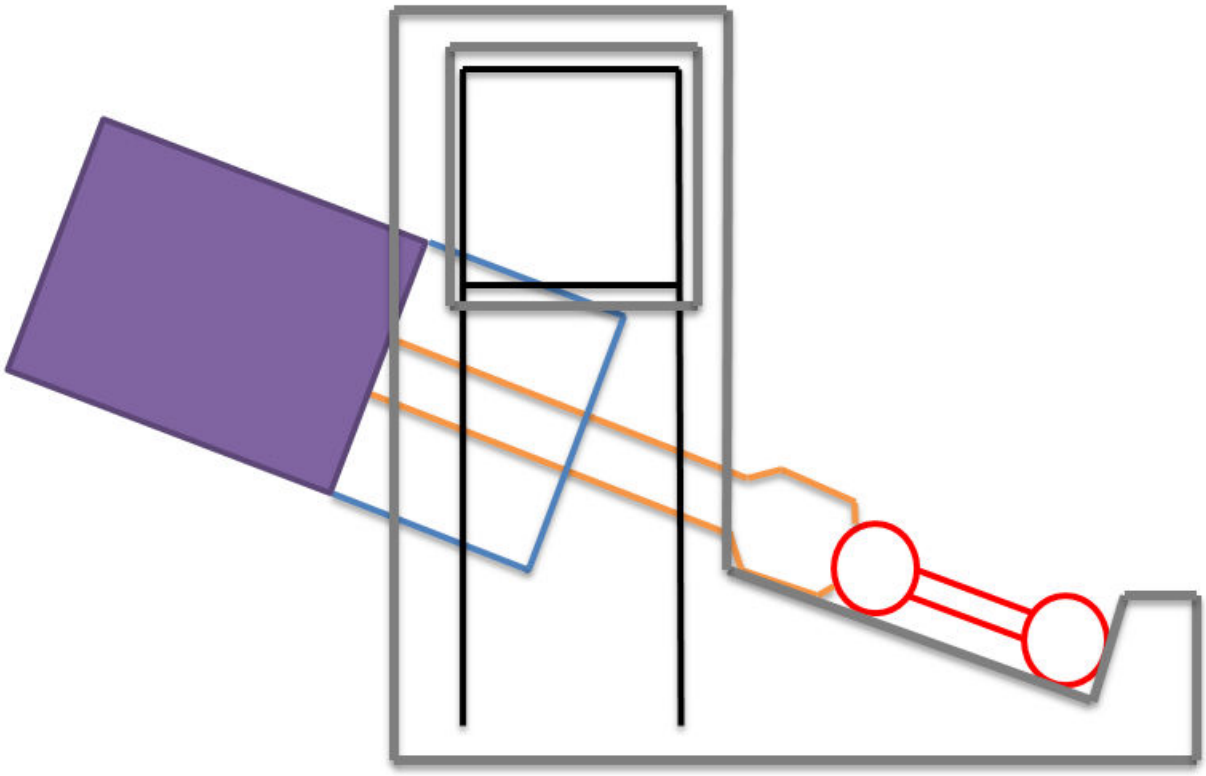

Figure 46: Design of tube, frame and attachment.

Figure 46 shows the design parameters that we are dealing with to scale.

- Black
  - Aluminum frame
- Red
  - Manifold
- Orange
  - Heat transfer pipes
- Blue and Purple
  - An evacuated tube, the purple is the absorber portion.
- Gray
  - Attachment design for the manifold to the frame, which will be referred to as the ‘claw’.

Figure 47: Real picture of manifold attachment.

Solutions

After many designs and materials we chose to go with our design called the 'claw' which is featured in Figure 46 and the material we chose it to made of was fiberglass. The following reasons led us to choose this design:

- The fiberglass "claw" will support the weight of the manifolds + 10 tubes.
- It will also provide a thermal barrier between the hot manifold tubes and the aluminum collector frame.
- Relatively cheap ($10 added cost / collector stand).

Now we must design the weatherproofing and maintenance access to the manifolds. It was decided that the weatherproofing should cover all sides of the manifolds. It does not have to be airtight, but it should provide general cover from rain, splashing, and restrict wind flow over the manifolds. Based on design constraint #2 above, any piece of weatherproofing that is actually touching the manifolds or vacuum tubes must be an insulating material (probably fiberglass). We also want to be able to have access to the manifold tubes and vacuum tube connection points to allow for easy installation and maintenance on the system.

5.2.3 Manifold Expansion

To account for the manifolds undergoing expansion it was critical that we understood by how much the copper manifold was going to expand and design a component that would allow for that expansion.

Table 18 shows the input data used for this calculation, and Table 19 shows the results of the calculation. It is shown that each manifold should expand by just over an inch. To account for this expansion we added steel braided flex hoses in-between for each manifold to manifold connection. Figure 48 is a picture of this type of connection installed.

Figure 48: Picture of our manifold to manifold connection with flex hoses.

Table 18: Input data for the expansion analysis of the manifold.

Input Data		
L_o = *length of pipe (in)*	89	
a= linear expansion coefficient(1/C)	1.70E-05	(Copper)
δt = *temperature difference (C)*	170	(~30C->200)
Calculated Data		
δl = *thermal expansion (in)*	0.25	

Table 19: The expansion results of the manifold for the temperature increase.

Number of Manifolds: In Series	1	2	3	**4**	5	6	7	8
δl = *thermal expansion (m)*	Length of pipe (in)							
Temp.diff. (degC)	89.01574794	178.0314959	267.0472	**356.063**	445.0787	534.0945	623.1102	712.126
30	0.04540	0.09080	0.13619	**0.18159**	0.22699	0.27239	0.31779	0.36318
40	0.06053	0.12106	0.18159	**0.24212**	0.30265	0.36318	0.42371	0.48425
50	0.07566	0.15133	0.22699	**0.30265**	0.37832	0.45398	0.52964	0.60531
60	0.09080	0.18159	0.27239	**0.36318**	0.45398	0.54478	0.63557	0.72637
70	0.10593	0.21186	0.31779	**0.42371**	0.52964	0.63557	0.74150	0.84743
80	0.12106	0.24212	0.36318	**0.48425**	0.60531	0.72637	0.84743	0.96849
90	0.13619	0.27239	0.40858	**0.54478**	0.68097	0.81716	0.95336	1.08955
100	0.15133	0.30265	0.45398	**0.60531**	0.75663	0.90796	1.05929	1.21061
110	0.16646	0.33292	0.49938	**0.66584**	0.83230	0.99876	1.16522	1.33168
120	0.18159	0.36318	0.54478	**0.72637**	0.90796	1.08955	1.27114	1.45274
130	0.19672	0.39345	0.59017	**0.78690**	0.98362	1.18035	1.37707	1.57380
140	0.21186	0.42371	0.63557	**0.84743**	1.05929	1.27114	1.48300	1.69486
150	0.22699	0.45398	0.68097	**0.90796**	1.13495	1.36194	1.58893	1.81592
160	0.24212	0.48425	0.72637	**0.96849**	1.21061	1.45274	1.69486	1.93698
170	0.25726	0.51451	0.77177	**1.02902**	1.28628	1.54353	1.80079	2.05804
180	0.27239	0.54478	0.81716	**1.08955**	1.36194	1.63433	1.90672	2.17911
190	0.28752	0.57504	0.86256	**1.15008**	1.43760	1.72513	2.01265	2.30017
200	0.30265	0.60531	0.90796	**1.21061**	1.51327	1.81592	2.11857	2.42123

6. Experimental Results

6.1 Solar Collector Performance

The instantaneous solar thermal collector output power is calculated by:

$$\dot{Q}_{sc} = \dot{m}_{oil} C_{p_{oil}} \Delta T_{sc} \quad \text{Equation 38}$$

The mass flow rate through the solar collectors was measured by a Coriolis flow meter, and the temperature difference is taken with two thermocouples placed at the input and output of the solar collectors. The available solar energy to the solar thermal collector system was calculated by:

$$\dot{Q}_{AVsc} = \Phi * A_{ap} \quad \text{Equation 39}$$

There was a precision spectral pyronameter on the collector plane which measures $\frac{power}{square\ area}$. Knowing this and the aperture area the available power to the solar thermal collector was calculated. Dividing equations 38 by 39 yields the efficiency of the solar collector thermal efficiency.

6.2 Chiller Performance

Conventionally a chiller's effectiveness is characterized by its coefficient of performance, COP. The COP is calculated by the following equation:

$$COP = \frac{Cooling\ Power\ Output}{Power\ Input} = \frac{Cooling\ Power\ Output\ of\ Chiller}{Solar\ Thermal\ Input\ to\ Chiller}$$

In our case the power input is the power provided directly by the collectors. This slightly de-rated the chiller performance by lumping in heat losses due to the glycol loop and heat exchanger.

The power input to the chiller by solar energy is calculated above.

In the natural gas mode the thermal input to the chiller is calculated by metering the natural gas consumption.

7. Results and Discussion

7.1 The Collectors

At the beginning of the summer it was noticed that the collectors were not performing very well. The efficiency of the system was in the twenties when it is projected to be in the thirties. These numbers were determined in the following manner: From Figure 13 we can see that the rated efficiency for the XCPC at an operational temperature of 170°C is 45%, with a direct normal incidence power of 800 W/m^2 and 20% diffuse; however, with this experiment we are conducting we are basing our available solar power off of the global radiance on the plane of the collector, which should yield, according to this model, roughly 35%.To diagnose why this was occurring we ran a test on July 18th that would tell us whether the performance loss was due to optical properties or heat loss.

The experiment consisted of running the system at ambient temperature and then seeing if the temperature difference between the inlet and outlet of the collectors was high [$\Delta T \geq 15°C$] or low[$\Delta T < 15°C$]. If the temperature difference across the collectors was low that would mean that there was some sort of optical loss. If the temperature difference across the collectors was high this would mean that there was a heat loss within the collectors that was preventing the energy from being conserved to the output.

Figure 49 shows the temperature difference of the collectors during our experiment. From the beginning of the day until 2:20pm the original experiment was run and the system was up to temperature, then at that time we began to cool down the experiment to ambient temperature. From about 2:45pm to 3:45 pm the experiment was running at ambient temperature producing a temperature difference of approximately 18°C which is more than double what it had been during operational temperatures of 180°C. This meant that our performance loss was due to heat loss.

Heat loss within the collectors is primarily due to the manifolds. Originally our team chose a new brand of insulation that comes in the form of a quilt. It was advised to us by the company that we could wrap it around a pipe; however, we would later find out that the company themselves had never done this before. When the insulation arrived at our lab it was already falling apart at the seams and when we tried to wrap it around the pipe the tension and stress it caused within the material caused most of the insulation to come undone and spill out at the seams. Therefore, we

already had an idea that the insulation we purchased was not going to work perfectly, but we did not see it performing this bad. Due to time constraints we decided to keep this insulation and on cover the old insulation with an extra inch of insulation using FiberFrax, which is a fiber ceramic.

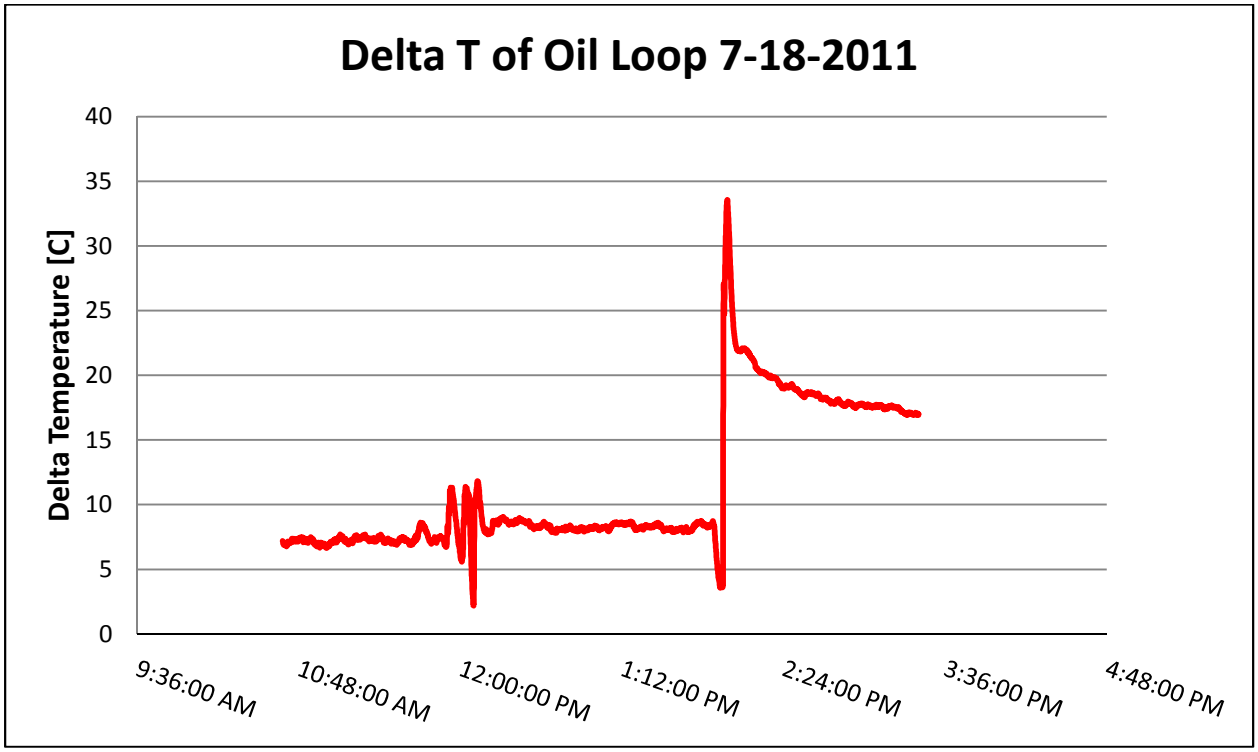

Figure 49: Delta T of the solar collectors during an efficiency experiment.

Figure 50 shows the results of the additional insulation on the manifolds by comparing the efficiencies of the collector before and after the insulation was added. The difference on average throughout the operational period of the experiment is an additional 3% putting our collectors averaging somewhere between 30-35% during operation, as compared to 26-31% before. Both of the graphs also show the efficiencies of the collector starting at the lower range and growing linearly with time towards the higher range. The reason for this being that the system is reaching steady state for its heat exchange. Meaning that the frame, insulation, etc. is warming up with the system and thereby taking away less heat from the working medium which increases the collector's efficiency.

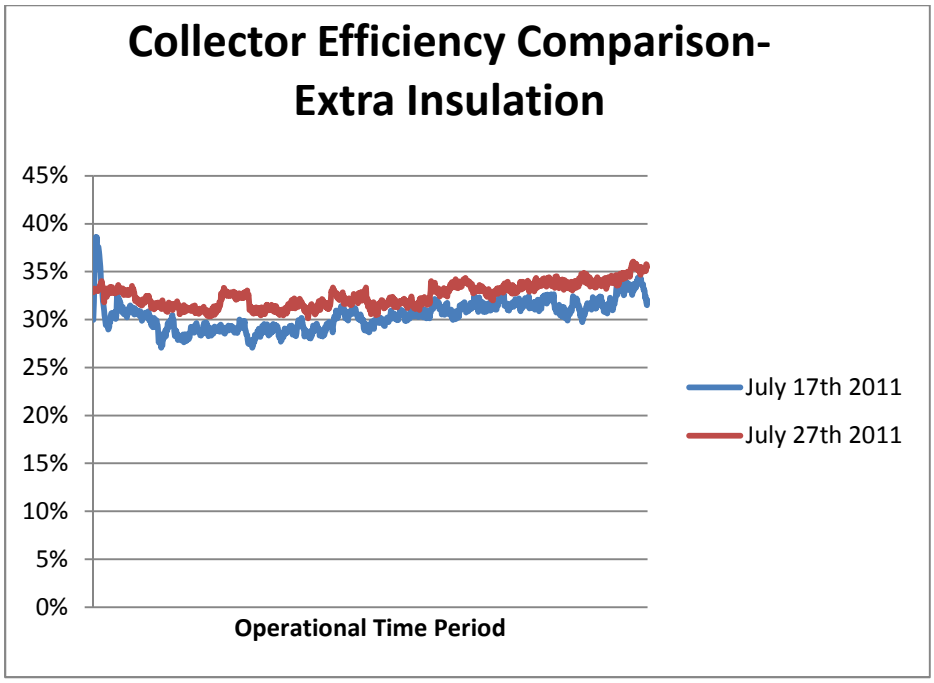

Figure 50: Collector efficiency comparison of extra insulation.

The collectors continued to perform with an average efficiency of 33% until early September. It was quickly observed that the collectors were quite dirty due to the farmers working on their land, which is within a 10 yards of our collectors, with very large tractors. Lots of dirt had settled on our collectors and they needed to be cleaned. Figure 51 shows the comparative difference of the collectors' efficiency before and after they were thoroughly cleaned. The average difference is about 5%, this is fairly large difference. This concludes that when the collectors are very dirty, ie: have so much dust on them it's difficult to tell the color of the tube, they must be cleaned. However, had it not been for the tractors these collectors would have performed fine as they had been, and we would have continued to clean them on a quarterly basis.

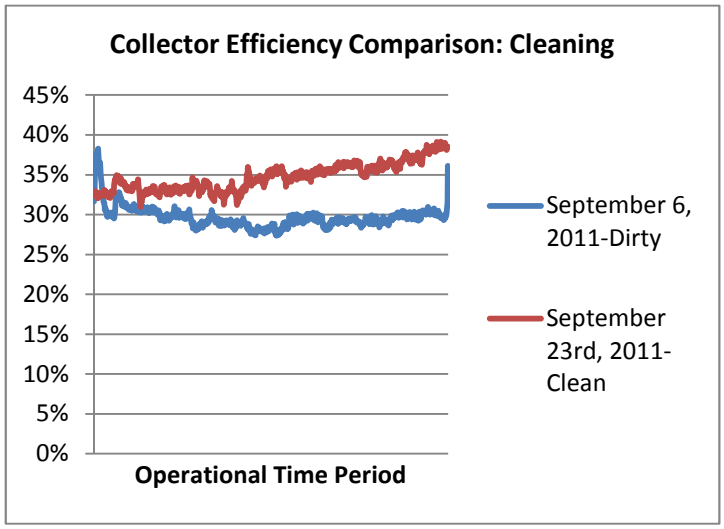

Figure 51: Collector efficiency comparison of the collectors dirty vs. clean.

7.2 The Chiller:

There are two critical variables to the chiller: The coefficient of performance, COP, and the outlet temperature of the chilled water. The double effect absorption chiller is designed to produce 7°C water at a rated COP of 1.1. COP is calculated by taking the outgoing cooling power of the machine divided by the incoming power of the machine; however, due to our glycol loop not producing reasonable answers we calculated our COP by dividing cooling power produced by collector power produced. This COP should be slightly less than what it's rated for at maximum capacity, approximately. .9.

It was observed through our experimentation that the chiller was neither producing water below 15°C nor maintaining a COP of .9. After running various experiments, we have concluded why our chiller was not performing well.

First, is that the chiller had a poor vacuum. Absorption chillers are directly dependent on how well the condensers are vacuumed, without a good vacuum the water being used in the absorber will be warm and the evaporative cooling will happen at a higher temperature; thereby, producing warmer water. Second, was that the load that was being put onto the chiller was too low. If there is too low of a load onto the chiller then the amount of heat the chiller can extract is less, and the COP will be low. Third, all of the filters within the chiller needed to be cleaned. Without the filters being cleaned the proper amount of water will not flow through the system and the rate at which the machine can cool will slow down and also produce warmer water. The final factor was that the city water line that was incoming to the chiller was $20\ °C$ hotter than it should have been. This water is used in the condenser and if it is $\sim 10°C$ warmer than the requirement it will not be able to condense the vapor which will prevent the condensation from entering into the evaporator.

All of these factors were fixed between the dates of the September 7, 2011 and September 22nd, 2011, and the results are in figures 4 and 5. The average COP went from .7 to .9, and the average outlet temperature of the chilled water went from 15°C to 7°C.

Figure 53 shows that for September 23rd the average COP of the chiller is .9 which is what we designed the system for. When the system is maintained, for example, chiller is vacuumed well and the collectors are clean, the average COP is .9 and it is stable.

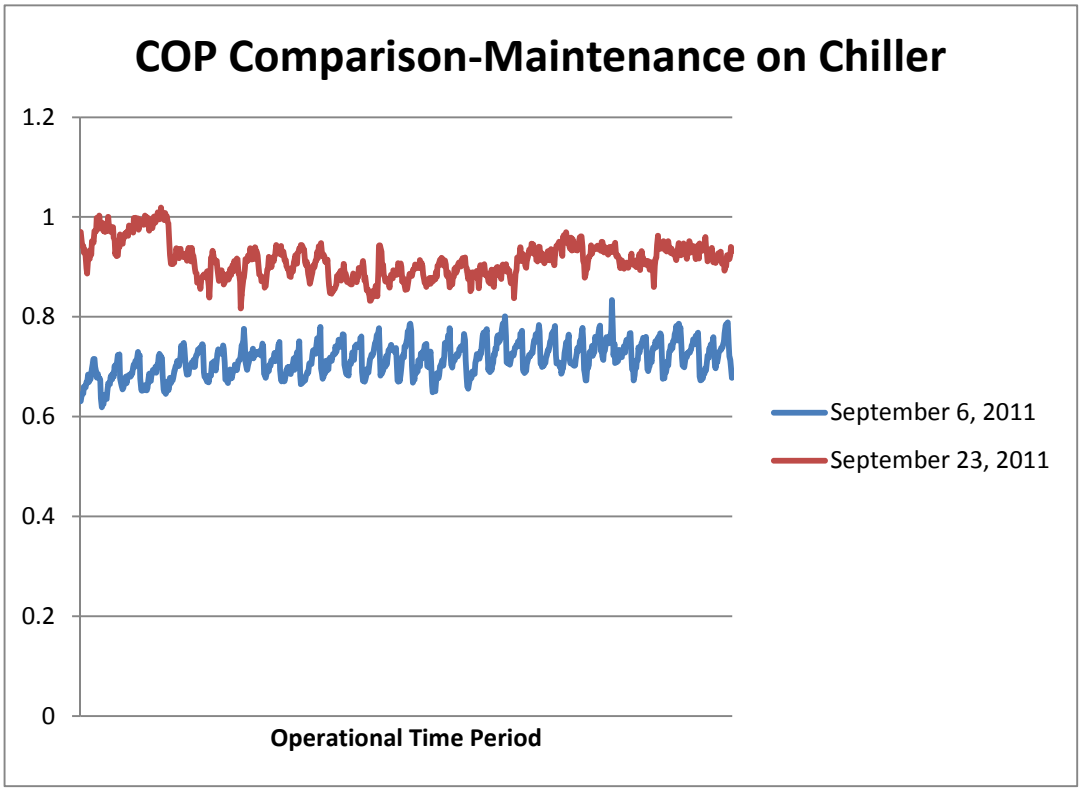

Figure 52: COP comparison on maintenance of chiller.

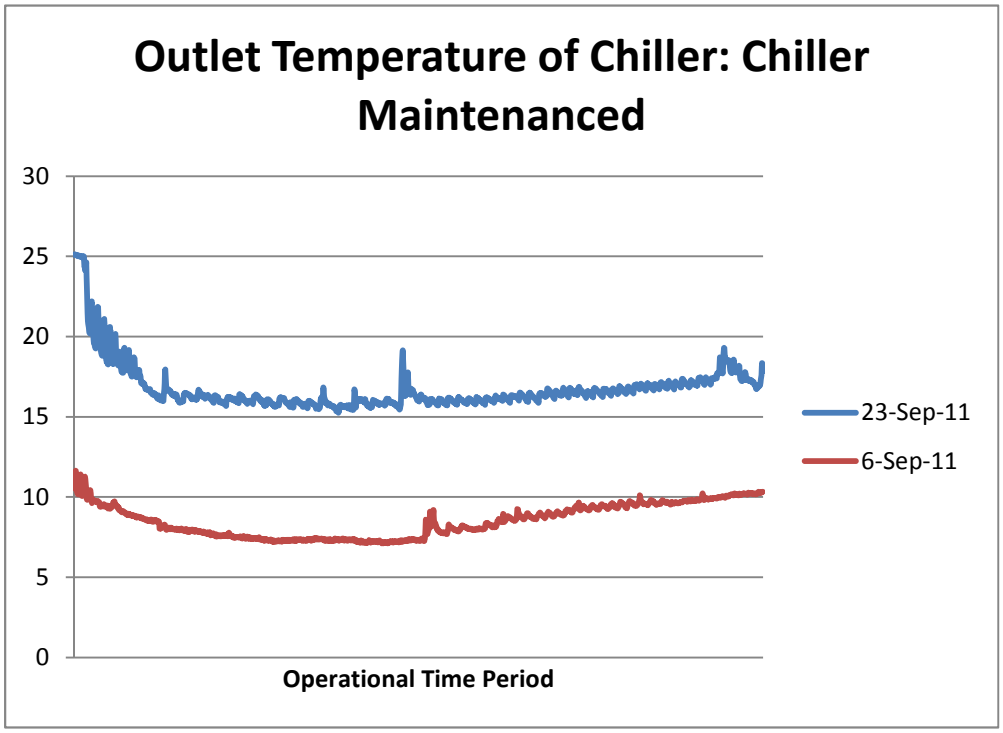

Figure 53: Outlet temperature of the chiller when it is maintained vs. when it is not.

7.3 The System:

Figure 54 shows that the non-tracking XCPC evacuated solar collector array at Castle Air Force Base provides enough energy for the double effect chiller to run on in order for the natural gas to turn off. Through all of our experiments it has been observed that once the solar collectors provide enough energy to run the system the natural gas does not need to be turned on again until approximately four hours after solar noon. It has also been shown that despite fluctuations with the solar insolation the COP of the chiller is fairly constant. This is primarily due to the chiller having a large high temperature generator which stores a lot of energy and does not fluctuate its performance with spikes in it incoming power. The fluctuations in the chiller towards the end of the day were caused by an inconsistent use of the radiator in the building. There were times when the original air conditioner in the building would kick on towards the end of the day and cause the temperature to fluctuate within the water loop of the chilled water.

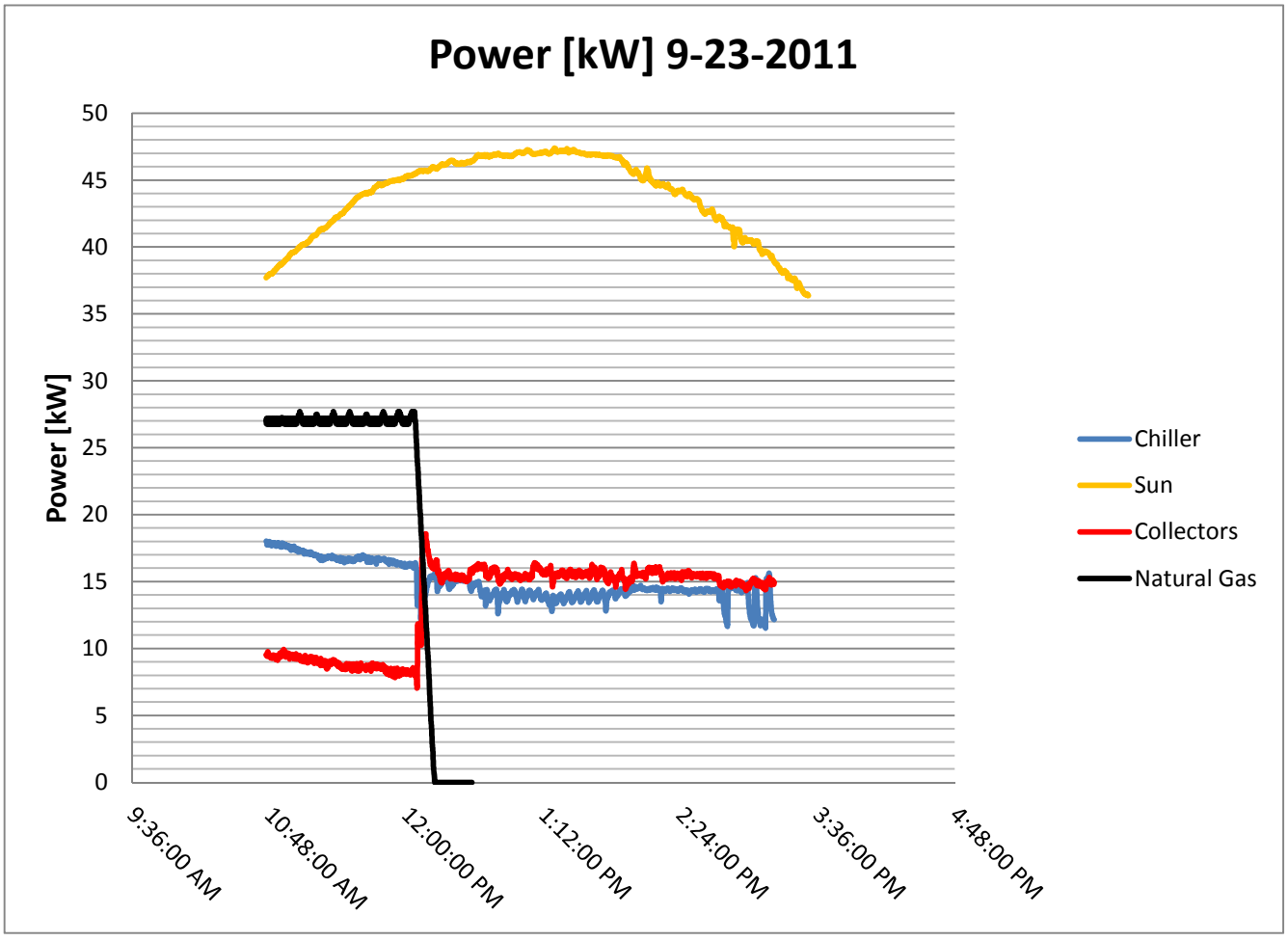

Figure 54: Power of solar, chiller, natural gas and sun vs. operational time.

8. Conclusion

There were a lot of lessons learned throughout the design, building and testing of this project.

A big lesson that was learned for designing the XCPC for the NS orientation was that it would be best if there was an alternative solution for cleaning the troughs. With the collectors having a plastic mold the static attracted dust and it was entirely enclosed so the dirt and debris would often get stuck at the bottom of the trough. Also the frame is fairly robust for such a design. At the time of designing it the team wanted to ensure that it wouldn't break and it would be sturdy; however, it cost a lot of money and took far more time to install that it should have. Looking at what is available for standard thermal systems and pv systems there is an opportunity for the frame cost to be reduced and become simpler.

Storage capacity was far too great for this system. There was a 50 gallon storage tank along with a 40 gallon expansion tank, that could have been the same 40 gallon tank and the entire system including these tanks only held 110 gallons of fluid. The original intention was to store the heat overnight to not cause the pump problems in the morning to turn on du to the viscosity of the fluid; however, what was observed was the fluid warmed up easily in the morning and there was no need to have the storage we had in place. Instead the storage caused the system hours of warm up time in the morning. In the future, try to combine the storage tank with the expansion tank and make it as small as possible.

Insulation is a key factor that should be more thoroughly evaluated. There was a 25% heat loss in the system that was primarily caused by bad insulation. For the manifolds there were responsible for majority of the heat losses. This was due to the insulation chosen, how it was installed and how it was weatherized. After many experiments it has been concluded that there are better insulation materials such as aerogel insulation that would be a better fit for the manifolds and there are off the shelf manifold boxes that enclose the insulation that do a remarkable job at weatherizing the insulation. Both of these are highly recommended to be looked into.

The glycol loop was incredibly difficult to design, install, find parts for and even maintain. Since this loop was pressurized it was difficult to find parts that could operate at a high temperature, high pressure and have a low power rating while being efficient. It was dangerous to have a 1 MPa pressurized loop with ethylene glycol. After many conversations with the chiller vendor, BROAD, it was decided that the glycol loop would be unnecessary and that the mineral oil in the collectors could be run through chiller. In the future it is advised that experiments be run without the glycol loop and for the oil to go from the collectors to the chiller.

A huge factor that prohibited research on a daily basis was all of the leaks from the tubes to the manifolds. The manifolds and tubes are connected by a threaded connection. As the system goes through a $\Delta T \sim 160°C$ the metals contract and expand, the working medium becomes less viscous and there were many leaks that came of this. To help prevent this in the future one should house the manifolds atop of the collectors and look into compression fittings rather than threaded fittings for the connection of tube to manifold.

To be done in the future, with this research project specifically:
On a tight budget:

1. Take out the storage tank on the oil loop.
2. Take out the glycol loop, run mineral oil from collector directly to the chiller.
    1. Be very careful to get out all water of chiller so as not to have steam!
3. Get the wind meter, ambient temperature thermometer and NIP to work on site so as to take more accurate data.

On a larger budget:

4. Redo all of the insulation on the manifolds and put in a manifold box.

On an even larger budget:

5. Manufacture new collectors out of aluminum
6. Orient collectors with manifolds on the top
7. New way to connect evacuated tubes to manifolds, such as compression fittings

Overall the XCPC solar powered double effect absorption cooling project was a success. What needs to be developed is a systematic approach to not only designing these systems but evaluating them as well. This will normalize data that is being researched around the world and will allow the technology and data to be easily understood on a global scale. Securing a strong foundation for the system to be analyzed will allow researchers to continue to develop state of the art solar collectors and chillers and integrating them into a well-designed system that fits in the overall goal of being energy efficient, environmentally friendly and economically reasonable.[xxiv]

9. Appendix

9.1 Acronyms

CEC California Energy Commission

COP Coefficient of Performance

CPC Compound Parabolic Concentrator

CSP Concentrated Solar Power

HTG High Temperature Generator

IAM Incidence Angle Modifier

ICPC Integrated Compound Parabolic Concentrator

EW East-West

kW Kilowatt

kWh Kilowatt hour

LiBr Lithium-Bromide

NS North-South

RT Reflectech

UCM University of California, Merced

USRT United States Refrigeration Ton

UT U-tube

VC Vapor Compression

XCPC External Compound Parabolic Concentrator

1.1 Nomenclature

$\eta_{EW} = Efficiency\ of\ EW \eta_{NS}$

$P_{EW} = Power\ int\ the\ collector, of\ EW$

$P_{NS} = Power\ into\ the\ collector, of\ NS$

$C = Concentration$

$C_{EW} = Concentration\ of\ EW$

$C_{NS} = Concentration\ of\ NS$

$\Phi, Total\ Irradiation\ accepted\ by\ concentrator, \frac{W}{m^2}$

$I_d = Diffuse\ Irradiation, based\ off\ of\ 1000 \frac{W}{m^2}$

$\dot{Q}_{wi} = Heat\ flow\ through\ unshaded\ windowns\ of\ Area\ A_{wi}$

$\dot{Q}_{wish} = Heat\ flow\ through\ shaded\ windowns\ of\ Area\ A_{wish}$

$\dot{Q}_{wa} = Heat\ flow\ through\ unshaded\ walls\ of\ Area\ A_{wia}$

$\dot{Q}_{wash} = Heat\ flow\ through\ shaded\ walls\ of\ Area\ A_{wash}$

$\dot{Q}_{rf} = Heat\ flow\ through\ roof\ Area\ A_{rf}$

$\dot{Q}_i = Heat\ load\ resulting\ from\ infiltration\ of\ ventilation$

$\dot{Q}_w = Latent\ heat\ load$

$I_{hb} = Beam\ component\ of\ insolation\ on\ horizontal\ surface$

$I_{hd} = Diffuse\ component\ of\ insolation\ on\ horizontal\ line$

$I_r = Ground - reflected\ component\ of\ insolation$

$W_o, W_i = Outside\ and\ Inside\ humidity\ ratios$

$U_{wi}, U_{wa}, U_{rf} = Overall\ heat$
$- transfer\ coefficients\ for\ windows, walls\ and\ roof, including\ radiation$

$m_a = Net\ infiltration\ and\ ventilation\ mass\ flow\ rate\ of\ dry\ air$

$C_{pa} = Specific\ heat\ of\ air$

$T_o = Outside\ dry - bulb\ temeprature$

$T_i = Indoor\ dry - bulb\ temprature$

$F_{sh} = Shade\ factor, 1 = unshaded, 0\ completely\ shaded$

$\alpha_{s,wa} = wall\ solar\ absorptance,$

$\alpha_{s,rf} = roof\ solar\ absorptance$

$i = solar\ incidence\ angle\ on\ walls, windows\ and\ roof$

$h_o, h_i = outside\ and\ inside\ air\ enthalpy$

$\alpha = solar\ altitude\ angle$

$\lambda_w = latent\ heat\ of\ water\ vapor$

$\tau_{b,wi} = window\ transmittance\ for\ beam\ (direct) insolation$

$\bar{\tau}_{d,wi} = window\ transmittance\ for\ diffuse\ insolation, and \bar{\tau}_{r,wi}$

$= window\ transmittance\ for\ ground\ reflected\ insolation$

9.2 Solar

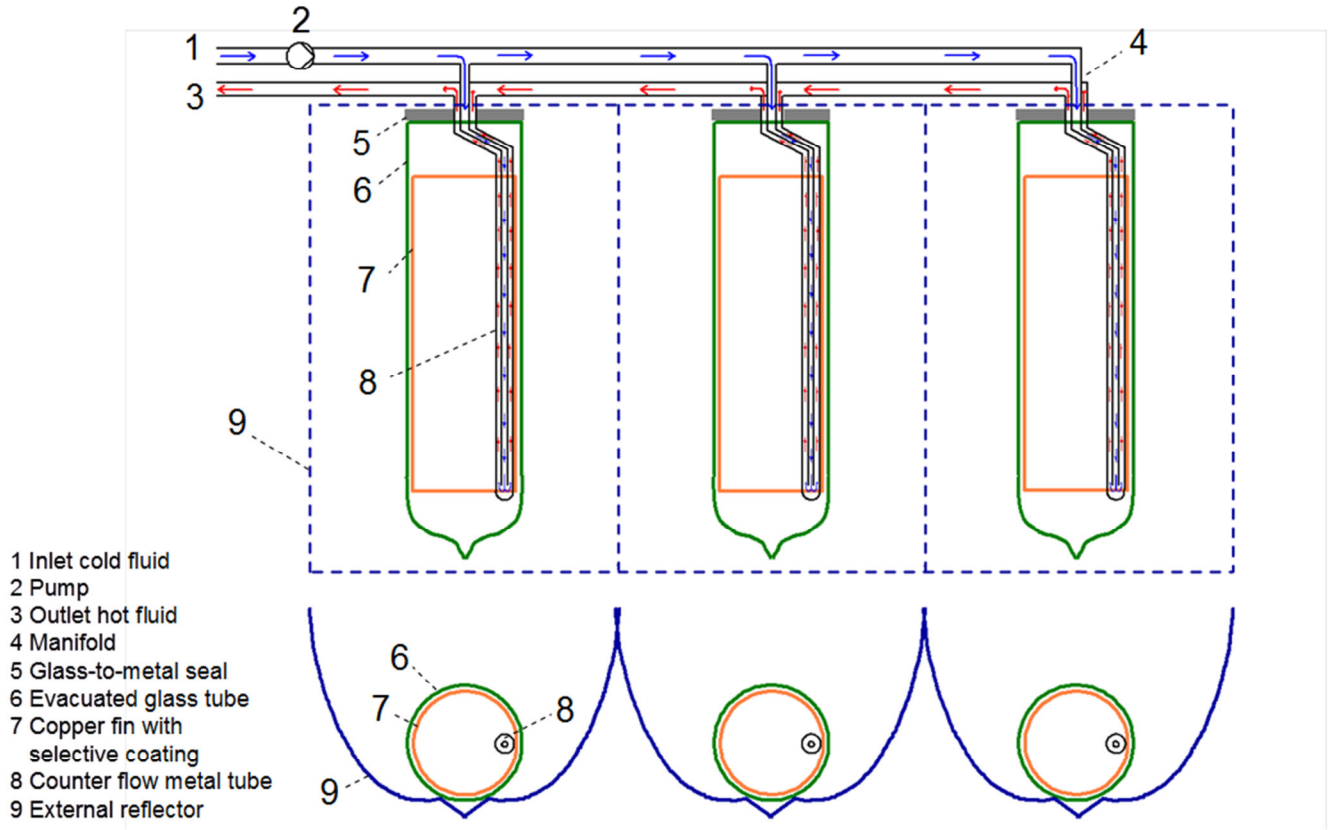

Figure 55: Top and cross sectional view of the XCPC with a counter flow tube.

9.2.1 Testing Method:

Collector Thermal Efficiency

The instantaneous collector efficiency η_{coll} can be defined as

$$\eta_{coll} = \frac{\dot{Q}_{coll}}{A_A G}$$

with

$$\dot{Q}_{coll} = \frac{\dot{Q}_{cal} \cdot \Delta T_{coll}}{\Delta T_{cal}},$$

$$G = G_{direct} + \frac{G_{diffuse}}{C_x},$$

$$G_{diffuse} = G_{hemi} - G_{direct}$$

Where

$\dot{Q}_{coll}$: useful power extracted from collector,

$\dot{Q}_{cal}$: calorimeter power,

ΔT_{coll}: temperature difference between collector fluid at collector outlet and inlet,

ΔT_{cal}: temperature difference between the fluid at the calorimeter outlet and inlet,

A_A: effective aperture area of collector – we define this area as the length of the active area of the absorber tube (which is the area covered by the selective coating) times the width of the reflector

G: solar irradiance captured by concentrating collector,

G_{direct}: direct normal irradiance (measured with a pyrheliometer),

$G_{diffuse}$: diffuse sky irradiance,

G_{hemi}: hemispherical irradiance (measured with a pyranometer).

C_x: geometric concentration of collector

Temperature dependence of collector efficiency

The temperature dependence of the instantaneous efficiency η_{coll} can be represented graphically as a function of the reduced temperature T^*. The thermal performance of the collector can then be characterized by the two coefficients a_1 and a_2, which are determined by a least square parabolic curve fit:

$$\eta_{coll} = \eta_o - a_1 T^* - a_2 G (T^*)^2$$

with

η_o: optical efficiency

T^*: reduced temperature

$$T^* = \frac{T_{in} - T_{amb}}{G}$$

where

T_{amb}: ambient temperature,

T_{in}: collector inlet temperature,

a_1 and a_2: coefficients determined from least squares parabolic curve fit, and the value of G in the formula above is assumed to be 1000 W/m^2.

Description of Test Loop

The test facility used is a closed loop system that includes a circulating oil temperature controller with integrated pump and expansion tank (see Figure 56). The circulating oil temperature controller provides a selectable constant temperature (up to 260°C) to the heat transfer fluid that is circulated through the collector. The loop further includes a flow meter and temperature sensors before and after the collector. There are flow mixers introduced into the loop before each temperature sensor. The solar collector is mounted on a dual axis tracker to allow the measurement of collector performance under controlled incidence angles.

The test facility further includes a meteorological station with a Precision Spectral Pyranometer and a Normal Incidence Pyrheliometer that are both mounted on the same tracker as the solar collector, a thermometer to measure the ambient temperature, and an anemometer.

In addition, a calorimeter was used as an improved method of determining the instantaneous thermal efficiency without depending on knowing the heat capacity of the oil.

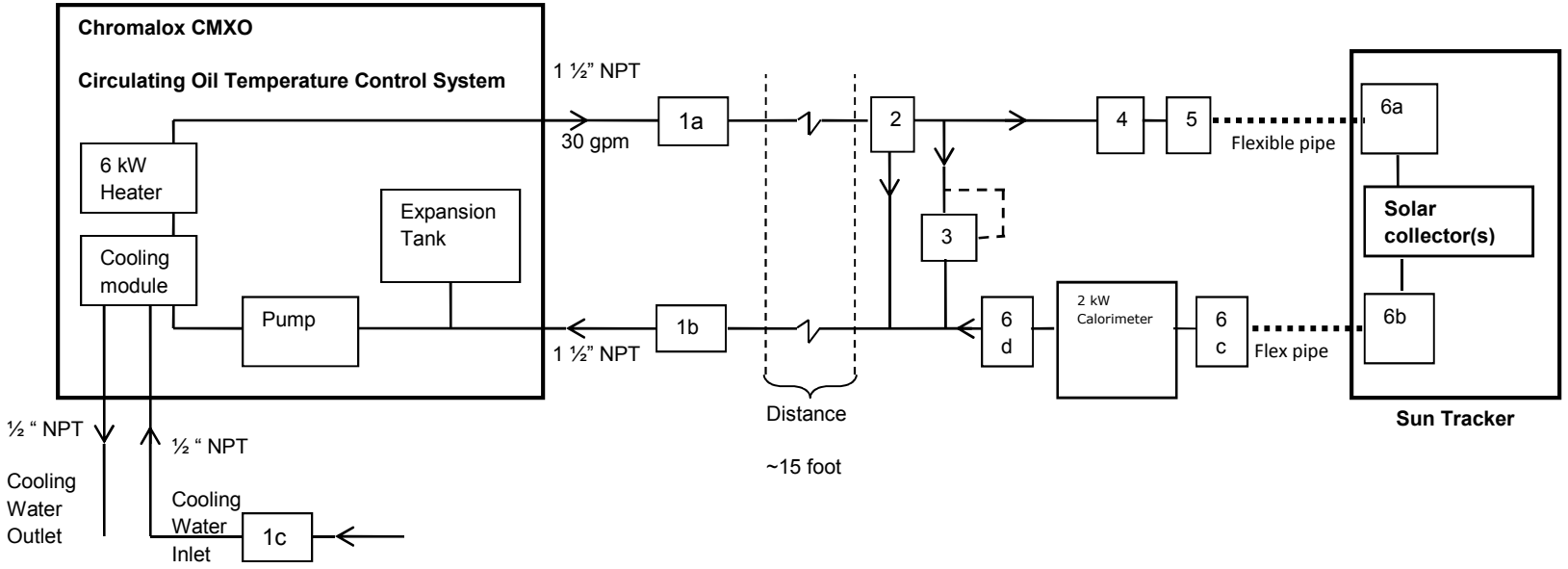

1abc	Ball valves
2	Diverter valve
3	(Back)pressure regulating valve
4	Flow control valve
5	Flow meter
6ab	Temperature sensors w/ flow mixers
7	Calorimeter (2kW)

1abc	Gate valves
2	Diverter valve
3	(Back)pressure regulating valve
4	Flow control valve
5	Flow meter
6abcd	Temperature sensors

Figure 56: Schematic of the test facility for CEC grant.

The data from the flow meter, the temperature sensors and the meteorological station were recorded through a data acquisition system.

Instrumentation

Circulating oil temperature controller: Chromalox CMXO 6kW (with integrated pump and expansion tank)

Temperature sensors:	Type-K thermocouples from Omega
Flow meter:	Micro Motion Coriolis F-Series sensor
Flow control valve:	Valtek ½" Flow Top Control Valve
Back pressure regulating valve:	Jordan: 1" 50-100-S6-I5-S6-Y-8-21-S6-MD Pressure Control Valve
Sun tracker:	Wattsun AZ-125 dual axis tracker
Calorimeter:	Custom made by Valin Inc.
Pyranometer:	Eppley Precision Spectral Pyranometer
Pyrheliometer:	Eppley Normal Incidence Pyrheliometer
Data Acquisition System 1:	Agilent 34970A Data Acquisition/Switch Unit
Data Acquisition System 2:	Acquisuite Data Acquisition System

9.3 The System

9.3.1 Chiller

Table 20: Chiller burner refrence table.

Burner and Heat Source Valve operation reference table		
HTG temp	Two levels burner(High/Low)	Four levels burner/valve(Heat source valve, 4-20mA burner)
4˚C above the target temperature / HTG maximum allowed temperature	Stop	Close/Stop
2˚C above the target temperature	maintain	maintain
Target temperature	Low(if stopped, now start)	lvl 1(If stopped, now start)
2˚C below the target temperature	maintain	lvl 2
4˚C below the target temperature	High	lvl 3
6˚C below the target temperature	High	lvl 4
Above the high burner starting temperature(about 90˚C)	Low to High	lvl 1 to lvl 2, 1 min later to lvl 3, 1 min later to lvl 4
Below the high burner starting temperature(about 90˚C)	High to Low	To lvl 1

9.3.2 Computer Programs

9.3.2.1EW vs NS

With the given matlab codes, despite your inlet temperature, diffuse irradiation or where you are located, this program should identify which CPC design type, East West or North South is optimal a solar thermal system, strictly in terms of energy only.

PlayId: This file has a for loop that iterates through the temperature and allows one to compute a string of values to use for different temperatures in the evaluation of the break even function. The plot is of the temperature vs. the diffuse level, Id.

fId: This file creates the break even function and takes as input the Id level and the string of values for the temperatures.

PlayID

```
clc
clear all
%The for loop runs through temperature iterations creating a string that I
%can use for input that will allow me to compute the break even function
%for multiple temperatures.
Ti = 70;
dT = 10;
for i = 1:14
    Ti = Ti + dT;
    Temp(i) = Ti;
    Id(i) = fzero(@(x)fId(x,Ti),100);
end
%This plot has the temperature as the x-axis ranging from 80-200C, and the
%Y-axis is the Diffuse level. (%Diffuse of Irradiation. Based on 1000w/m^2)
plot(Temp,Id,'x-')
xlabel('Inlet Temperature [C]')
ylabel('Diffuse [W/m^2]')
title('Break Even for NS,EW AL,UT,ambient = 35')
```

fID

```
function f = fId(Id, Ti)%Evaluates the function, which is the break even analysis of EW vs. NS
atany temperature, and any diffuse level, Id.
Ta=35;          %Ambient Temperature
c1=1.8;         %EW Concentration
c2=1.15;        %NS Concentration
N1=.664;        %No for Ew
N2=.691;        %No for NS
a1=.908;        %The first co-efficient for the equation for EW
a2=.00239;      %The second ""
b1=1.08;        %The first coefficient for the equation for NS
b2=.00351;      %The second ""
Pew=(((1-c1)/(c1))*Id +1000);  %Power of EastWest because assumed 1m^2 area
Pns=(((1-c2)/(c2))*Id +1000);  %Power of NorthSouth because assumed 1m^2 area
New=N1-a1*((Ti-Ta)/(Pew))-a2*Pew*((Ti-Ta)/(Pew))^2;       %Efficiency for EW
Nns=N2-b1*((Ti-Ta)/(Pns))-b2*Pns*((Ti-Ta)/(Pns))^2;       %Efficiency for NS
f = New*Pew-Nns*Pns;
return
```

9.3.3 Cooling Load Program

```
B=90;
L=37;
Hs=0;
N=204;
Ss=-23.44*cosd((360/365)*(N+10));
To=100;
Ti=72;
Arf=11*56;
AwaNS=12*56;
AwaEW=12*11;
Awi=12.5;
Awish=0;
Awash=0;
Alpha=.12;
Fsh=.1;
Tbwi=.6;
Tdwi=.81;
Trwi=.6;
Ihb=185;
Ihd=80;
Ir=70;
Uwa=0.19;
Uwi=1.09;

Urf=0.061;
Qw=.3;

IncidenceAngle=cosd(B)*cosd(L-Ss)+sind(B)*sind(L-Ss)
SolarAltitude=cosd(L-Ss)

SouthFacingWindowLoad_BTUperHR=
Awi*(Fsh*Tbwi*Ihb*(IncidenceAngle/SolarAltitude)+Tdwi*Ihd+Trwi*Ir+Uwi*(To-Ti))

ShadedWindowLoad_BTUperHR=Awish*Uwi*(To-Ti)

SouthFacingWallLoad_BTUperHR=(AwaNS-
Awi)*(Alpha*(Ir+Ihd+Ihb*(IncidenceAngle/SolarAltitude))+Uwa*(To-Ti))

ShadedWallLoad_BTUperHR=Awash*(Uwa*(To-Ti))

RoofLoad_BTUperHR=Arf*(Alpha*(Ihd+Ihb*(IncidenceAngle/SolarAltitude))+Urf*(To-Ti))

LatentHeatLoad_BTUperHR=Qw*(AwaNS*2+AwaEW*2-12*Awi)*(Uwa*(To-Ti))
```

TotalLoad_BTUperHR=SouthFacingWindowLoad_BTUperHR+ShadedWindowLoad_BTUperHR+SouthFacingWallLoad_BTUperHR+ShadedWallLoad_BTUperHR+LatentHeatLoad_BTUperHR+RoofLoad_BTUperHR

TotalLoad_USRT=(TotalLoad_BTUperHR)/12000

9.3.4 Heat Exchanger: Oil to Glycol

Specification Sheet

Unit : B3-052-30-M

Ref : U of C Merced **Date : 07-24-2009**

Design Duty : 21.9 kW

			Side 1	Side 2
Fluid Name		:	Dowtherm 4000 40%	Duratherm 600
Inlet Temperature	°C	:	161	180
Outlet Temperature	°C	:	170.34	168
Mass Flow Rate	GPM	:	9.16	16
Pressure	bar	:	-	-

Physical Properties of Fluid :

Reference Temperature	°C	:	165.67	174
Viscosity	mPas	:	0.288	1.4
Viscosity Wall	mPas	:	0.284	1.505
Density	kg/m³	:	962.8	749
Specific Heat Capacity	kJ/kg,°K	:	3.944	2.417
Thermal Conductivity	W/m,°K	:	0.446	0.134

Designed Plate Heat Exchanger :

Heat Load	kW	:	21.9	
Total Heat Transfer Area	m²	:	1.43	
Log Mean Temperature Difference	°K	:	8.26	
Overall H.T.C.	W/m²,°K	:	2193/1860	
Calculated Pressure Drop	psi	:	1.77	4.14
Number of Channels		:	1*14M	1*15M
Port Hole Diameter	mm	:	25	25
Number of Heat Transfer Units	NTU	:	1.131	1.453
Total Number of Plates		:	30	
Over surfacing	%	:	18	
Fouling Factor	m²,°K/kW	:	0.0818	
Volume	dm3	:	1.358	1.455
Length Of Plate Package	mm	:	82.5	
Weight (Empty)	kg	:	8.7	
Max. Operating Pressure	bar	:	45	
Test pressure	bar	:	56	
Max. Operating Temperature	°C	:	195	
Flow Type		:	Q3=>Q4	Q1=>Q2

9.3.5 Fluids

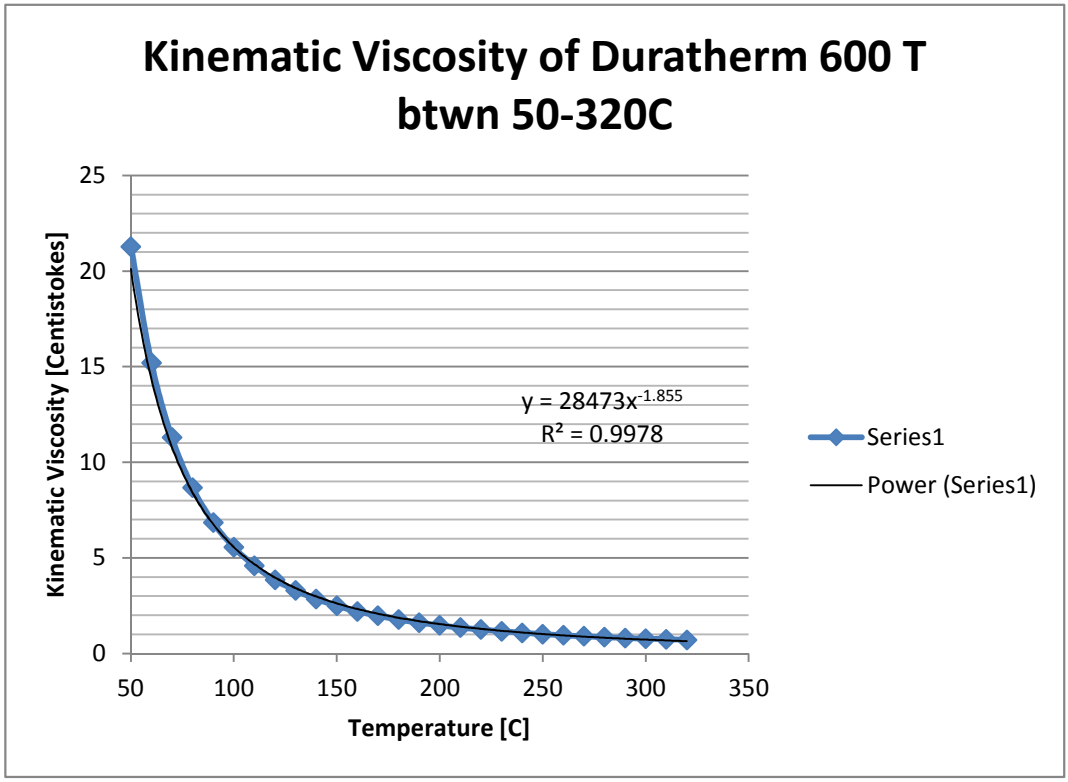

Figure 57: Kinematic Viscosity vs. temperature for the mineral oil.

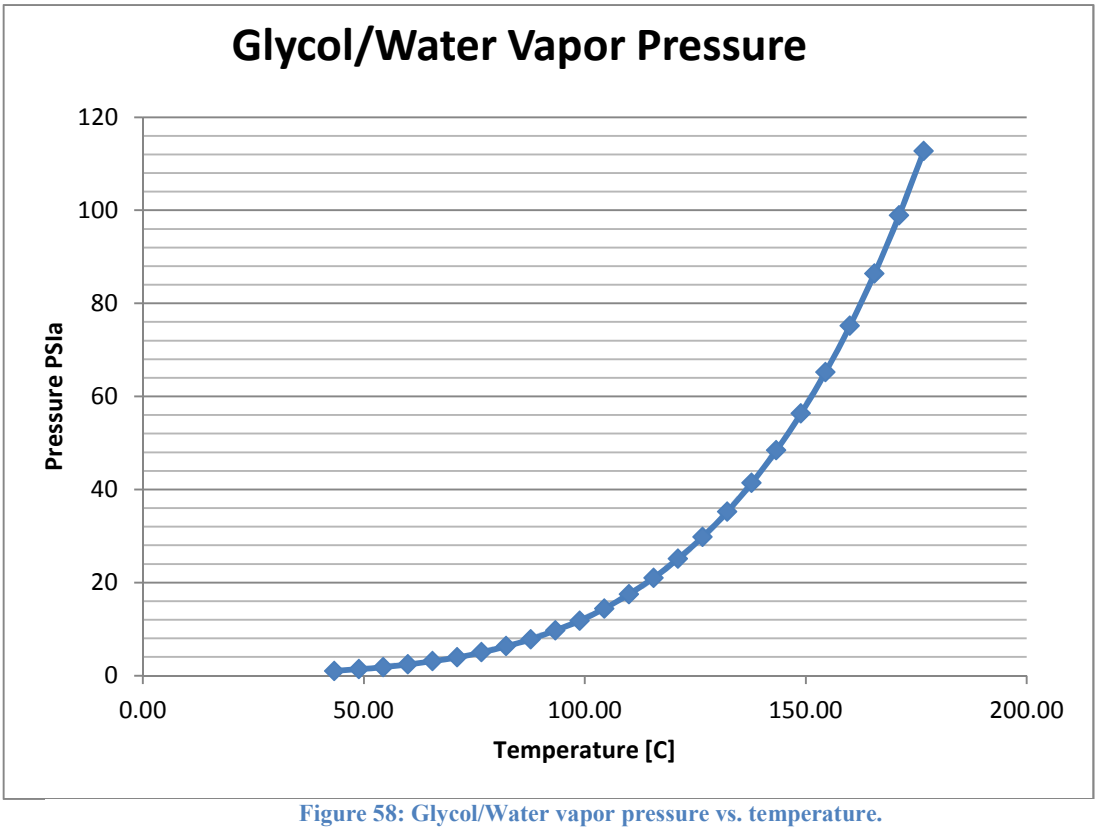

Figure 58: Glycol/Water vapor pressure vs. temperature.

[i] Foneseca, Alfonso Tovar. *Performance Assessment of Three Concentrating Solar Thermal Units Designed with XCPC Reflectors and Evacuated Tubes, Using an Analytical Thermal Model*. Thesis. University of California, Merced, 2008. Print.

[ii] *U.S. Energy Information Administration (EIA)*. Web. 1 July 2009. <http://www.eia.gov>.

[iii] Kreith, F., Lof, G.O.G., Rable, A. and Winston, R. (1980) "Solar collectors for low and intermediate temperature applications". Progress in Energy and Combustion Science 6(1):1-34

[iv] Balaras, C. A., Grossman, G., Henning, H.-M., Infante Ferreira, C.A., Podesser, E., Wang, L. and Wiemken, E. (2007) "Solar air conditioning in Europe-an overview" Renewable and Sustainable Reviews **11**(2):299-314

[v] Smitabhindu, R., Jajai, S. and Cahnkong, V. (2008) "Optimization of a solar-assisted drying system for drying bananas". Renewable Energy 33(7): 1523-1531

[vi] Mills, D. (2004) "Advances in solar thermal electricity technology". Solar Energy 76(1-3):19-31

[vii] Winston, R. 2009. *Design and Development of Low-cost, High-temperature, Solar Collectors for Mass Production*. California Energy Commission PIER Public Interest Energy Research Program Report: CEC-500-05-021

[viii] Lazzarin, R. M., P. Romagnoni, and L. Casasola. "Two Years of Operation of a Large Solar Cooling Plant." Print.

[ix] Hang, Yin, Ming Qu, and Fu Zhao. "3. Economical and Environmental Assessment of an Optimized Solar Cooling System for a Medium-sized Benchmark Office Building in Los Angeles, California."Renewable Energy 36.1 (2010): 648-58. Print.

[x] Marc, Olivier, Jean-Philippe Praene, Alain Bastide, and Franck Lucas. "Modeling and Experimental Validation of the Solar Loop for Absorption Solar Cooling System Using Double- glazed Collectors."Applied Thermal Engineering 31 (2011): 268-77. Print.

[xi] Syed, A., M. Izquierdo, G. Maidment, J. Missenden, A. Lecuona, and R. Tozer. "A Novel Experimental Investigation of a Solar Cooling System in Madrid." International Journal of Refrigeration 28 (2005): 859-71. Print.

[xii] Tsur, Yacov, and Amos Zemel. "Long-Term Perspective on the Development of Solar Energy." Solar Energy 68.5 (2000): 379-92. Print.

[xiii] Agyenim, Francis, Ian Knight, and Michael Rhodes. "Design and Performance of a Solar Powered Heating and Cooling System Using Silica Gell Water Adsorption Chiller." Solar Energy 84 (2010): 735-44. Print.

[xiv] K. Gommed and G. Grossman, Experimental investigation of a liquid desiccant system for solar cooling and dehumidification, Solar Energy 81 (2007), pp. 131–138

[xvxv] Zhai, X. Q., and R. Z. Wang. "Experimental Investigation and Performance Analysis on a Solar Adsorption Cooling System With/without Heat Storage." Applied Energy 87 (2010): 824-35. Print

[xvi] Luo, H. L., Y. J. Dai, R. Z. Wang, J. Y. Wu, Y. X. Xu, and J. M. Shen. "Experimental Investigation of a Solar Adsorption Chiller Used for Grain Depot Cooling." Applied Thermal Engineering 26 (2006): 1218-225. Print.

[xvii] Goswami, D. Yogi., Frank Kreith, Jan F. Kreider. "Solar Cooling."*Principles of Solar Engineering*. Philadelphia, PA: Taylor & Francis, 2000. Print.

[xviii] Balaras, Constantinos A., Gershon Grossman, Hans-Martin Henning, Carlos A. Infante Ferreira, Erich Podesser, Lei Wang, and Edo Wiemken. "Solar Air Conditioning in Europe-an Overview."Renewable & Sustainable Energy Reviews 11 (2007): 299-314. Print.

[xix] Causone, Francesco, Stefano P. Corgnati, Marco Filippi, and Bjarne W. Olesen. "Solar Radiation and Cooling Load Calculation for Radiant Systems: Definition and Evaluation of the Direct Solar Load."Energy and Buildings 42 (2009): 305-14. Print.

[xx] http://www.eere.energy.gov/de/thermally_activated/tech_basics.html

[xxi] Frost and Sullivan Report #7501-19, 2000

[xxii] Ari Rabl, “Active Solar Collectors and Their Applications,” Oxford University Press, 1985

[xxiii] Munson, Bruce Roy, Donald F. Young, and T. H. Okiishi. *Fundamentals of Fluid Mechanics*. Hoboken, NJ: J. Wiley & Sons, 2006. Print.

[xxiv] Qu, Ming, David H. Archer, and Hongxi Yin. "Proceedings of ES2008." Experiment Based Performance Analysis of a Solar Absorption Cooling and Heating System in Carnegie Mellon University. Proc. of Energy Sustainability Florida, Jacksonville. ASME. Print.